LEVEL

AD A082313

DTIC
SELECTED
MAR 27 1980

A

DDC FILE COPY

ENSCO, INC. ®

80 3 26 057

SAR(01)-TR-79-04
8 November 1979

# AN EVALUATION OF THE SEISMIC RESEARCH OBSERVATORIES: FINAL REPORT

TECHNICAL REPORT NO. 4

PREPARED BY

LEONARD C. WELTMAN, HELMUT Y.A. HSIAO, AND ROBERT R. OLIVER

PREPARED FOR

AIR FORCE TECHNICAL APPLICATIONS CENTER
ALEXANDRIA, VIRGINIA 22314

DTIC
ELECTE
S   D
MAR 27 1980

ENSCO, INC.

SEISMIC APPLIED RESEARCH DIVISION
813 NORTH ROYAL STREET
ALEXANDRIA, VIRGINIA 22314

REPORT DOCUMENTATION PAGE

READ INSTRUCTIONS
BEFORE COMPLETING FORM

1. REPORT NUMBER

2. GOVT ACCESSION NO.

3. RECIPIENT'S CATALOG NUMBER

(9) Final rept.

4. TITLE *(and Subtitle)*

(6) AN EVALUATION OF THE SEISMIC RESEARCH
OBSERVATORIES. FINAL REPORT

5. TYPE OF REPORT & PERIOD COVERED

11 Dec 78 — 31 Mar 84,

Technical

6. PERFORMING ORG. REPORT NUMBER

(14) SAR(01)-TR-79-04, *TR-4*

7. AUTHOR(s)

(10) Leonard C. Weltman   Helmut Y.A. Hsiao
and Robert R. Oliver

8. CONTRACT OR GRANT NUMBER(s)

(5) F08606-79-C-0014, *ARPA*

9. PERFORMING ORGANIZATION NAME AND ADDRESS

ENSCO, INC.
SAR Division
Alexandria, Virginia 22314

10. PROGRAM ELEMENT, PROJECT, TASK AREA & WORK UNIT NUMBERS

Order-2551

VELA T/9705/B/PMP

11. CONTROLLING OFFICE NAME AND ADDRESS

Advanced Research Projects Agency
Nuclear Monitoring Research Office
Arlington, Virginia   22209

12. REPORT DATE

(11) 8 Nov 1979

13. NUMBER OF PAGES

132

14. MONITORING AGENCY NAME & ADDRESS*(If different from Controlling Office)*

Air Force Technical Applications Center
VELA Seismological Center
Alexandria, Virginia   22314

15. SECURITY CLASS. *(of this report)*

UNCLASSIFIED

15a. DECLASSIFICATION/DOWNGRADING SCHEDULE

16. DISTRIBUTION STATEMENT *(of this Report)*

APPROVED FOR PUBLIC RELEASE, DISTRIBUTION UNLIMITED

(12) 135

17. DISTRIBUTION STATEMENT *(of the abstract entered in Block 20, if different from Report)*

18. SUPPLEMENTARY NOTES

ARPA Order No. 2551

19. KEY WORDS *(Continue on reverse side if necessary and identify by block number)*

Abbreviated Seismic Research Observatories
Seismic Research Observatories
Data Quality
RMS Noise Levels

20. ABSTRACT *(Continue on reverse side if necessary and identify by block number)*

This report concludes a four-year evaluation of the Seismic Research Observatories (SRO) and the Abbreviated SROs (ASRO). Five stations are evaluated here:

- SRO: Ankara, Turkey (ANTO)
         Bogota, Columbia (BOCO)
         Graffenburg, Germany (GRFO)
         Shillong, India (SHIO)

DD FORM 1473   **EDITION OF 1 NOV 65 IS OBSOLETE**
1 JAN 73

19. (continued)

Noise Spectral Content
Detection Capability

20. (continued)

● ASRO: Kongsberg, Norway (KONO).

Major areas of investigation included the analysis of
noise levels, trends, and spectral content, and the estima-
tion of the detection capability of each station with regard
to specified geographic regions. Estimates were also made
of data quality, station reliability, and mixed-event prob-
ability. In addition to the above, long-period noise analy-
ses were extended over a full year for the following pre-
viously evaluated stations:

● · SRO: Chiang Mai, Thailand (CHTO)
● ASRO: Zongo (LaPaz), Bolivia (ZOBO)
           Kabul, Afghanistan (KAAO)
           Matsushiro, Japan (MAJO).

The detection capability of station ZOBO with respect to
South American events was also determined.

Finally, the results of the four-year study were sum-
marized. The average station was operational 90% of the time.
Data quality was excellent.

GUMO and BOCO are the only poor stations in the network.
Data from the former station were affected by ocean noise;
data from the latter station were sometimes degraded by cor-
rectable hardware malfunctions.

Noise studies showed that, as expected, instrument burial
reduces and stabilizes the recorded noise field. Station noise
measurements and detection capabilities are tabulated in Sec-
tion V of this report.

AFTAC Project Number: VELA T/9705/B/PMP

Project Title: VELA Network and Automatic
                               Processing Research

ARPA Order Number: 2551

Name of Contractor: ENSCO, Incorporated

Contract Number: F08606-79-C-0014

Effective Date of Contract: 11 December 1978

Contract Expiration Date: 31 March 1980

Project Manager: Theodore J. Cohen
                               (703) 548-8666

SUMMARY

This report concludes a four-year evaluation of the Seismic Research Observatories (SRO) and the Abbreviated SROs (ASRO). Five stations are evaluated here:

- SRO - Ankara, Turkey, (ANTO)
       Bogota, Colombia, (BOCO)
       Grafenburg, Germany, (GRFO)
       Shillong, India, (SHIO)
- and ASRO - Kongsberg, Norway, (KONO).

Major areas of investigation included the analysis of noise levels, trends, and spectral content, and the estimation of the detection capability of each station with regard to specified geographic regions. Estimates were also made of data quality, station reliability, and mixed-event probability. In addition to the above, long-period noise analyses were extended over a full year for the following previously evaluated stations:

- SRO - Chiang Mai, Thailand, (CHTO)
- and ASRO - Zongo (LaPaz), Bolivia, (ZOBO)
         Kabul, Afghanistan, (KAAO)
         Matsushiro, Japan, (MAJO).

The detection capability of station ZOBO with respect to South American events was also determined.

ENSCO, INC.   iii

Finally, the results of the four-year study were summarized. The average station was operational 90% of the time. Data quality was excellent.

GUMO and BOCO are the only poor stations in the network. Data from the former station were affected by ocean noise; data from the latter station were sometimes degraded by correctable hardware malfunctions.

Noise studies showed that, as expected, instrument burial reduces and stabilizes the recorded noise field. Station noise measurements and detection capabilities are tabulated in Section V of this report.

ENSCO, INC.   iv

ACKNOWLEDGMENTS

ENSCO, INC.

TABLE OF CONTENTS

ENSCO, INC.

LIST OF FIGURES

LIST OF FIGURES
(continued)

LIST OF FIGURES
(continued)

LIST OF FIGURES
(continued)

LIST OF FIGURES
(continued)

LIST OF TABLES

SECTION I
INTRODUCTION

A.   THE SEISMIC RESEARCH OBSERVATORY SYSTEM

Sorrels et al. (1971) noted that seismic data recorded by surface-sited instruments may be degraded by atmospheric loading at the earth's surface. Theoretical data (Sorrels, 1971) and tests (Sorrels et al., 1971) proved that the atmospheric contribution to the seismic noise field decreases with depth. These studies suggested instrument burial as one way to eliminate these transients, and such research culminated with the construction of the Seismic Research Observatories (SRO), a world-wide network of borehole seismometers.

The SRO data acquisition and recording system has been described in detail by Strauss (1976). Briefly, broadband seismic energy is recorded by force-balance type seismometers which produce an output proportional to earth acceleration over the frequency range 0.02 to 1.0 Hz. Both long-period and short-period data are produced from each sensor by selectively filtering the broadband output. The long-period data are digitized and recorded continuously on an 800 bit per inch magnetic tape.

The short-period data recorder is a save-only-signal system, the operation of which is governed by an automatic power threshold detector (Eterno et al., 1974). This detector permits recording to occur only when certain operator-specified

conditions are met (e.g., detection threshold and power average time constants). The detector works well at quiet sites (Weltman and Oliver, 1978; Peterson et al., 1976) and effectively conserves magnetic tape. Its operation at noisy sites is less effective because of higher false alarm rates.

Magnetic tapes, once loaded, are shipped to the Albuquerque Seismological Laboratory at Kirtland Air Force Base, New Mexico. Copies of these tapes are then sent to the Seismic Data Analysis Center at Alexandria, Virginia, for subsequent distribution and analysis.

Data are recorded in the following manner. Long-period data are sampled once per second. The instrument response peaks at a period of 25 seconds with a quantization factor of 5 computer counts per millimicron of ground motion.

Short-period data are sampled 20 times per second. The instrument response peaks at a period of 1 second. The 1 second quantization factor is 2000 computer counts per millimicron of ground motion with the following exceptions. Beginning 1 May 1976, at Guam; 14 April 1976, at Wellington, New Zealand; and 13 May 1976, at Taipei, Taiwan; short-period data were quantized at 2 computer counts per millimicron of ground motion to prevent data clipping.

In addition to the analyses performed on data from selected SRO stations, data from selected Abbreviated Seismic Research Observatories (ASRO) are also evaluated. The latter stations feature surface-vault seismometers rather than instruments of the borehole type. Data sampling rates are identical, and response characteristics are very similar, to those

of the SRO sites. Normalized response characteristics for
SRO and ASRO instruments are shown in Figure I-1. Quantiza-
tion factors at 1- and 25-second periods are 10 and 1000 com-
puter counts per millimicron, respectively, for the ASRO
sites.

B.   THE EVALUATION TASK

The specific goals of this evaluation are:

- To estimate the data quality from, and reliability
  of, selected stations.

- To investigate the short-period and long-period
  noise field characteristics of selected stations.

- To estimate the detection capability of selected
  stations.

- To summarize the results of the four-year study
  and to determine the detection capability of the
  combined SRO-ASRO network.

These evaluation goals are addressed in the following
manner. First, suites of seismic events and noise samples
were assembled from event lists. The procedure for event
suite selection is described in Section II. Section II
also describes the manner in which the events and noise
samples were processed, estimates the quality of the SRO
data, and quantifies the reliability of the individual sta-
tions.

In Section III, the local noise field characteristics at
each evaluated SRO station are presented. The local noise

ENSCO, INC.   I-3
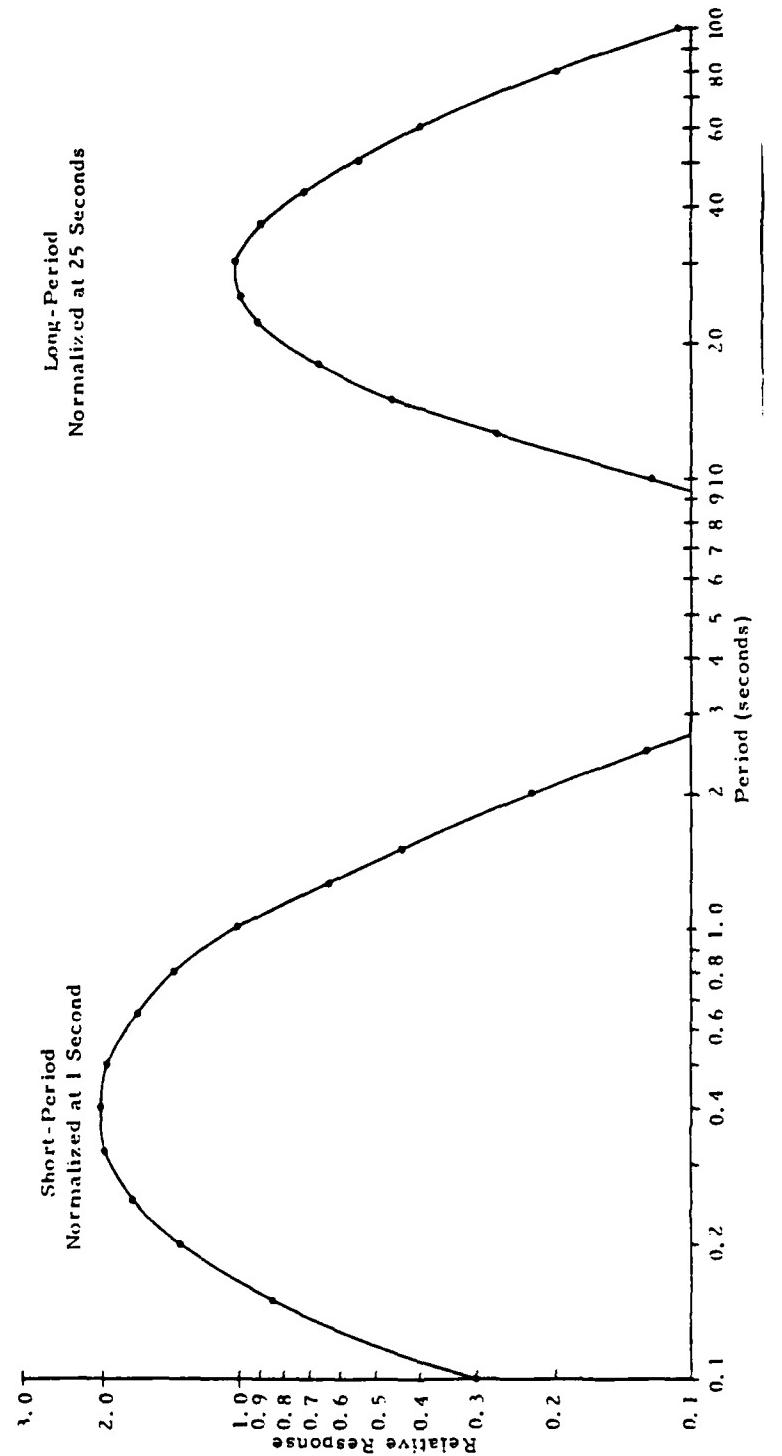
FIGURE I-1

NORMALIZED INSTRUMENT RESPONSE CURVES

ENSCO, INC.   I-4

field is characterized by the RMS noise levels, monthly RMS noise level trends, peak noise amplitudes, and spectral content of the noise.

Section IV presents the detection capability of each station. In the course of estimating detection capabilities, the effects of mixed events and system malfunctions on these estimates are also discussed.

Section V summarizes the results of the four-year SRO/ASRO study, and includes an estimate of the network detection capability.

Finally, Section VI lists the references cited.

SECTION II
THE DATA BASE

A.   DATA AVAILABILITY

The SRO network presently consists of the eighteen sta-
tions listed in Table II-1 and shown in Figure II-1. Stations
evaluated in this report are located at Ankara, Turkey (ANTO);
Bogota, Columbia (BOCO); Chiang Mai, Thailand (CHTO); Grafen-
burg, Germany (GRFO); Shillong, India (SHIO); Zongo, Bolivia
(ZOBO); Kabul, Afghanistan (KAAO); Matsushiro, Japan (MAJO);
and Kongsberg, Norway (KONO).

Figure II-2 shows data availability during the period
June 1977 through May 1979. Data availability is good for
all stations except for BOCO (this station was disabled for
an extended period because of equipment failure).

B.   FORMATION OF THE EVENT DATA BASES

ANTO, BOCO, GRFO, SHIO, ZOBO, and KONO were the stations
to be evaluated with respect to detection capability and sev-
eral factors were considered before forming an event data
base.

First, the traditional emphasis on an SRO/ASRO Eurasian
detection capability was considered inappropriate for two
stations: ZOBO and BOCO. These stations were expected to be

ENSCO, INC.   II-1

TABLE II-1

SEISMIC RESEARCH OBSERVATORIES

Station Number	Location	Designator	Type	Coordinates	
				Latitude	Longitude
30	Albuquerque, New Mexico	ANMO	SRO	34°56'30"N	106°27'30"W
31	Ankara, Turkey	ANTO	SRO	39°52'12"N	32°47'24"E
Unknown	Bangui, Central African Republic	BCAO	SRO	Unknown	Unknown
32	Bogota, Columbia	BOCO	SRO	4°35'46"N	74°2'57"W
33	Chiang Mai, Thailand	CHTO	SRO	18°47'24"N	98°58'37"E
50	Charters Towers, Australia	CTAO	ASRO	20°5'18"S	146°15'16"E
39	Grafenburg, Germany	GRFO	SRO	49°41'24"N	11°13'12"E
35	Guam, Marianas Islands	GUMO	SRO	13°35'16"N	144°51'59"E
52	Kabul, Afghanistan	KAAO	ASRO	34°32'27"N	69°2'34"E
54	Kongsberg, Norway	KONO	ASRO	59°39'00"N	9°36'00"E
36	Mashhad, Iran	MAIO	SRO	36°18'00"N	59°29'40"E
53	Matsushiro, Japan	MAJO	ASRO	36°32'30"N	138°12'32"E
38	Narrogin, Western Australia	NWAO	SRO	32°55'42"S	117°14'9"E
Unknown	Quetta, Pakistan	QUPO	SRO	Unknown	Unknown
40	Shillong, India	SHIO	SRO	25°34'12"N	91°52'48"E
42	Wellington (South Karori), New Zealand	SNZO	SRO	41°18'37"S	174°42'17"E
41	Taipei, Taiwan	TATO	SRO	24°58'34"N	121°29'20"E
51	Zongo, Bolivia	ZOBO	ASRO	16°16'12"S	68°7'30"W
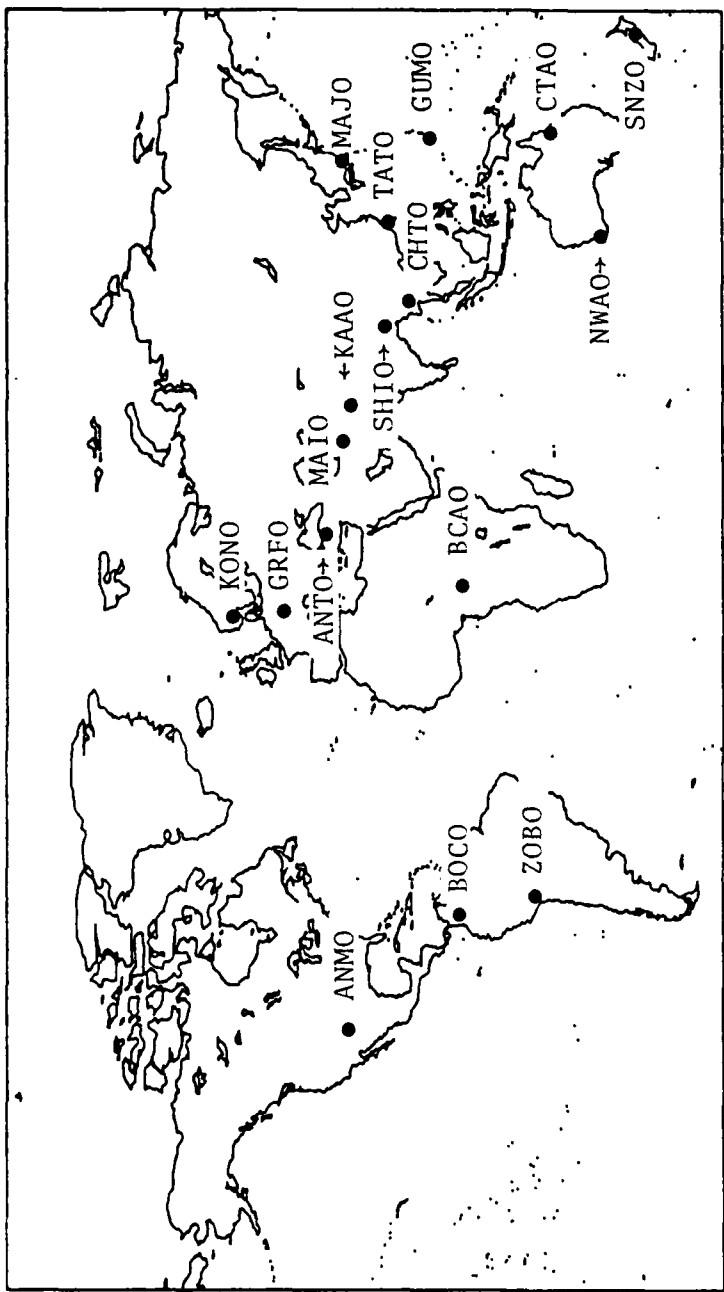
FIGURE II-1

THE SRO/ASRO NETWORK

ENSCO, INC.   II-3
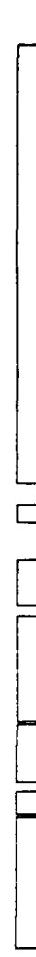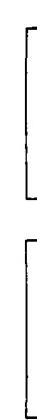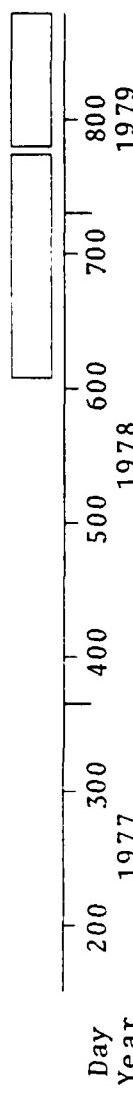
FIGURE II-2

AVAILABLE SRO DATA FOR EVALUATED STATIONS FROM
JUNE 1977 THROUGH MAY 1979

of greatest value in the detection of South American events and so, a data base was formed from that region for these two stations.

Second, it was decided that to the extent possible, events should be chosen to lie between 20 and 80 degrees epicentral distance from the station being evaluated. This distance range was chosen because more distant events evidence a marked increase in attenuation (see for example, Veith and Clawson, 1972), while near events are almost always detected.

For the reasons given above, individually tailored data bases were formed from Norwegian Seismic Array (NORSAR) event lists for each station. The mean and standard deviations for the epicentral distances of the events comprising each data base are listed in Table II-2, along with their associated evaluation time frames. The choice of time frame was governed by data and event bulletin availability. These data bases were used for the determination of both short- and long-period detection capabilities for the Eurasian stations. The South American short-period data bases, however, are truncated versions of their long-period counterparts.

A detailed description of the noise sample data base is given in Section III. In brief, the short-period noise samples were selected from time gates immediately preceding the observed signals which triggered the automatic detector. Long-period noise samples were arbitrarily processed at noon (GMT) of each day. Short-period and long-period noise samples were edited every fourth field tape day. Noise samples were quality checked by visual examination of seismograms, and samples containing signals were rejected.

ENSCO, INC.   II-5

TABLE II-2

THE EVENT DATA BASES

Station	Data Type*	Data Base Begins	Data Base Ends	$\overline{\Delta}$** (degrees)	Region
ANTO	LP SP	November 1978 November 1978	February 1979 February 1979	32±2 32±2	Eurasia Eurasia
GRFO	LP SP	November 1978 November 1978	February 1979 February 1979	46±4 46±4	Eurasia Eurasia
SHIO	LP SP	November 1978 November 1978	February 1979 February 1979	21±6 21±6	Eurasia Eurasia
KONO	LP SP	November 1978 November 1978	February 1979 February 1979	45±5 45±5	Eurasia Eurasia
BOCO	LP SP	October 1978 October 1978	May 1979 February 1979	42±16 42±16	South America South America
ZOBO	LP SP	October 1978 October 1978	April 1979 February 1979	49±17 49±17	South America South America

* LP = Long-Period, SP = Short-Period

** Mean and standard deviation of station-to-epicenter distances

ENSCO, INC.

II-6

C. DATA PROCESSING

Long-period signal and noise data, and short-period noise data, were processed in two stages: 1) a pre-analysis processing stage, which involved the use of the multi-purpose program TISSPROG (Schmidt, 1978), and 2) an analysis processing stage. A description of TISSPROG, as it processes SRO data, follows (refer to Figure II-3).

Given input data consisting of epicentral locations and origin times, TISSPROG estimates short- or long-period arrival times, and edits events or noise samples from a field tape. Short-period data are resampled to a one-tenth of a second time interval, and long-period data are resampled from a one-second to a two-second time interval. Long-period edit gates are automatically set at 4096 seconds, and short-period edit gates are determined by the 'on time' of the short-period detector. Short-period edit gates are limited to 204.8 seconds. Trace means are next removed, and long-period data are rotated from their vertical, north, east configuration to a vertical, transverse, radial configuration. At this stage, samples are saved on an event tape for further analysis. Finally, TISSPROG produces 0.5-4.0 Hz bandpass filtered short-period or 0.023-0.059 Hz bandpass filtered long-period plots.

Noise and signal analyses follow. Since procedures are detailed in later sections, only brief descriptions will be included here.

All data samples were visually checked for quality. Long-period events were analyzed to determine detection capability. Long-period noise samples yielded 512-point noise analysis

ENSCO, INC.   II-7
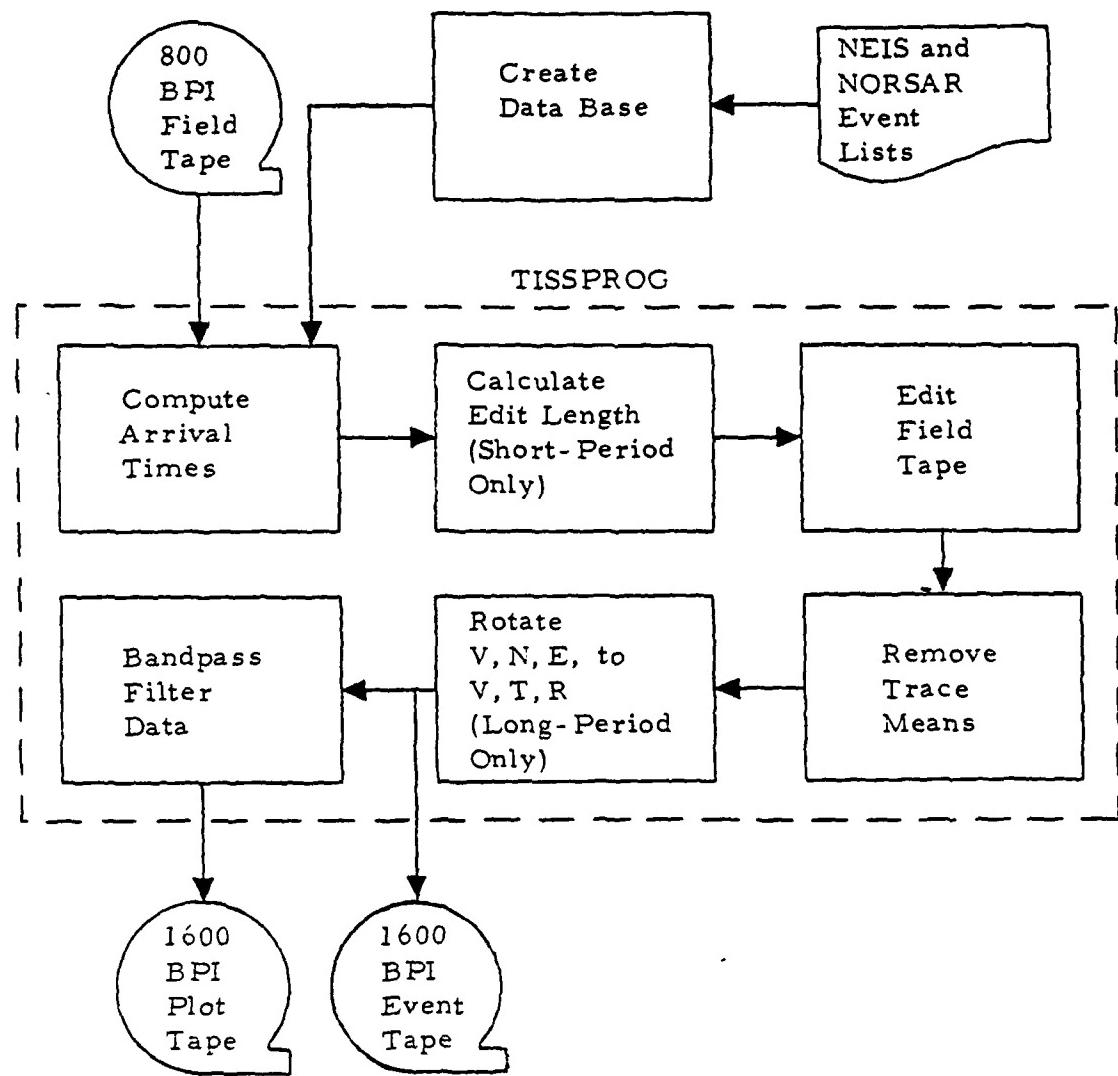
FIGURE II-3

DATA PROCESSING FLOW CHART

gates. These noise gates were further processed to produce peak 25 second noise amplitudes, RMS noise amplitudes in the 17-41 second spectral band, and power spectra. Values were later grouped as averages and/or functions of time.

Since short-period data were recorded only when the SRO detector is signal activated, acceptable extended noise gates are non-existent. However, each time the detector triggers, the preceding 20 seconds of data are recorded as a lead-in buffer. Therefore, the first 12.8 seconds of short-period detections were used for noise analyses. Following visual inspection, an analysis processing routine was employed to produce a peak one-second amplitude, 0.5-4.0 Hz RMS amplitude, and power spectrum.

Short-period detection capabilities were estimated with the aid of microfiche analyses, and no short-period events were computer processed.

D. PROCESSING SUMMARY

Table II-3 summarizes results of event analyses performed during the current contract period on the SRO/ASRO evaluation task. In this table, the 'SP' and 'LP' under the heading "DATA TYPE' refer to short- and long-period data, respectively. The heading 'EVENTS DETECTED' refers to the number of events which were visually detected (Calcomp plot for LP; microfiche or Calcomp plot for SP) under the detection criteria of Section V. The heading 'EVENTS NOT DETECTED'

TABLE II-3

SUMMARY OF SRO/ASRO EVENT PROCESSING

Station	Data Type	Events Detected	Events Not Detected	No Detection Because Of Mixed Events	Events For Which No Data Were Recorded	Events Not Detected Because Of Malfunction	Total Events
ANTO	LP	34	164	44	13	2	244
	SP	27	108	2	18	0	155
BOCO	LP	86	19	22	8	4	139
	SP	25	27	0	1	0	53
GRFO	LP	34	112	41	3	9	196
	SP	30	170	2	0	0	202
SHIO	LP	62	118	34	42	2	258
	SP	24	29	4	54	0	116
ZOBO	LP	138	33	39	3	0	213
	SP	39	17	1	1	0	58
KONO	LP	52	116	43	6	3	220
	SP	12	151	3	57	0	223

ENSCO, INC.

II-10

refers to the number of events for which only seismic noise was observed in the signal gate. The heading 'NO DETECTION BECAUSE OF MIXED EVENTS' refers to the number of events obscured by the presence of some other signal within the signal gate. The heading 'EVENTS FOR WHICH NO DATA WERE RECORDED' refers to the number of events for which the recording system at a SRO/ASRO station was disabled. The heading 'EVENTS NOT DETECTED BECAUSE OF MALFUNCTION' refers to the number of events for which a detection status could not be determined because of data degradation (e.g., power spikes) within the signal gate.

The quality of the data recorded at the SRO/ASRO stations was excellent with the following exceptions. The long-period north-south component data recorded at station ANTO showed an intermittent high noise level. The data received from station BOCO were sometimes degraded by power spikes and by short-term data dropouts. These dropouts, which were caused by telemetry problems (John Hoffman, Personal Communication, 1979), were typically of a duration on the order of 1 second. These malfunctions rarely interfered with data processing or analyses, and they are not reflected in Table II-3.

Estimates of station reliability were made using the following argument. If a station is 'perfect' in that it always produced seismic recordings which an analyst can check for detections, it is considered to have a reliability factor of 1.0. If, on the other hand, the station never produced seismic recordings because of instrumentation problems (instruments recording improperly or not at all), it is considered to have a reliability factor of 0.0. In practice, the reliability factor lies between these extremes. Since station

down time and station malfunction time are the two factors
which render the station reliability less than 1.0, the re-
liability factor is defined as follows:

Reliability Factor = 1.0 - (percentage of time station
was down + percentage of
time station malfunctioned)

where the two percentages are estimated from the data of
Table II-3. Thus, the percentage of time a station was down
is estimated from the number of events for which no data were
recorded, divided by the total number of events for which
processing was attempted. The percentage of time a station
malfunctioned is the number of events for which malfunctions
(spikes, glitches, and data drop-outs) masked the seismic
data, divided by the total number of events for which process-
ing was attempted.

Station reliability estimates are presented in Table II-4.
As can be inferred by the low number of malfunctions listed in
Table II-3, these estimates are more dependent upon station
down time. With the exception of station SHIO, all long-
period reliability estimates exceeded 0.91.

In some cases, a station continued to function in its
long-period mode though the short-period recording system had
been disabled. This circumstance expressed itself in the
differences between the short- and long-period reliability
estimates for some stations, notably SHIO and KONO. Such
hardware difficulties are correctable, and so, reliabilities
are expected to improve. Excepting the two stations, the
short-period reliability estimates exceeded 0.88.

ENSCO, INC.   II-12

TABLE II-4
STATION RELIABILITY ESTIMATES

Station	Short-Period	Long-Period
ANTO	0.88	0.94
BOCO	0.98	0.91
GRFO	1.00	0.94
SHIO	0.53	0.83
ZOBO	0.98	0.99
KONO	0.74	0.96

Estimates were also formed of the probability that a signal of interest will be masked by another signal (a 'mixed' event). From the data of Table II-3, one can see that the probability of a mixed short-period event is small, ranging from 0.00 at BOCO to 0.03 at SHIO. The low probability of short-period event mixing results from the typically brief signal coda relative to the average time between signals.

There is a greater probability for long-period event mixing, however, because of the greater duration of long-period signal codas. Table II-5 presents estimates of the probability of long-period event mixing, which ranged from 0.18 to 0.21. Roughly 20 percent of the events analyzed exhibited mixing of signatures.

TABLE II-5
LONG-PERIOD MIXED EVENT PROBABILITY ESTIMATES

Station	Probability Estimate
ANTO	0.18
BOCO	0.16
GRFO	0.21
SHIO	0.12
ZOBO	0.19
KONO	0.18

SECTION III
NOISE ANALYSES

A. DISCUSSION

The purpose of this section is to characterize the noise field at each SRO/ASRO site under evaluation. Presented in this section are mean, peak 1- and 25-second noise values, average RMS values in the 0.25-2.0 and 17-41 second passbands, RMS trends in the 0.25-2.0 and 17-41 second passbands, and average short- and long-period spectra.

The characteristics of the local noise field largely define a station's potential detection capability, and in the short-period case, indirectly determine the time-averaging constants of the automatic signal detector (see Operation and Maintenance Manual, Seismic Research Observatory Data Recording System, Unitech, Inc.).

All noise values are presented without instrument response correction since an analyst is primarily concerned with the noise as he or she will see it (i.e., after it has passed through the sensing, filtering, and recording instrumentation).

B. VERTICAL COMPONENT SHORT-PERIOD NOISE

Short-period noise analyses were performed for five stations; ANTO, BOCO, GRFO, SHIO, and KONO. The time periods of the analyses are shown in Table III-1.

ENSCO, INC.   III-1

TABLE III-1
THE SHORT-PERIOD NOISE DATA BASE

Station	Data Base Start	Data Base Finish	Number Of Samples
ANTO	1 September 1978	25 March 1979	48
BOCO	4 September 1978	27 April 1979	32
GRFO	1 October 1978	31 March 1979	42
SHIO	1 September 1978	30 March 1979	46
KONO	1 October 1978	24 March 1979	39

Noise samples were selected as the first 12.8 seconds of automatic detector edits (see Section I). Three candidate noise samples were chosen for every fourth day, subject to the constraint that each noise sample be separated from previous automatic detections by at least one hour. This constraint prevented one of a series of multiple detections from being mistaken for a noise sample. The three samples were visually screened, and a noise sample obviously free of signal contamination was chosen to represent that day.

The final samples selected were filtered in order to allow a 0.5-4.0 Hz passband RMS noise level measurement which was computed by the equation

$$\text{RMS NOISE} = \left[\frac{\sum_{i=1}^{n} (x_i)^2}{n} \right]^{\frac{1}{2}}$$

where

n   =   number of data points

x_i =   the ith data point.

The calculated RMS noise values (in millimicrons) were plotted against Julian day (Figures III-1 to III-3), and monthly RMS noise trends were then derived from these values (Figures III-4 to III-6).

The SRO stations, in general, are characterized by a relatively stable noise level as compared to the ASRO station, KONO (which showed more scattering of the data). This was not unexpected as a more stable noise field should result when using borehole seismometers. Station KONO is also subject to ocean noise which results from storms in the North Sea.

ENSCO, INC.   III-3
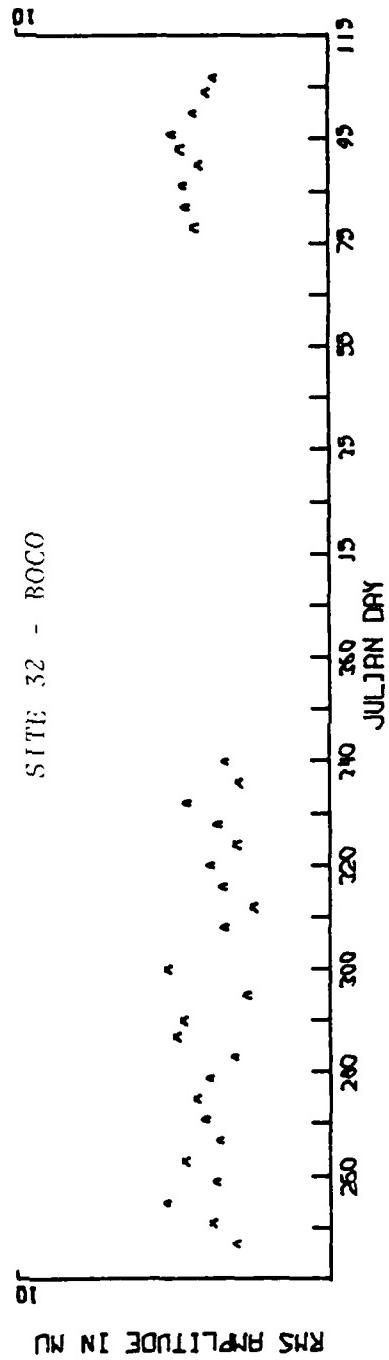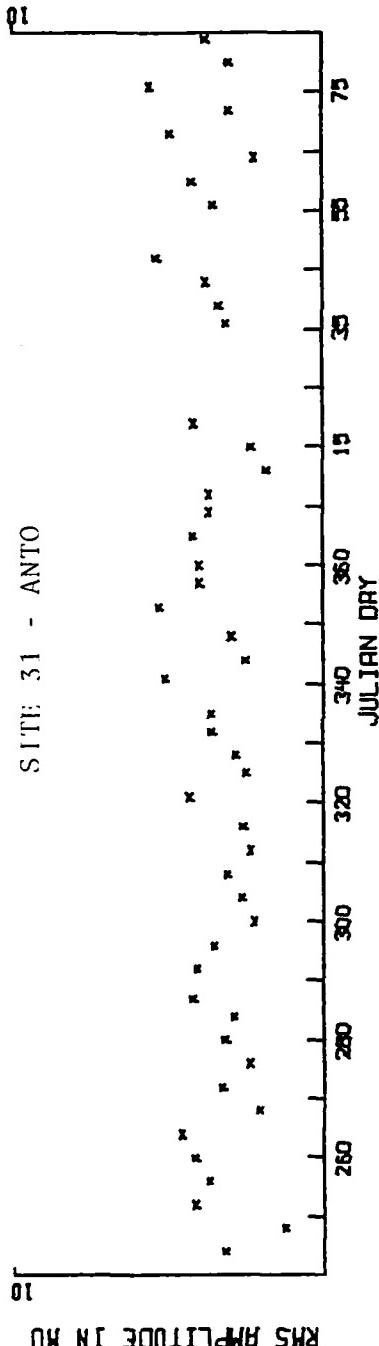
FIGURE III-1

ANTO AND BOCO SHORT-PERIOD RMS NOISE

SITE: 39 - GRFO
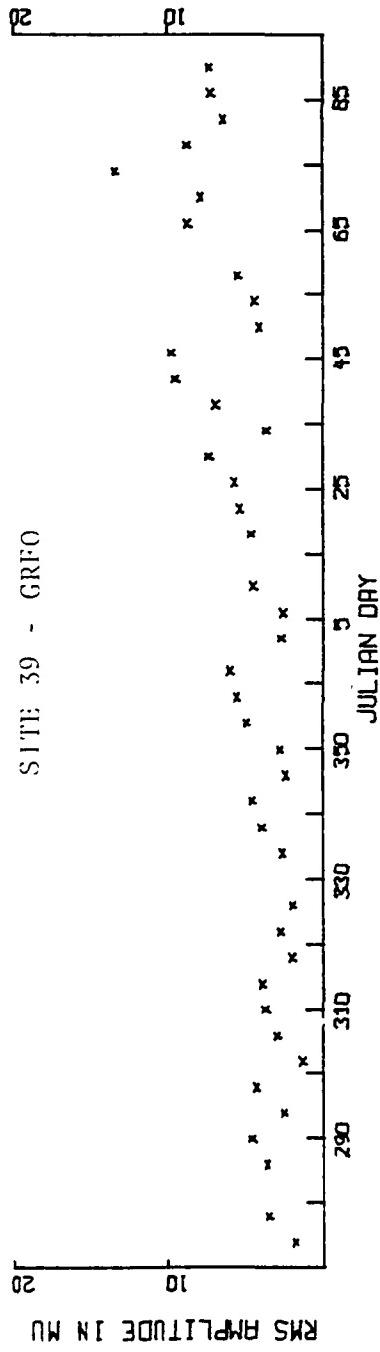
SITE: 40 - SHIO
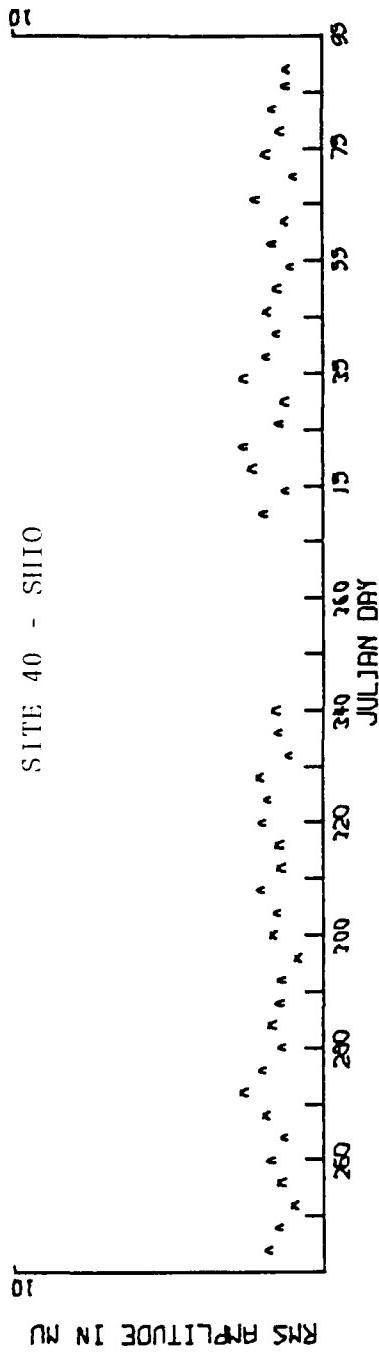
FIGURE III-2

GRFO AND SHIO SHORT-PERIOD RMS NOISE

SITE 54 - KONO

JULIAN DAY

RMS AMPLITUDE IN MU
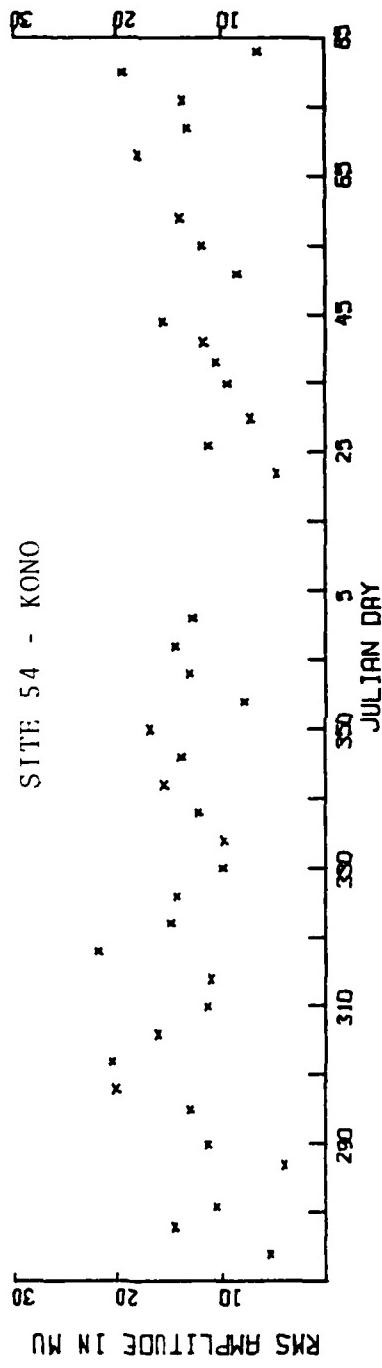
FIGURE III-3

KONO SHORT-PERIOD RMS NOISE
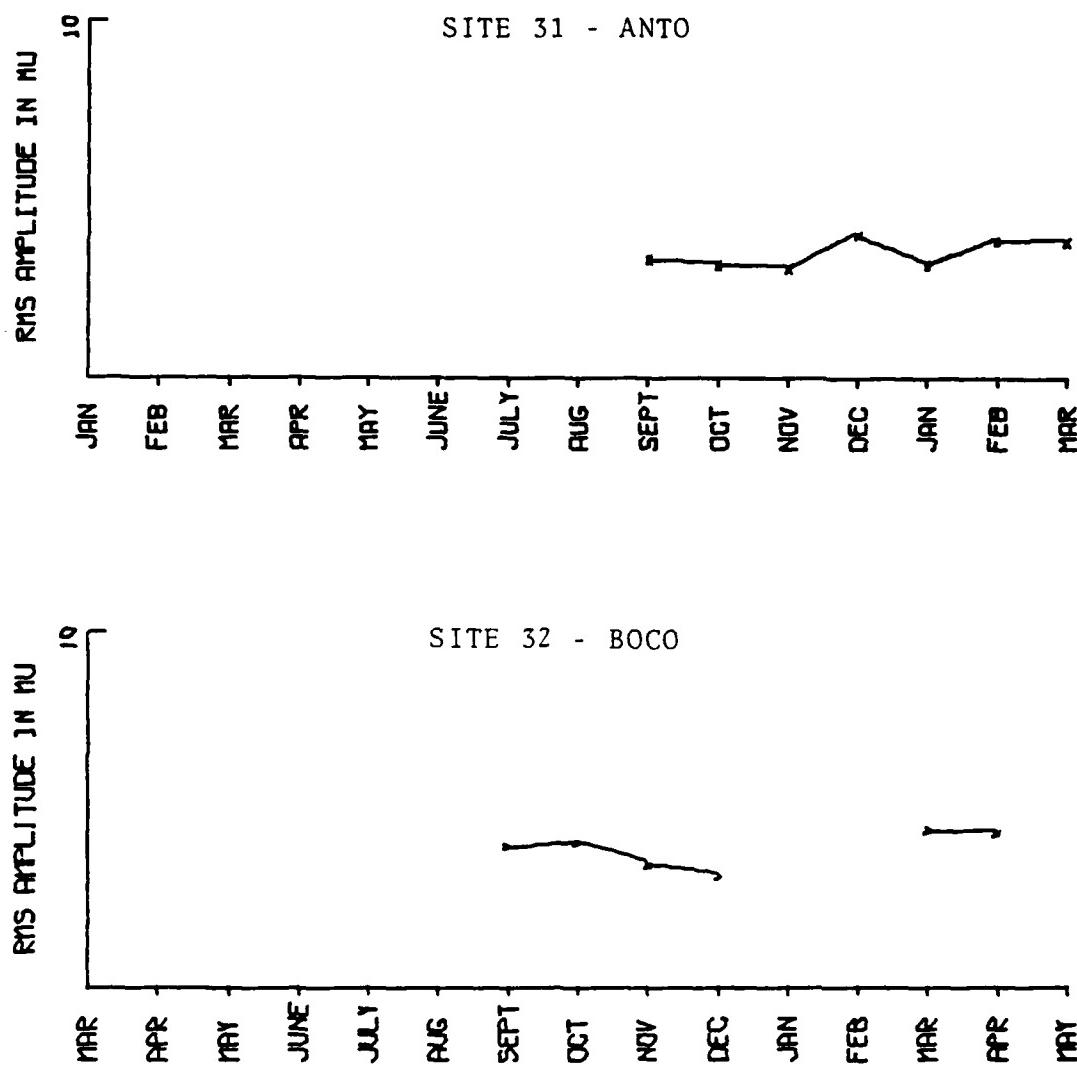
FIGURE III-4

ANTO AND BOCO SHORT-PERIOD RMS NOISE TRENDS

SITE 39 - GRFO
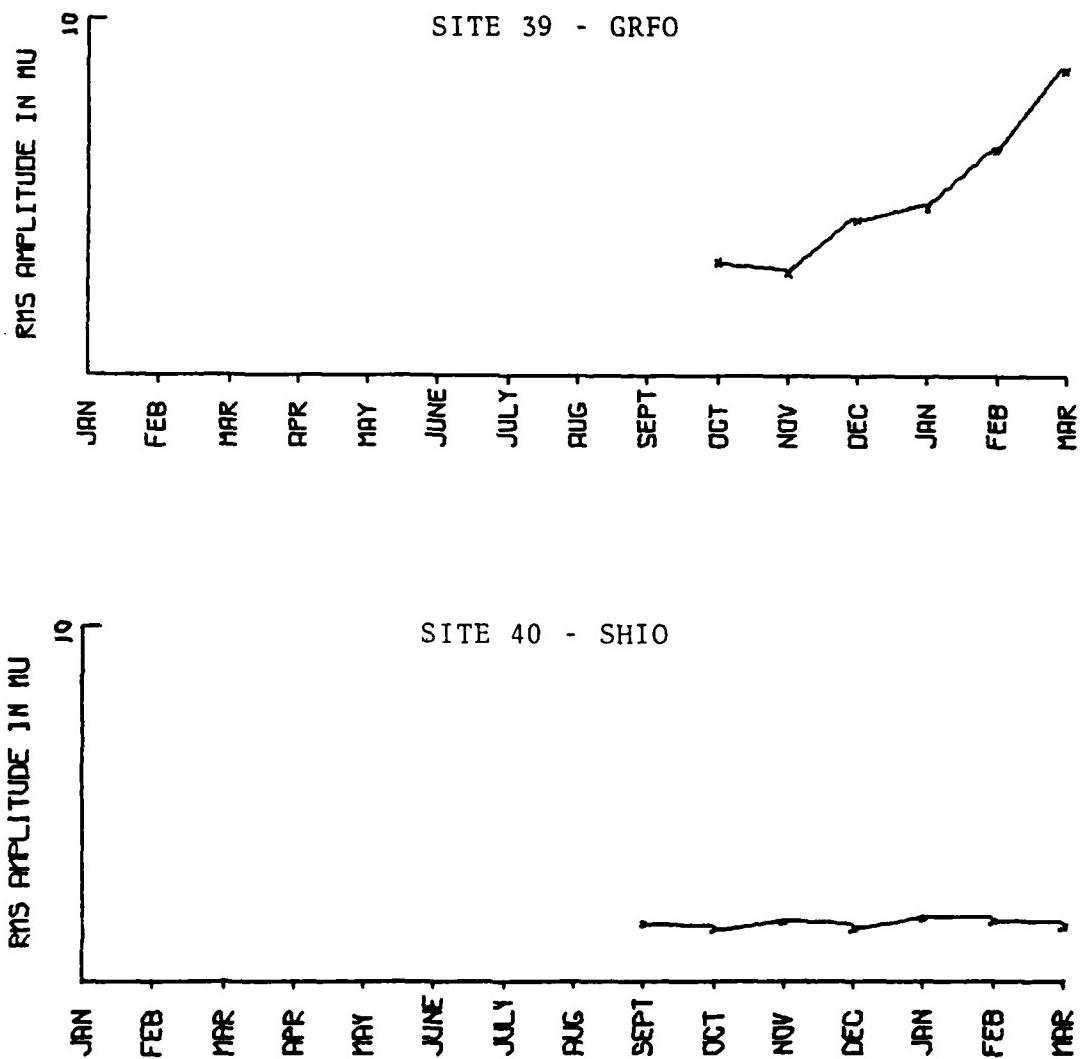
FIGURE III-5
GRFO AND SHIO SHORT-PERIOD RMS NOISE TRENDS

SITE 54 - KONO

RMS AMPLITUDE IN MU

JAN FEB MAR APR MAY JUNE JULY AUG SEPT OCT NOV DEC JAN FEB MAR
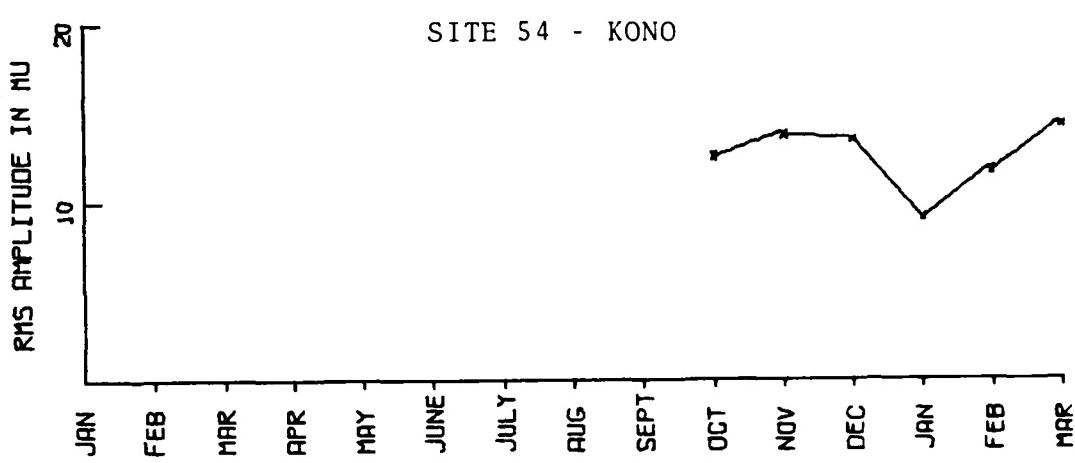
FIGURE III-6

KONO SHORT-PERIOD RMS NOISE TRENDS

ENSCO, INC.   III-9

The short-period noise trends of stations ANTO, BOCO, and SHIO showed little change with time. The noise level at station GRFO, however, appeared to have risen steadily from October 1978 through March 1979, perhaps responding to winter storm activity. The noise level at station KONO dropped in January 1979, but returned to earlier levels by March. This behavior may reflect data variability or a seasonal trend.

Caution must be exercised in interpreting noise trend data. Each monthly average represents six to eight RMS values, and so, one abnormal sample may bias an average. Therefore, noise trend data should be studied for overall patterns, and little weight should be given one anomalous monthly average.

Table III-2 contains the mean, short-period RMS noise values and associated standard deviations. As noted else-where (Weltman and Oliver, 1978; Strauss and Weltman, 1977), inland stations tend toward lower short-period noise levels as compared to coastal stations. The unexpectedly high noise level at station GRFO, however, proved an exception to this observation. No definite reason could be found to explain station GRFO's noise level.

Maximum zero-to-peak one second noise values were also measured for each noise sample. At the request of Dr. Filson, formerly of the Advanced Research Projects Agency, the statis-tics of these measurements are presented in Table III-3 in terms of the mean and standard deviation of the logarithm of the measured values. Both the RMS value standard deviations of Table III-2 and the log peak standard deviations of Table III-3 reflect the aforementioned greater noise variance at ASRO station KONO as compared to that at the SRO stations.

ENSCO, INC.   III-10

TABLE III-2
MEAN SHORT-PERIOD RMS NOISE (VERTICAL COMPONENT)

Station	Station-To-Coast Distance (km)	Mean RMS Noise (mμ)	Standard Deviation	Number Of Samples
ANTO	200	3.46	0.96	48
BOCO	350	3.88	0.81	33
GRFO	500	5.01	2.57	42
SHIO	350	1.62	0.42	42
KONO	33	12.64	4.27	39

TABLE III-3

SHORT-PERIOD NOISE

LOG_{10}(PEAK ONE-SECOND NOISE AMPLITUDE) STATISTICS

Station	Mean Log_{10} Peak 1-Second	Standard Deviation Log_{10} Peak 1-Second	Number Of Samples
ANTO	0.815	0.171	48
BOCO	0.867	0.127	33
GRFO	0.717	0.177	35
SHIO	0.428	0.188	37
KONO	0.828	0.233	26

Finally, representative short-period noise spectra were constructed for each station. Each sample was filtered with a 0.5-4.0 Hz bandpass filter, and the mean and standard deviation of the amplitude spectrum were calculated for each frequency increment. The mean spectral density and the logarithm of the mean spectral density with standard deviations are plotted in Figures III-7 to III-11.

Spectral peaks were found in the SHIO short-period noise spectra at periods of 0.3 and 0.5 seconds. Only a 0.5 second noise peak was apparent in the ANTO, BOCO, and GRFO spectra, however. The KONO short-period spectra were so dominated by noise at periods greater than 0.6 seconds that higher-frequency noise peaks were indiscernible. This noise is thought to result from storm activity in the North Sea.

In a study of ambient earth motion, Fix (1972) also observed peaks in the spectral density at the approximate periods of 0.3 and 0.5 seconds, with the 0.5 second peak being slightly less prominent. These peaks proved to be mainly fundamental mode Rayleigh waves (Douze, 1967).

C.   THREE COMPONENT LONG-PERIOD NOISE

The goals of the long-period noise analyses were to estimate long-period RMS noise levels, peak noise amplitudes, and the spectral content of the noise field for each of the three components (V, N, E) at stations ANTO, BOCO, CHTO, GRFO, SHIO, ZOBO, KAAO, MAJO, and KONO.

SITE 31
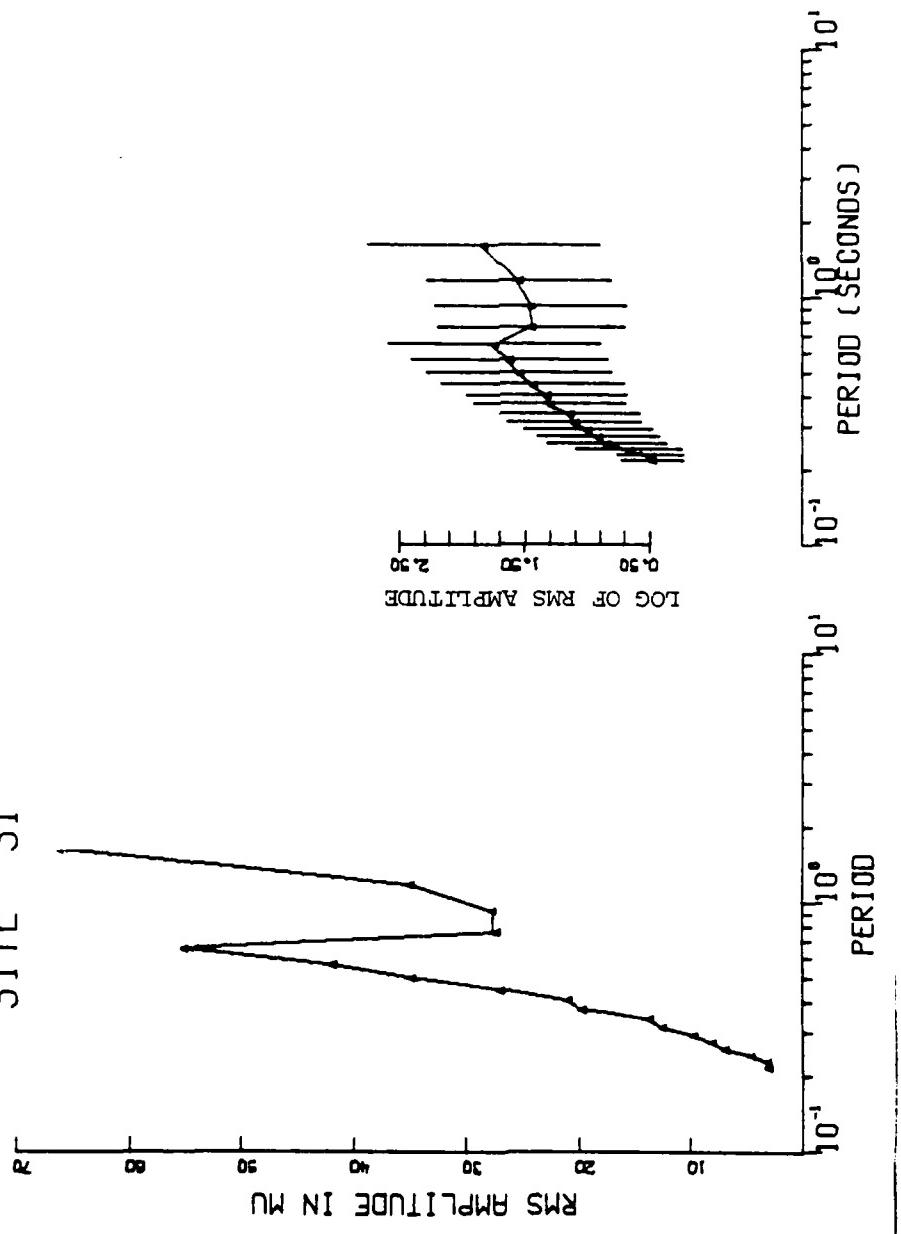
FIGURE III-7

AVERAGE RMS AMPLITUDE SPECTRA - ANTO SHORT-PERIOD NOISE
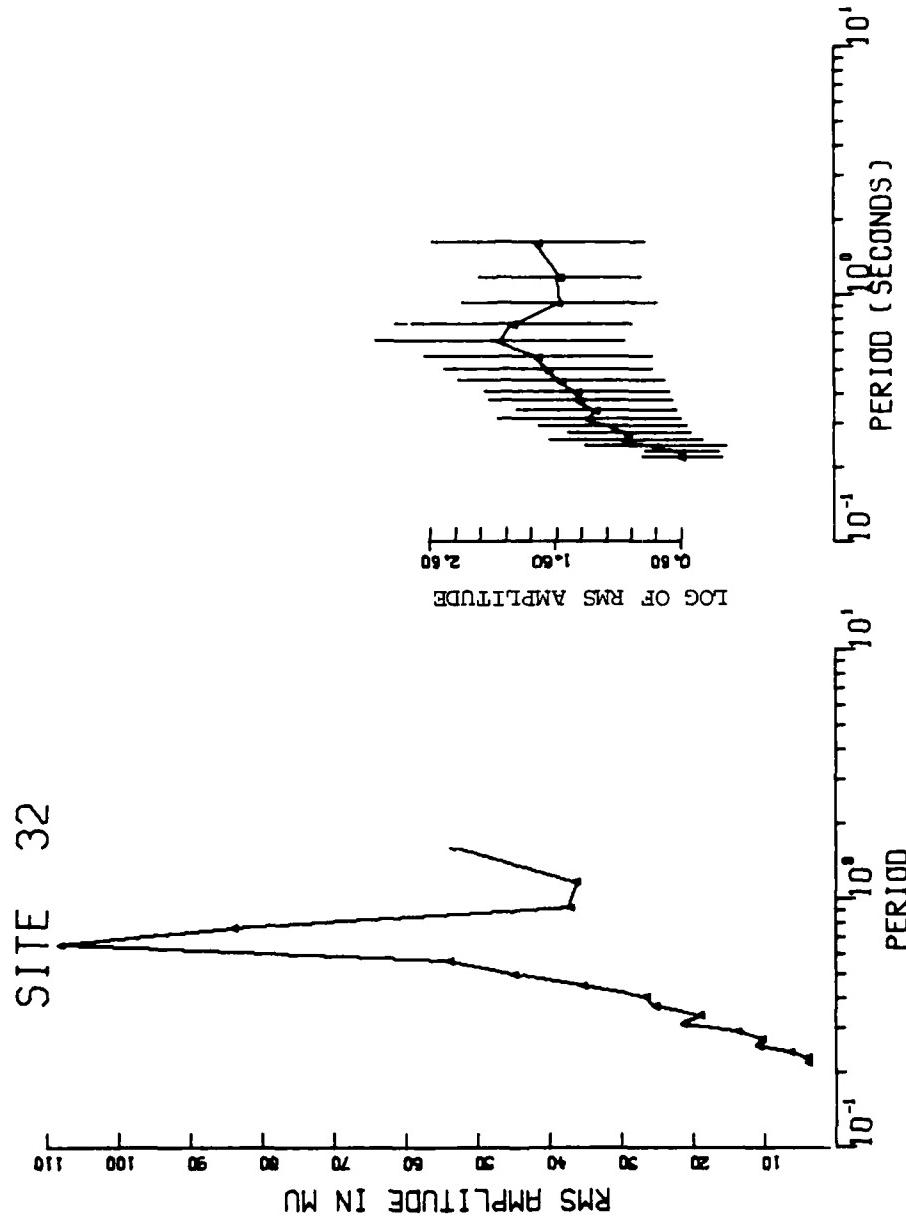
SITE 32

FIGURE III-8

AVERAGE RMS AMPLITUDE SPECTRA - BOCO SHORT-PERIOD NOISE

SITE 39
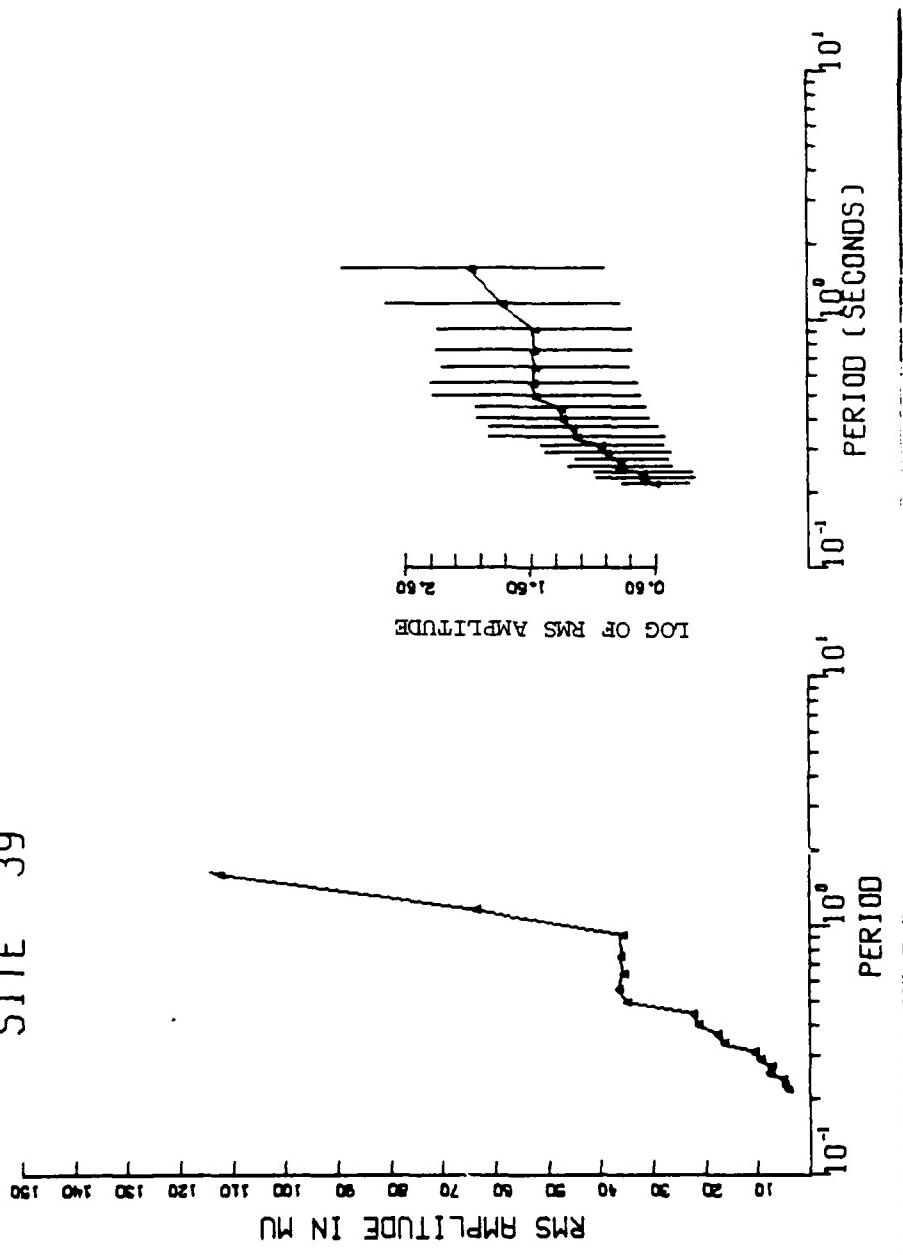
FIGURE III-9

AVERAGE RMS AMPLITUDE SPECTRA - GRFO SHORT-PERIOD NOISE

SITE 40
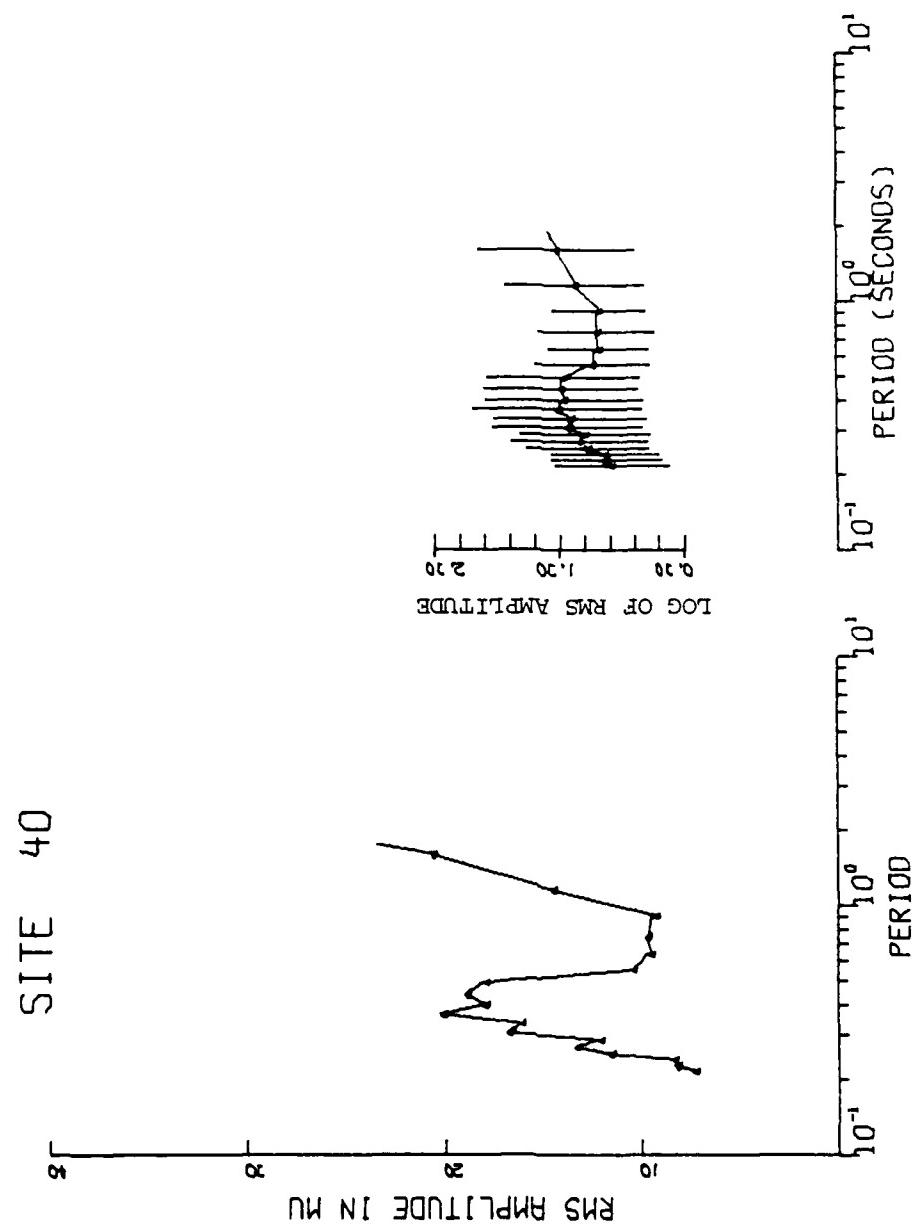
FIGURE III-10

AVERAGE RMS AMPLITUDE SPECTRA - SHIO SHORT-PERIOD NOISE

SITE 54

LOG OF RMS AMPLITUDE

PERIOD (SECONDS)
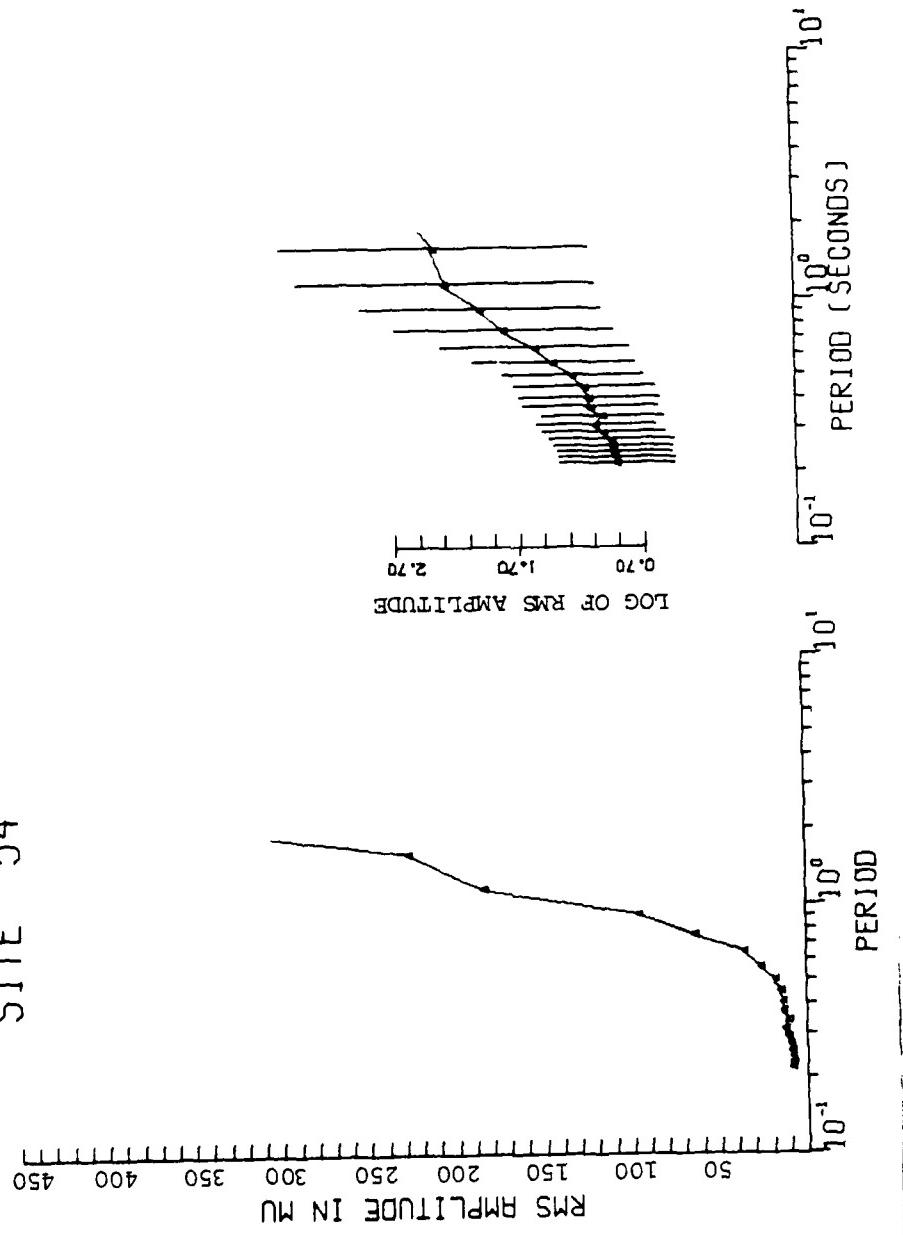
PERIOD

RMS AMPLITUDE IN MU

FIGURE III-11

AVERAGE RMS AMPLITUDE SPECTRA - KONO SHORT-PERIOD NOISE

ENSCO, INC.   III-18

Long-period noise processing usually began on a station's declared operational date and continued as long as time and computer availability permitted. Processing was delayed up to two months if evidence of station malfunction appeared. The processing time periods for each station are shown in Table III-4. Noise analysis time frames were limited to one data year, and periods of known hardware malfunction were deleted from the noise data base.

The 4096-second noise samples were processed as described in Section II. The V, N, E configuration was maintained. Where possible, samples were processed at 1200 hours every fourth day. Samples were visually screened for signals and unreported system malfunctions, and 1024-second noise analysis gates were selected. If an entire sample proved unacceptable, a second attempt followed, and an acceptable noise sample was usually found at an edit time within two hours of the first. Noise samples and analysis gates were then processed by a primary analysis program which performed the following functions:

- Computed RMS noise values without instrument response in the 17-41 second passband.

- Measured zero-to-peak 25 second noise magnitudes.

- Computed power spectra.

The variety of measurements were made for the following reasons. The RMS value describes the noise level over a frequency band which is traditionally of interest from a detection and discrimination viewpoint. The 25 second noise magnitudes are important in the determination of theoretical detection capability and, in fact, were used in the network detection

TABLE III-4
THE LONG-PERIOD NOISE DATA BASE

Station	Data Base Start	Data Base Finish	Number Of Samples
ANTO	2 September 1978	17 March 1979	43
BOCO	17 April 1978	26 March 1979	52
CHTO	8 September 1977	3 October 1978	75
GRFO	1 November 1978	25 February 1979	26
SHIO	5 September 1978	29 March 1979	40
ZOBO	2 June 1977	27 June 1978	54
KAAO	10 July 1977	23 June 1978	77
MAJO	30 July 1977	29 December 1978	85
KONO	15 September 1978	26 February 1979	37

capability estimate of Section V. The noise spectra most ac-
curately describe the noise field detected at a station.

Long-period RMS noise values (uncorrected for instrument
response) in the 17-41 second passband for the vertical, north,
and east components are plotted versus Julian day in Figures
III-12 through III-20 for stations ANTO, BOCO, CHTO, GRFO,
SHIO, ZOBO, KAAO, MAJO, and KONO. Data gaps of up to eight
days usually reflect an inability to find uncontaminated noise
samples. Larger gaps usually imply station down-time.

Visual inspection reveals that noise level variability
remains the same over time for all stations with the exception
of that at station CHTO (Figure III-14). Noise levels for
CHTO increased in both level and variability over a period ex-
tending from July through September 1978. These increases
were most probably caused by summer storm activity.

The 17-41 second passband RMS noise values were grouped
into monthly averages which are presented as noise trends in
Figures III-21 through III-29. The aforementioned late sum-
mer rise in noise level at CHTO is clearly visible in Figure
III-23. The ZOBO and KAAO noise levels, shown in Figures
III-26 and III-27, respectively, changed little with time,
though the KAAO noise trends reached a minimum in November
1977. MAJO's noise trends, which are shown in Figure III-28,
rose steadily from March through December 1978. The other
stations showed no visibly consistent long-period noise trends
within their evaluation time frames. Again, caution should be
exercised in the analysis of these trends, since each monthly
average represents, at most, eight noise samples.

SITE 31
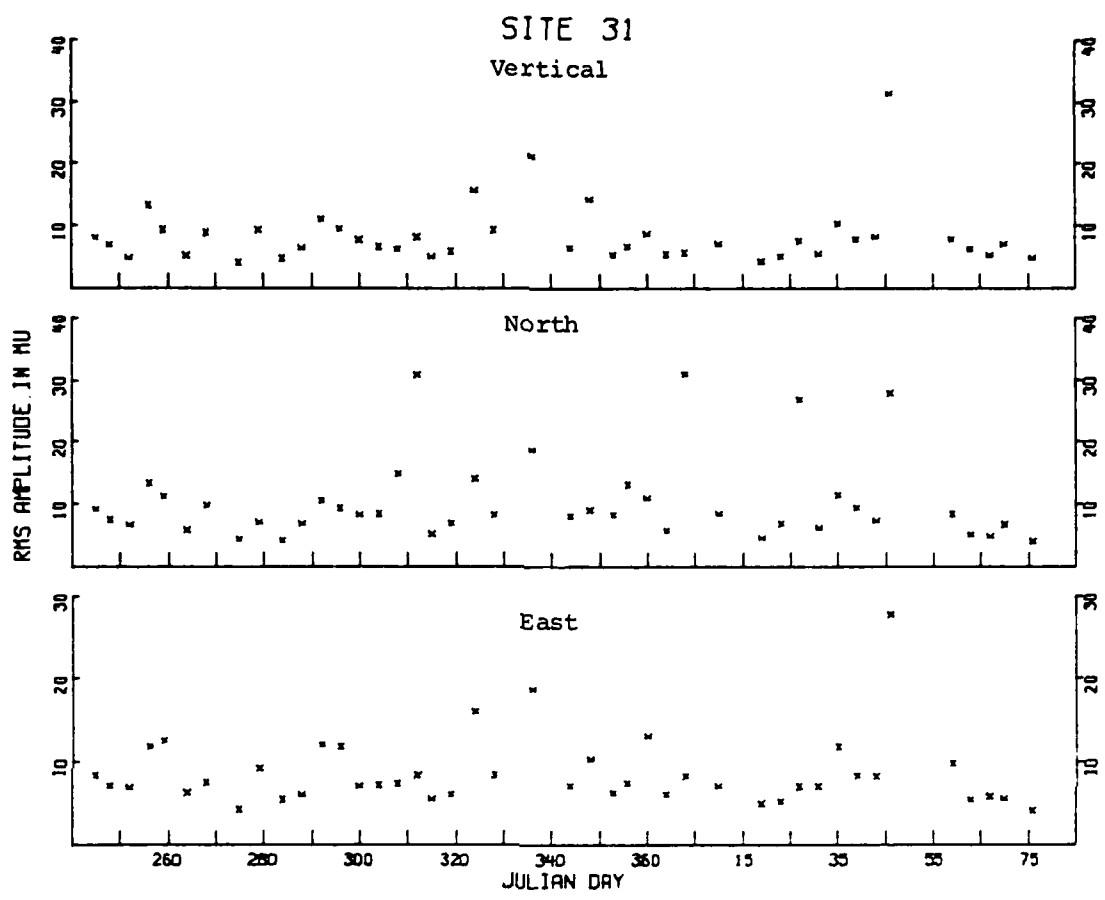
FIGURE III-12
ANTO 17-41 SECOND RMS NOISE

ENSCO, INC.   III-22
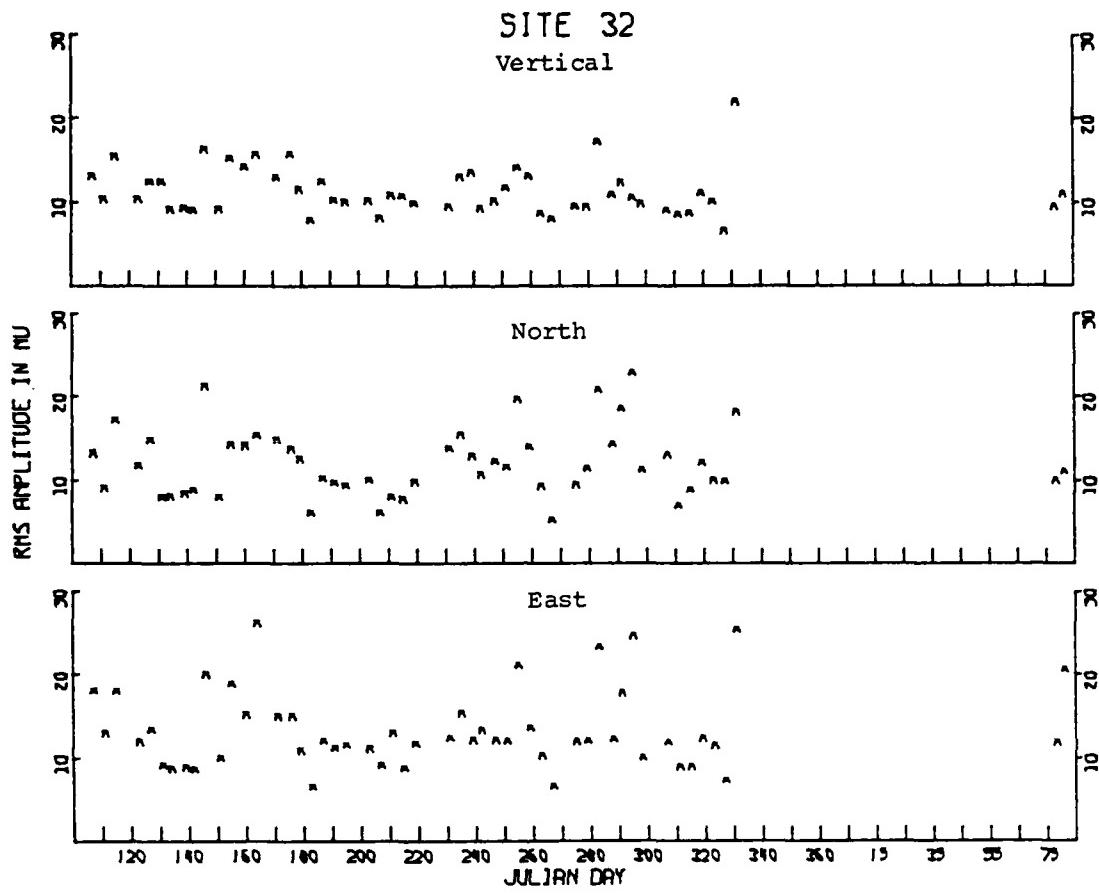
FIGURE III-13

BOCO 17-41 SECOND RMS NOISE

SITE 33
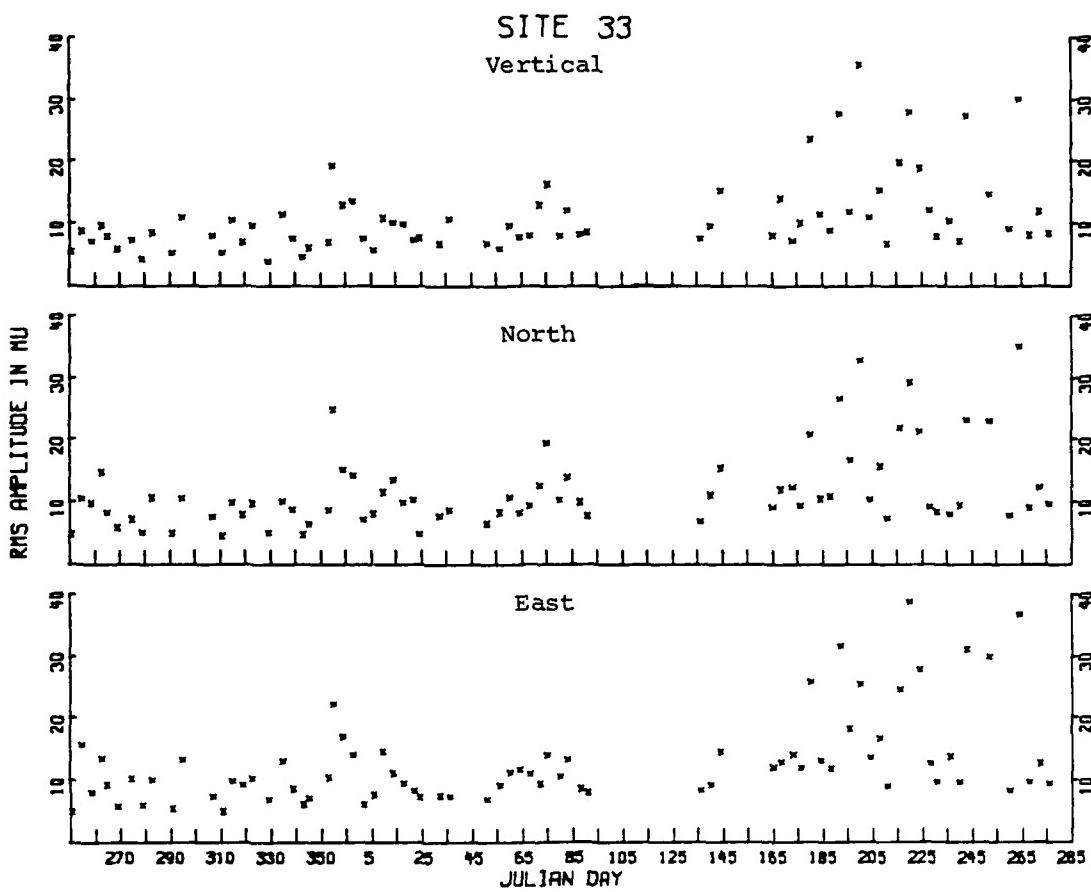
FIGURE III-14

CHTO 17-41 SECOND RMS NOISE

ENSCO, INC.   III-24

SITE 39
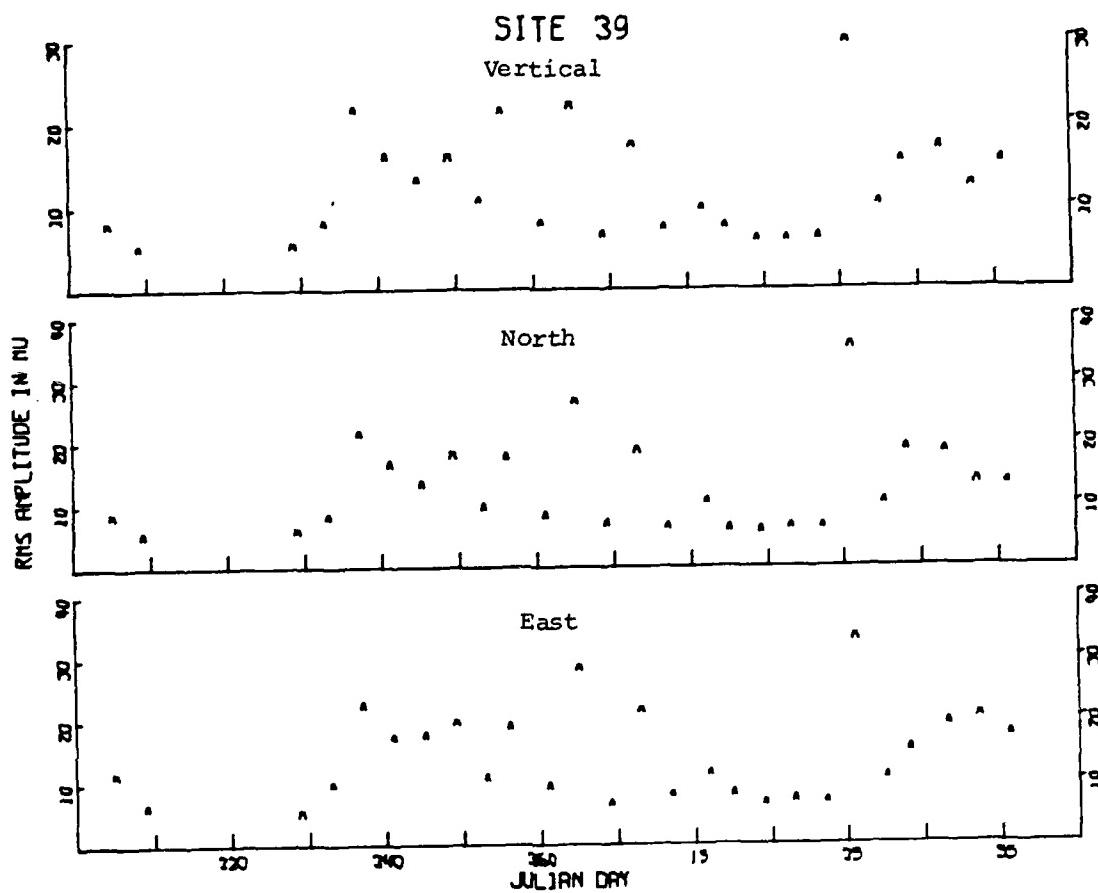
FIGURE III-15
GRFO 17-41 SECOND RMS NOISE

ENSCO, INC.   III-25

SITE 40
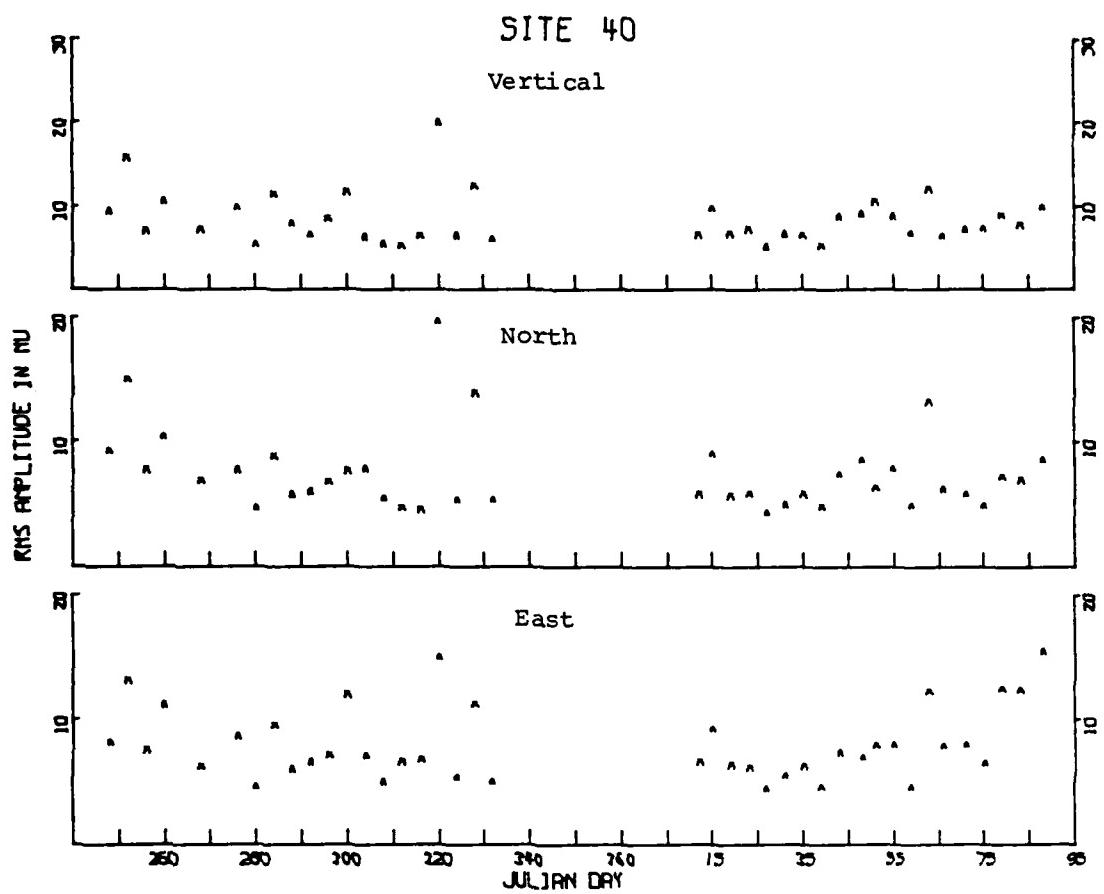
FIGURE III-16

SHIO 17-41 SECOND RMS NOISE

SITE 51
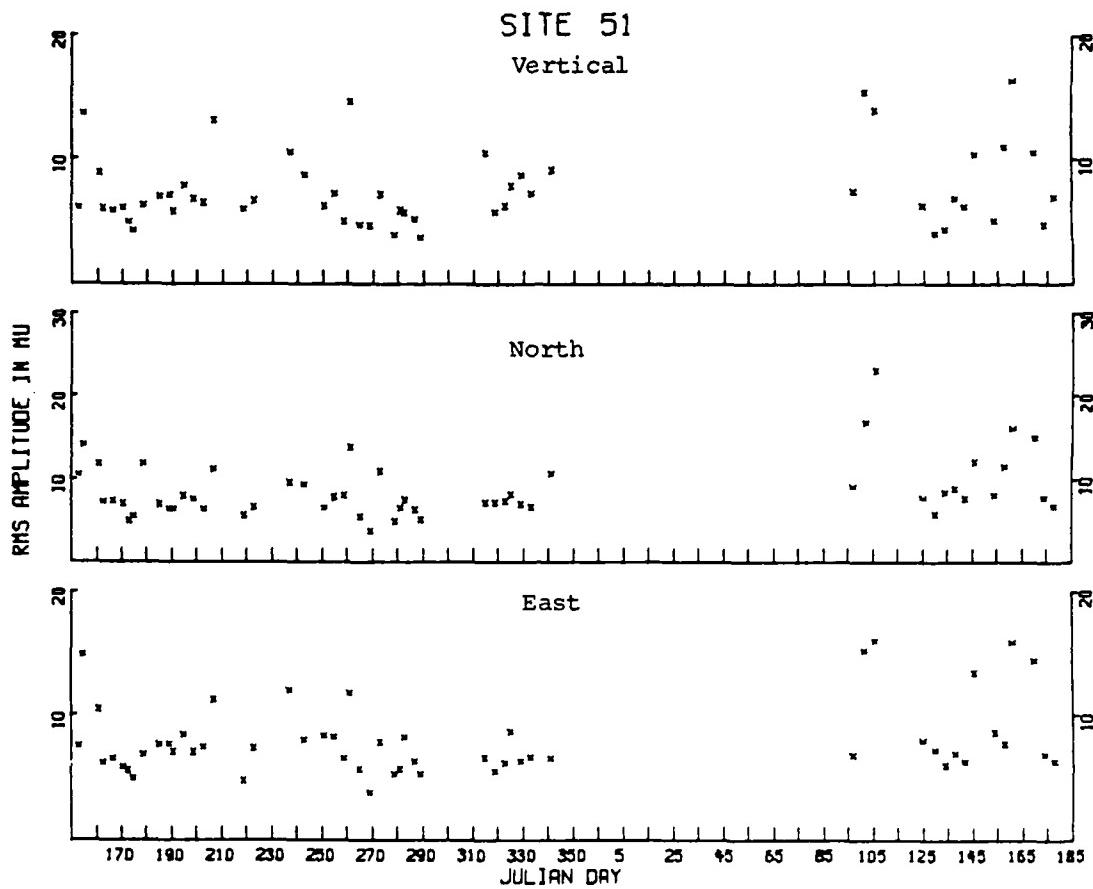
FIGURE III-17

ZOBO 17-41 SECOND RMS NOISE

ENSCO, INC.   III-27
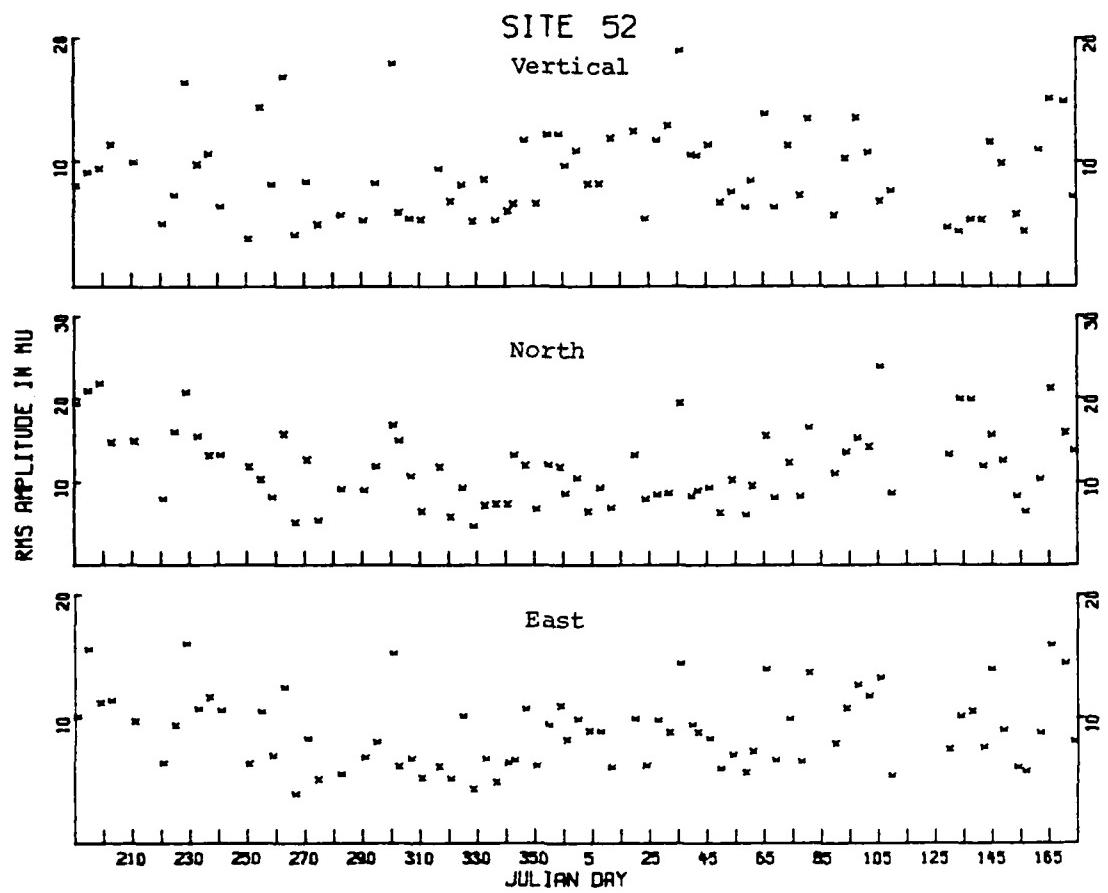
FIGURE III-18

KAAO 17-41 SECOND RMS NOISE
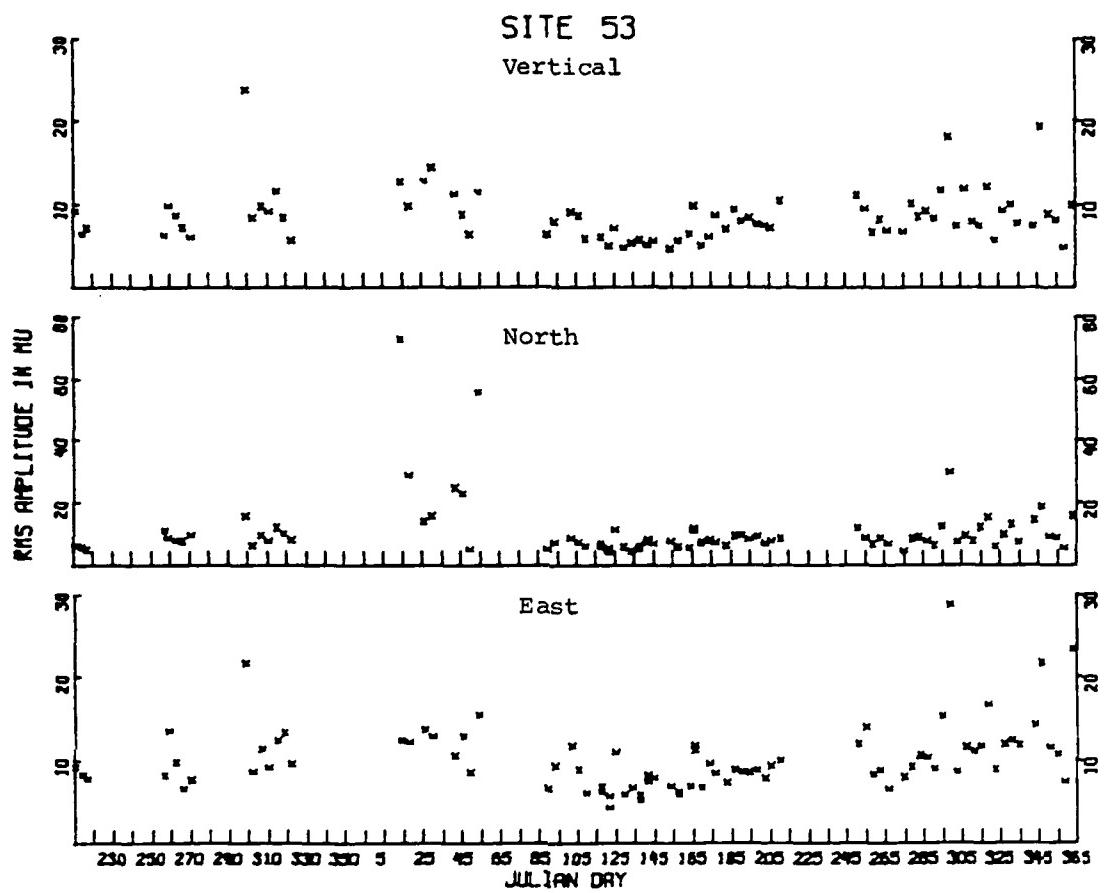
FIGURE III-19

MAJO 17-41 SECOND RMS NOISE
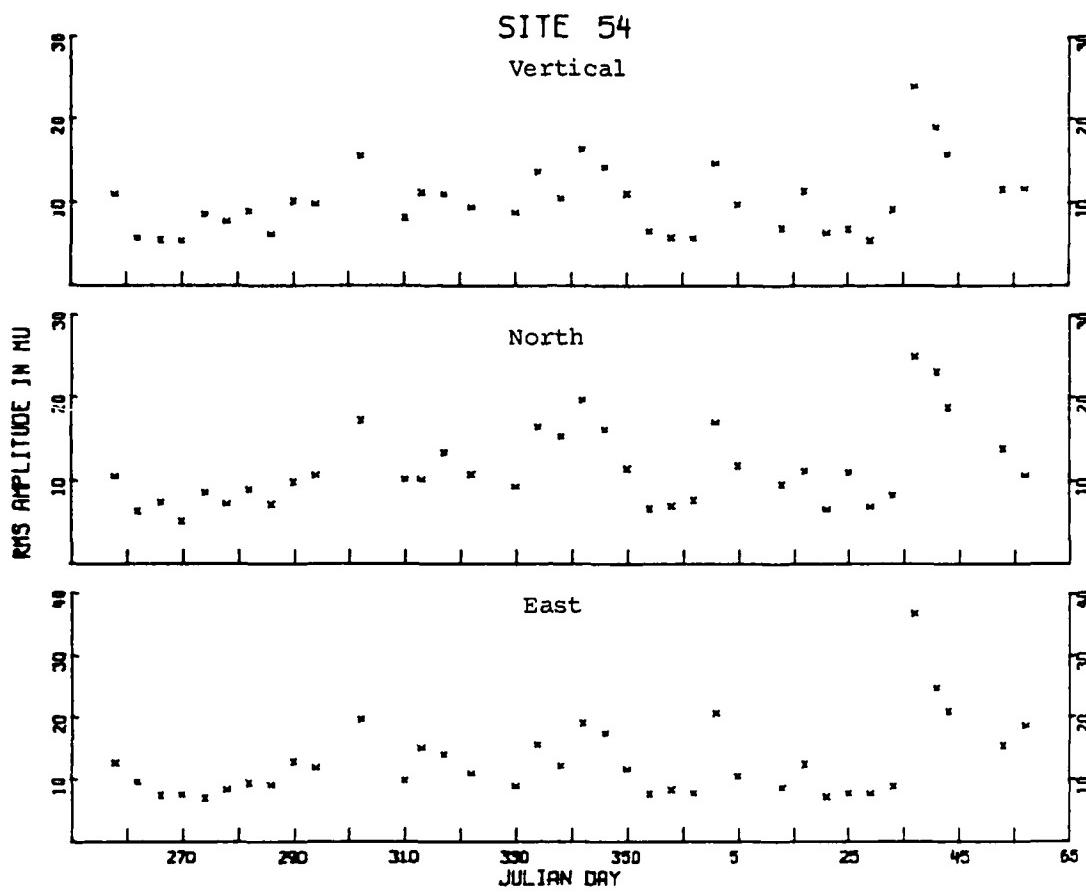
FIGURE III-20

KONO 17-41 SECOND RMS NOISE
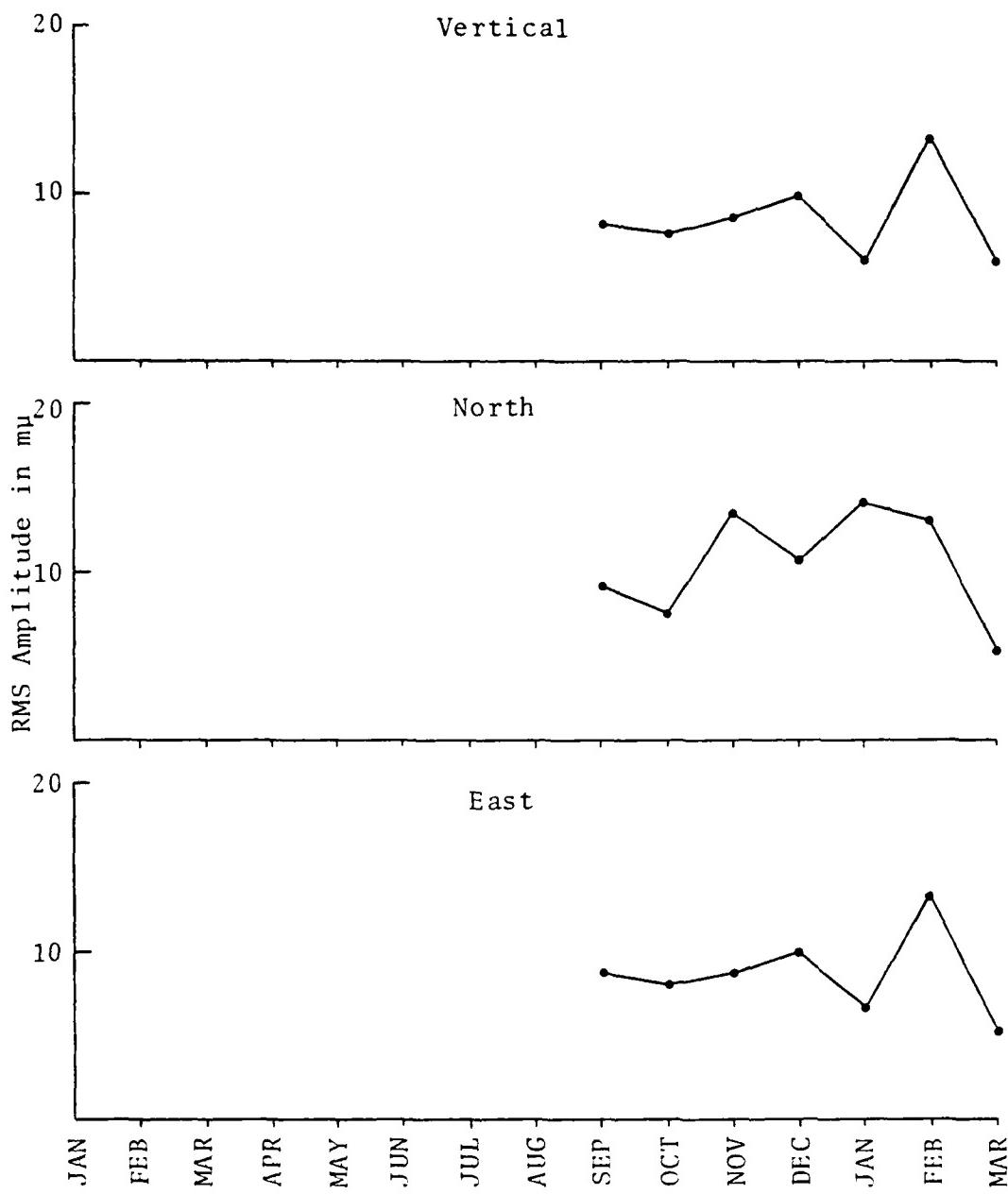
FIGURE III-21

ANTO 17-41 SECOND RMS NOISE TRENDS
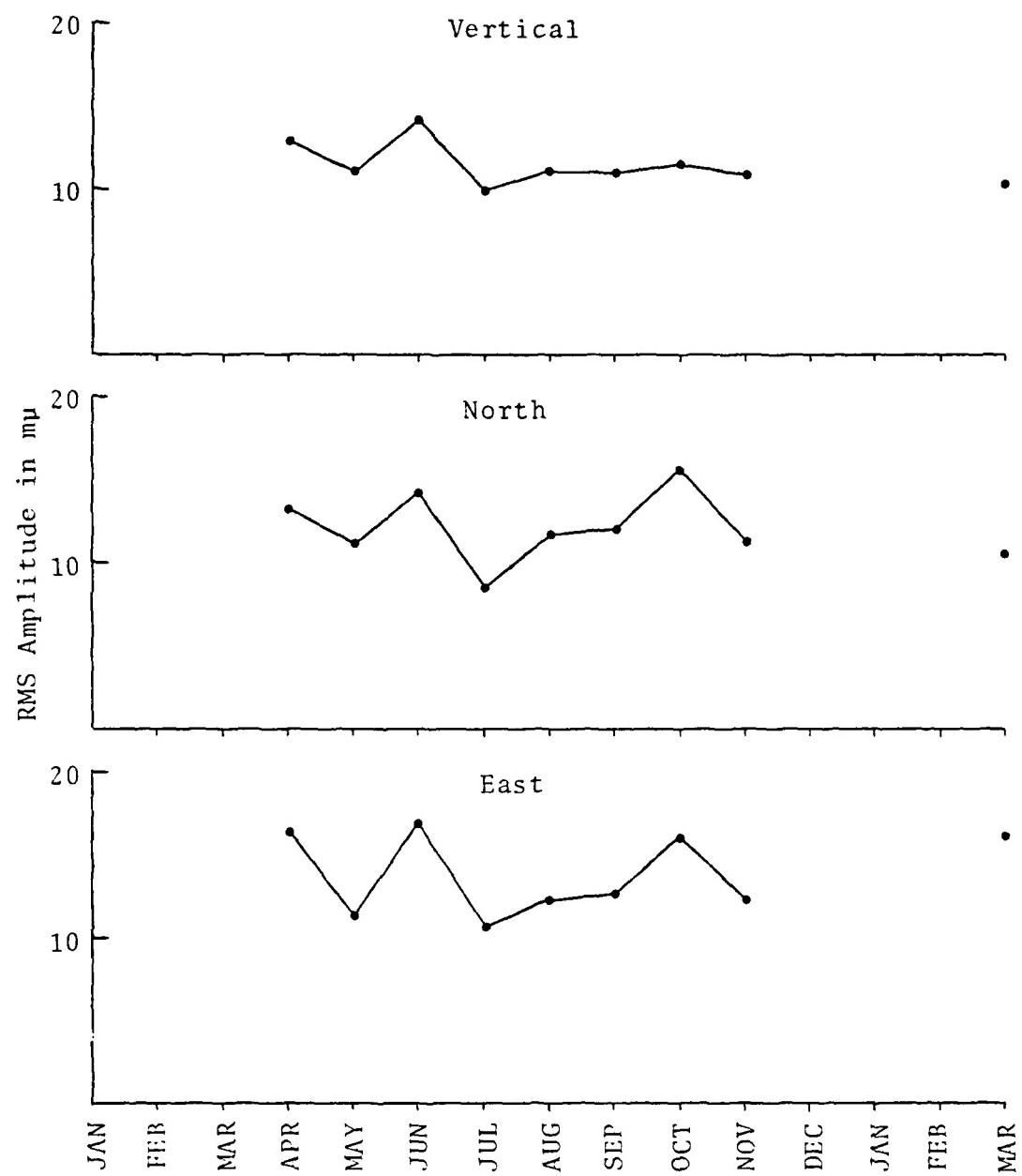
ENSCO, INC.   III-31

FIGURE III-22

BOCO 17-41 SECOND RMS NOISE TRENDS
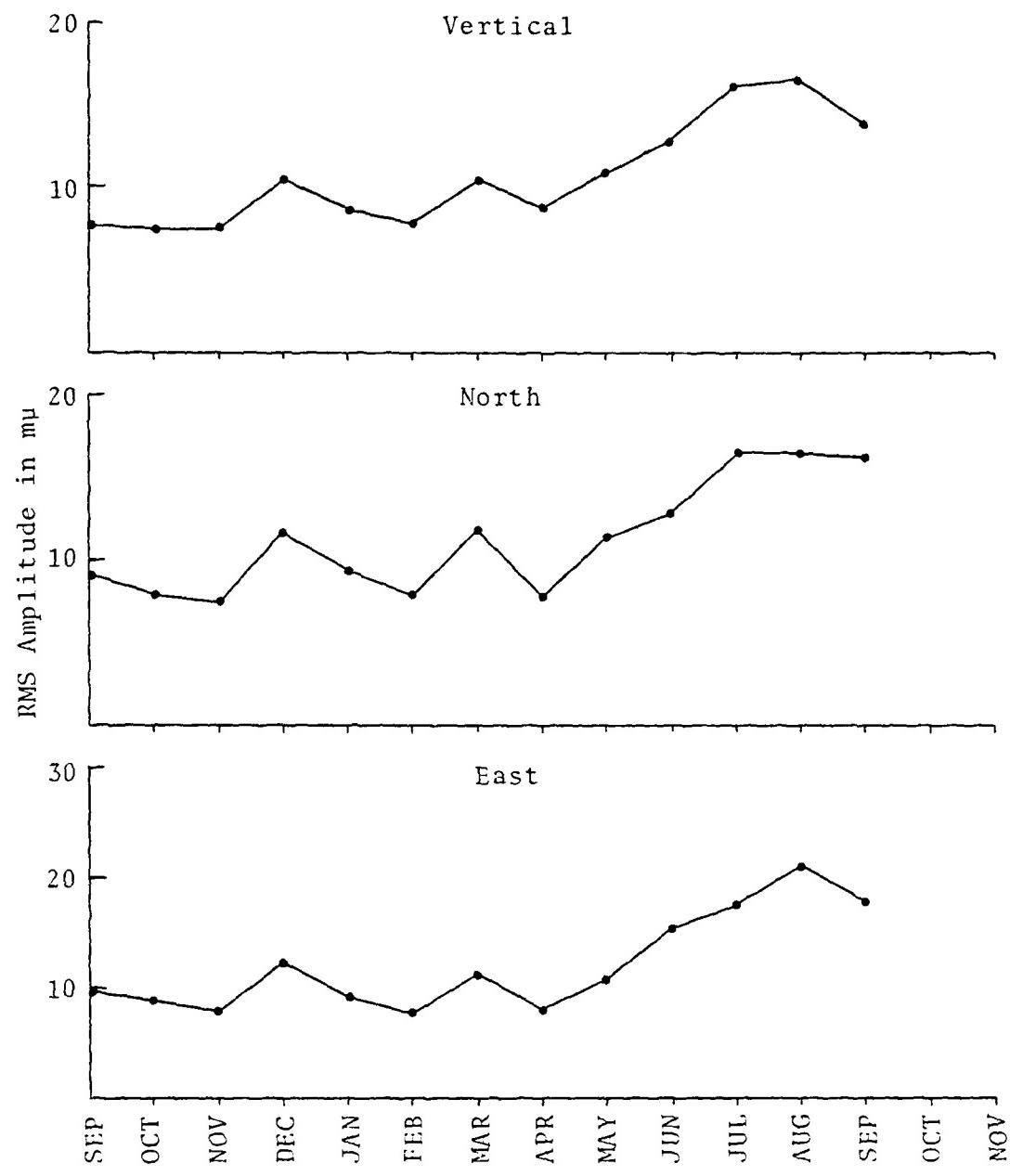
FIGURE III-23

CHTO 17-41 SECOND RMS NOISE TRENDS
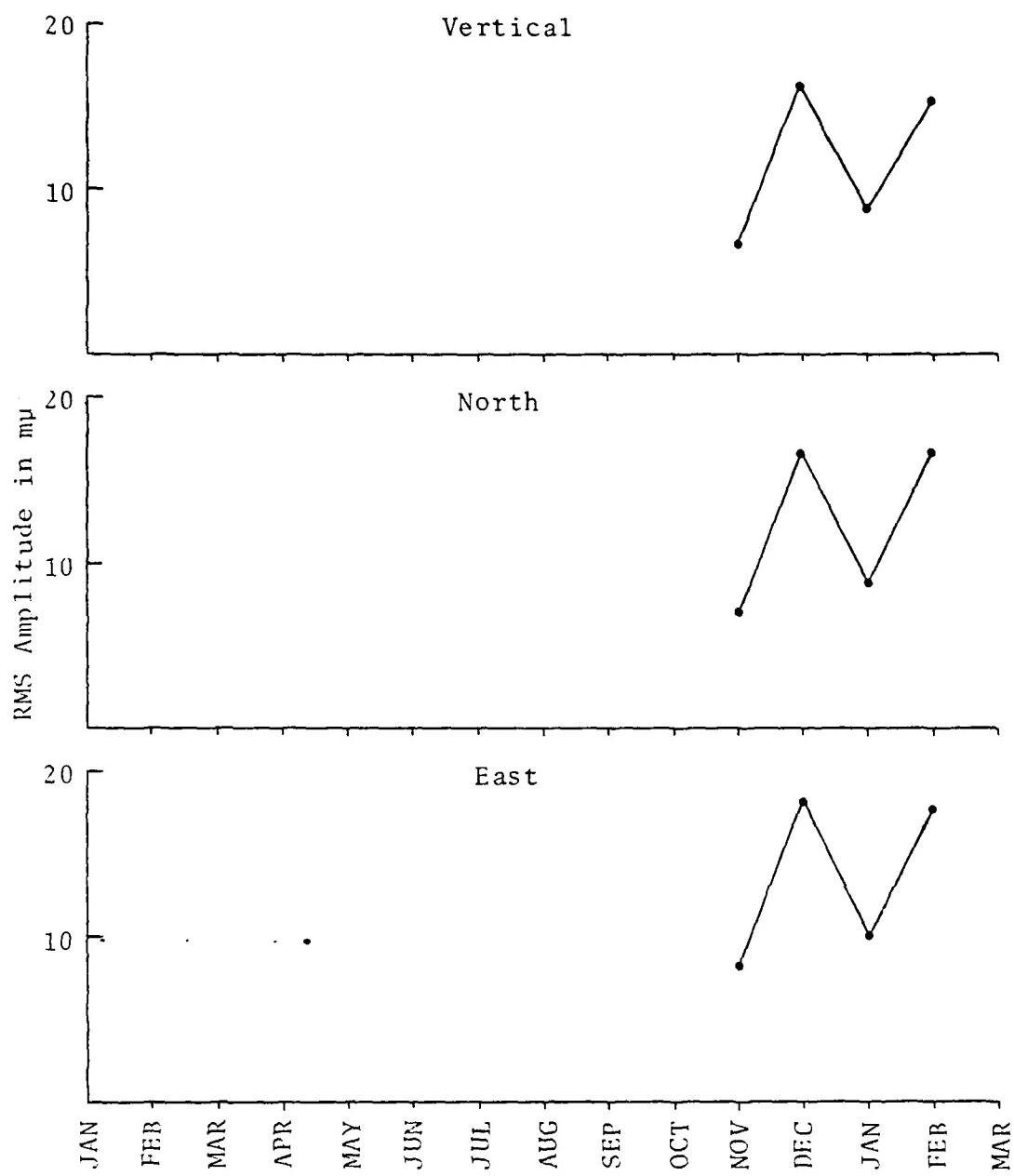
FIGURE III-24

GRFO 17-41 SECOND RMS NOISE TRENDS
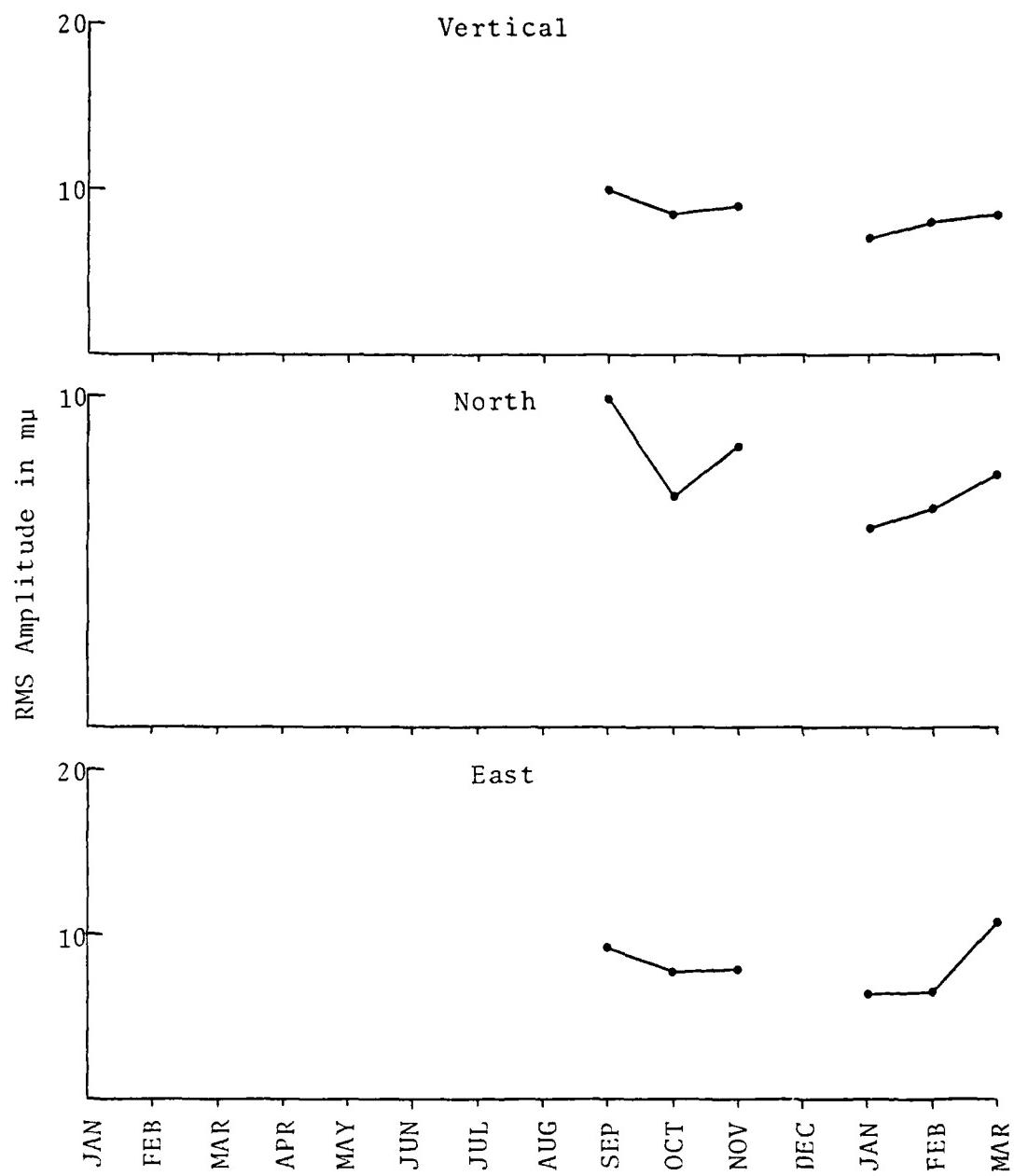
FIGURE III-25

SHIO 17-41 SECOND RMS NOISE TRENDS
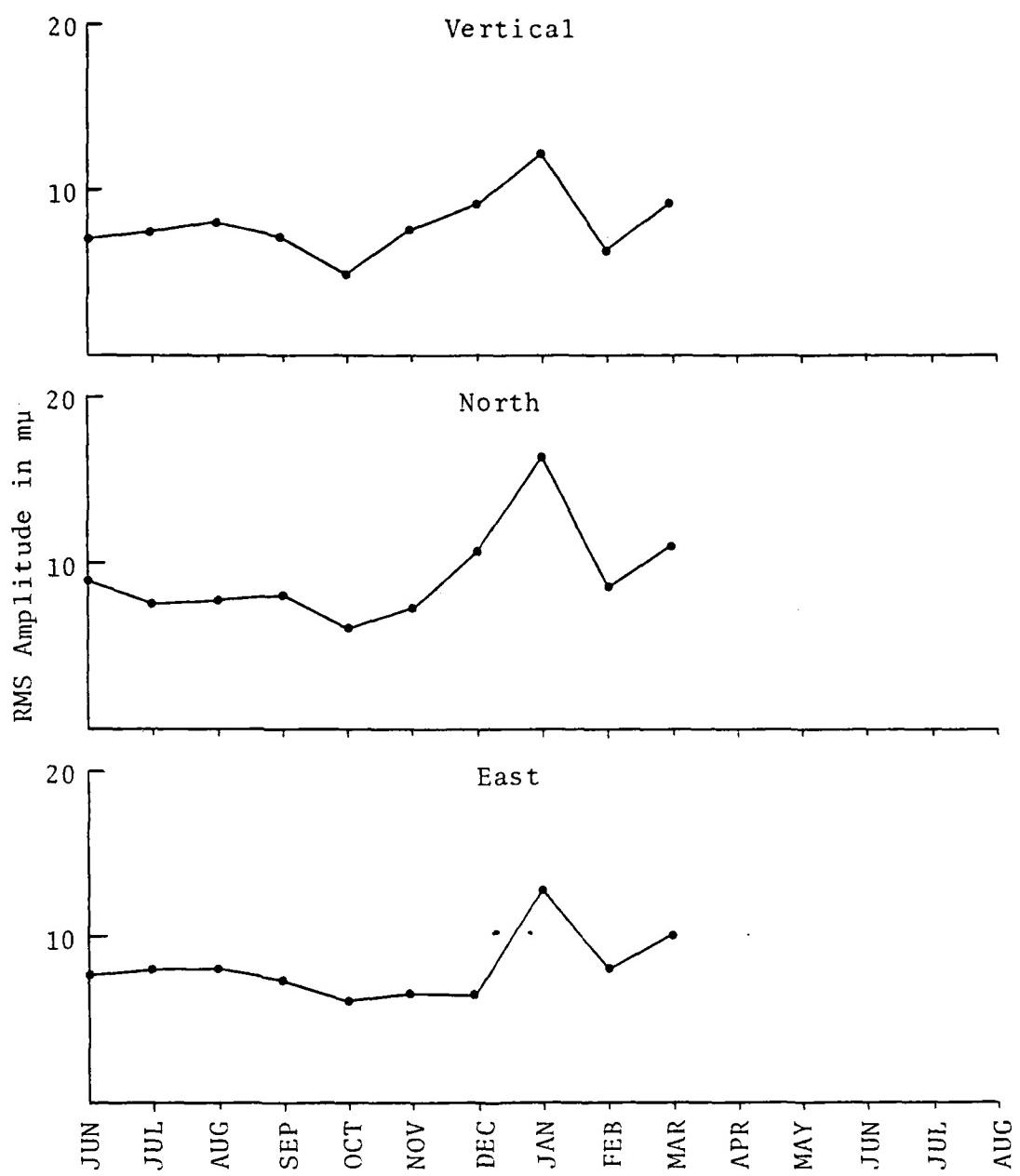
ENSCO, INC.   III-35

FIGURE III-26

ZOBO 17-41 SECOND RMS NOISE TRENDS
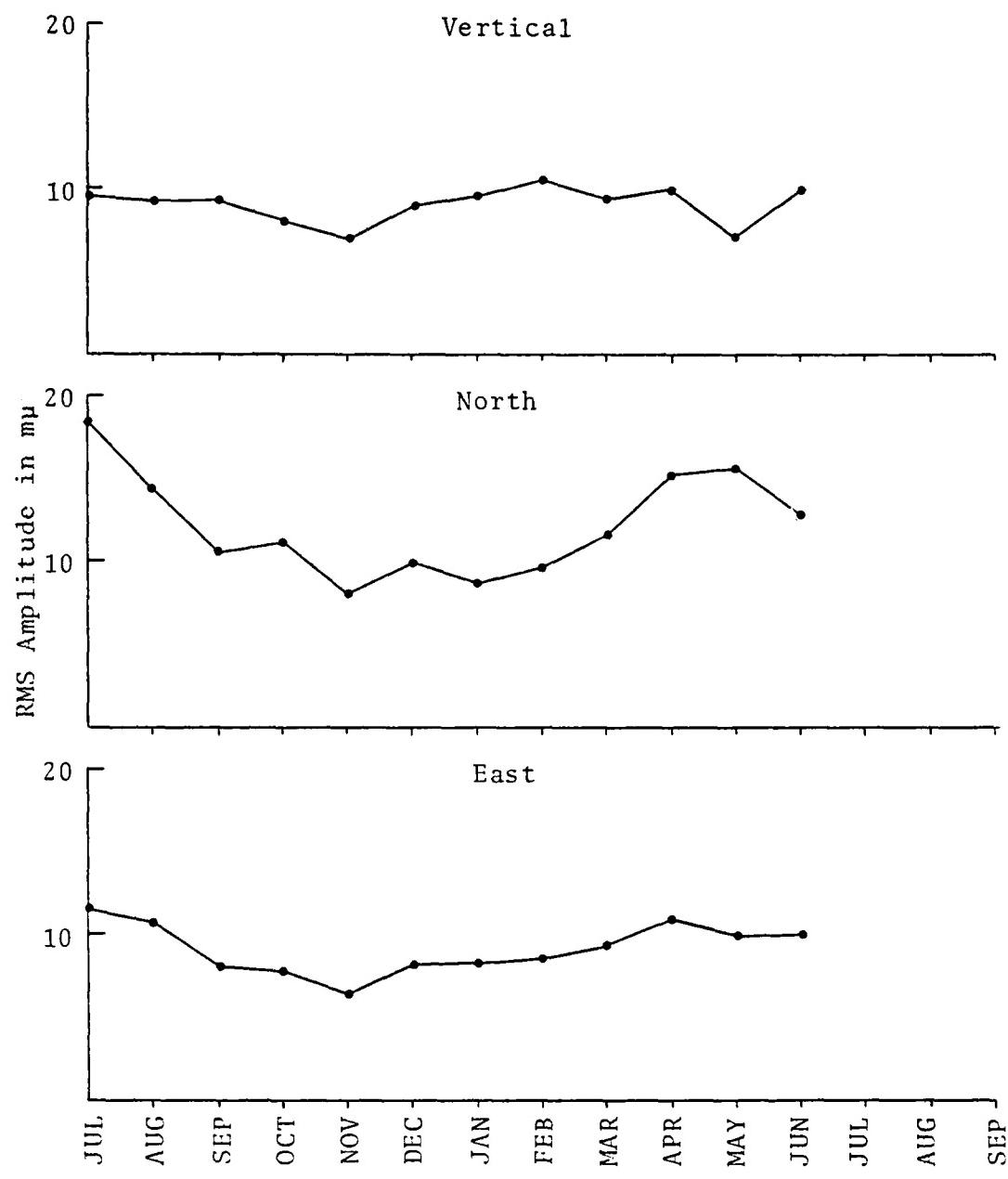
FIGURE III-27

KAAO 17-41 SECOND RMS NOISE TRENDS
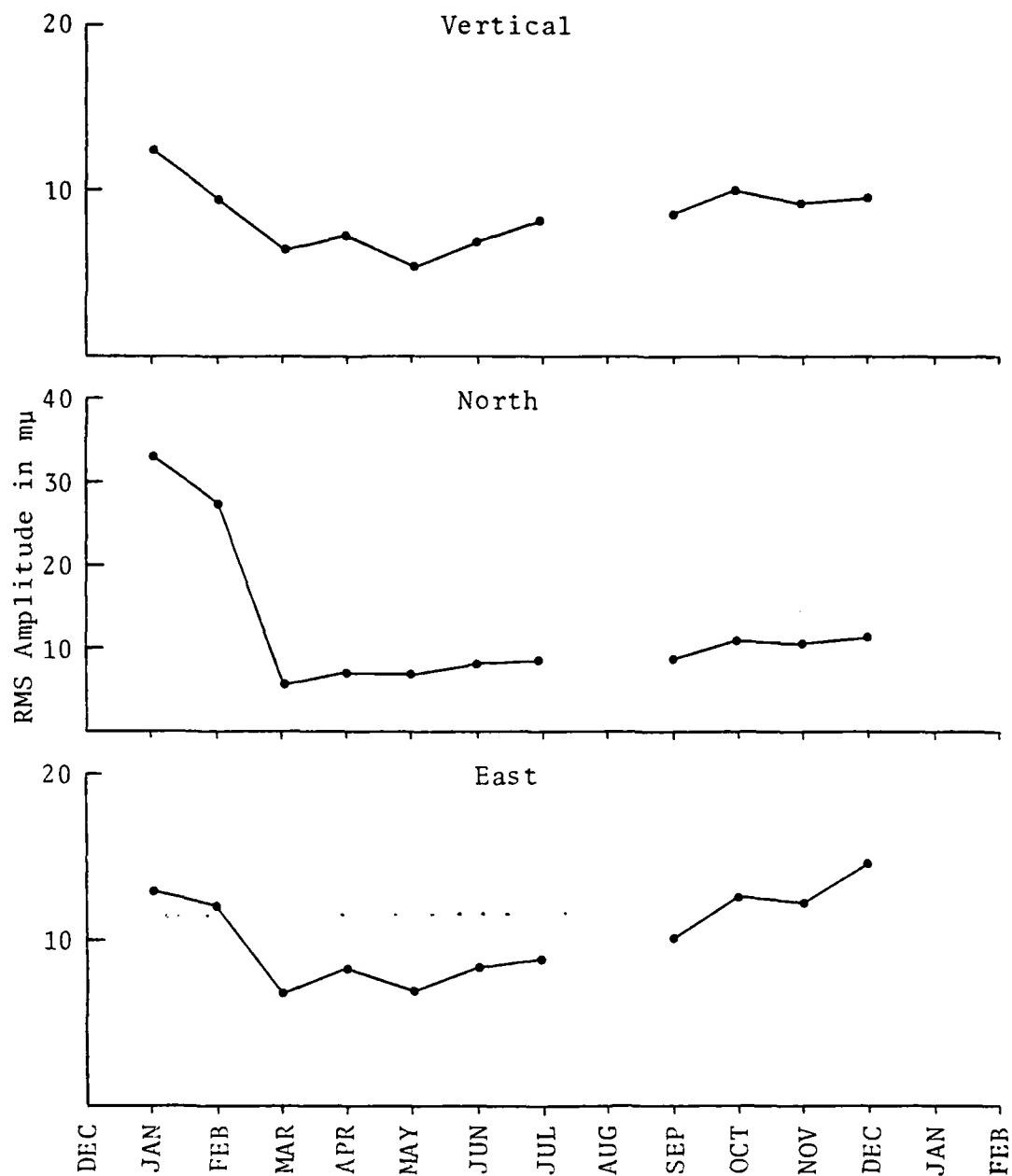
FIGURE III-28

MAJO 17-41 SECOND RMS NOISE TRENDS
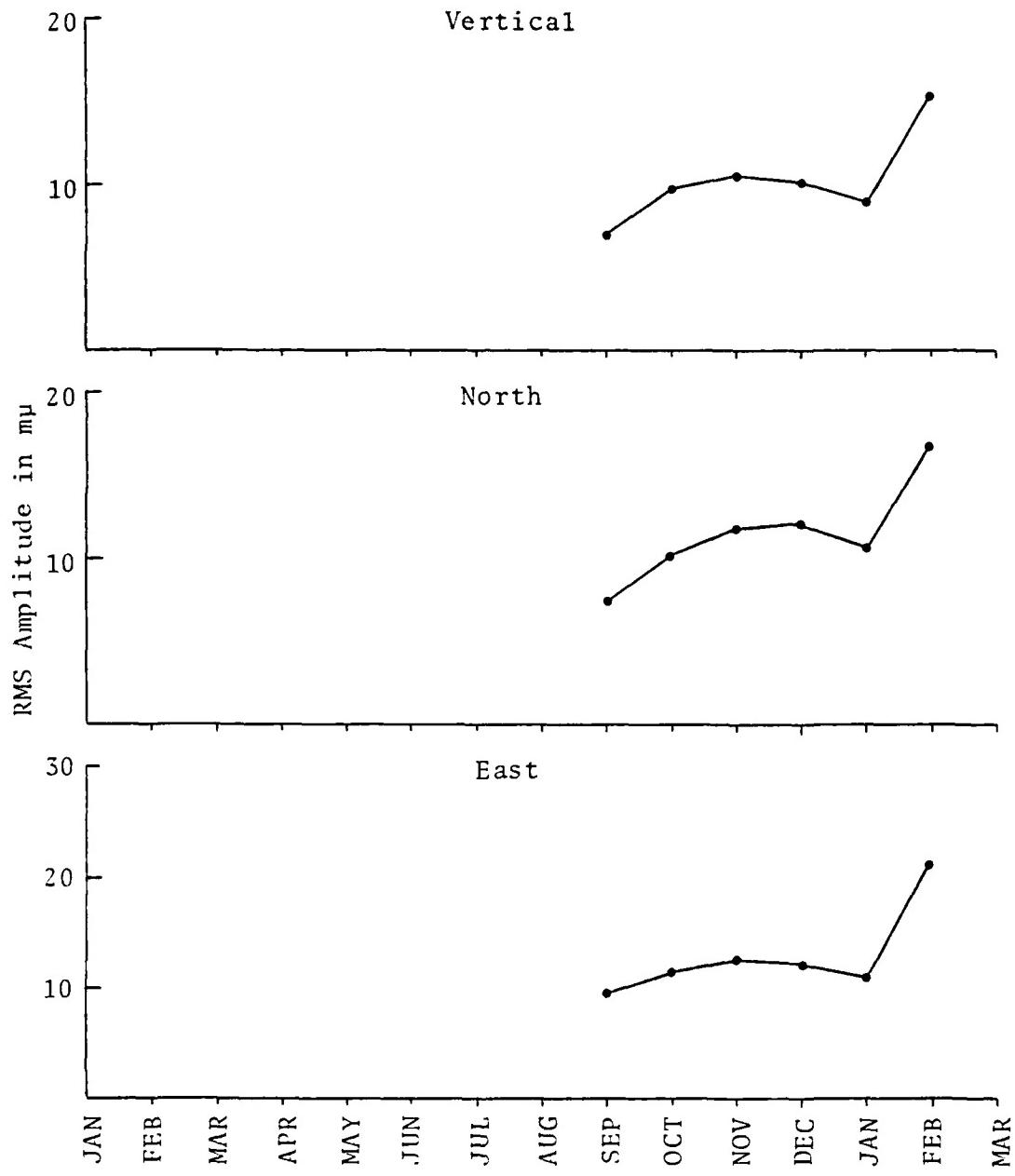
ENSCO, INC. III-38

FIGURE III-29

KONO 17-41 SECOND RMS NOISE TRENDS

ENSCO, INC.   III-39

Table III-5, contains station mean RMS noise values and
their associated standard deviations for the 17-41 second
passband. Note that the standard deviations generally in-
crease with increasing mean. The mean RMS amplitude long-
period noise spectra, Figures III-30 through III-38, display
the same characteristic. The left-hand spectra in these fig-
ures show the mean amplitudes while the right-hand spectra
show the standard deviations about those means.

The general character of a long-period noise spectrum
is that of a peak and a trough at approximately 16 and 27
seconds period, respectively, followed by an almost continu-
ous amplitude increase at longer periods (Fix, 1972; and
others). This description generally fits the spectra which
are presented here, with the following exceptions. The
north-south component at station ANTO displayed a spectrum
which is unlike those of the other components. This is
caused by an intermittent rise in the noise level on that
component only, and suggests a hardware problem. The unchar-
acteristic noise spectra which represented station BOCO are
caused by degradation of the data (also hardware related as
described in Section II).

Peak 25 $\pm$ 2 second noise amplitudes were measured on
all long-period noise samples. Each peak measured represent-
ed the largest absolute value zero-to-peak excursion of a
waveform within the given period range.   bles III-6 and
III-7 list the means and standard deviations of the peak and
log peak measured amplitudes. Note that there is little cor-
relation between instrument type and long-period noise level
as evidenced by RMS level and peak amplitude measurements.
These long-period peak noise measurements are used in

TABLE III-5

MEAN 17-41 SECOND RMS NOISE AMPLITUDES IN MILLIMICRONS (mμ)

Station	Vertical		North		East	
	Mean	S.D.*	Mean	S.D.*	Mean	S.D.*
ANTO	8.37	4.88	8.62	4.31	16.42	40.50
BOCO	13.50	16.00	20.02	48.89	14.60	19.13
CHTO	11.13	6.30	12.93	7.35	11.87	6.49
GRFO	12.48	6.38	14.36	7.34	13.05	7.41
SHIO	8.42	3.01	8.08	2.94	7.50	3.18
ZOBO	7.57	3.07	8.06	2.97	8.75	3.53
KAAO	9.06	3.51	9.05	3.02	11.86	4.56
MAJO	8.40	3.22	10.20	4.08	10.85	9.75
KONO	10.34	4.23	12.94	6.17	11.59	4.84

*S.D. = Standard Deviation

SITE 31
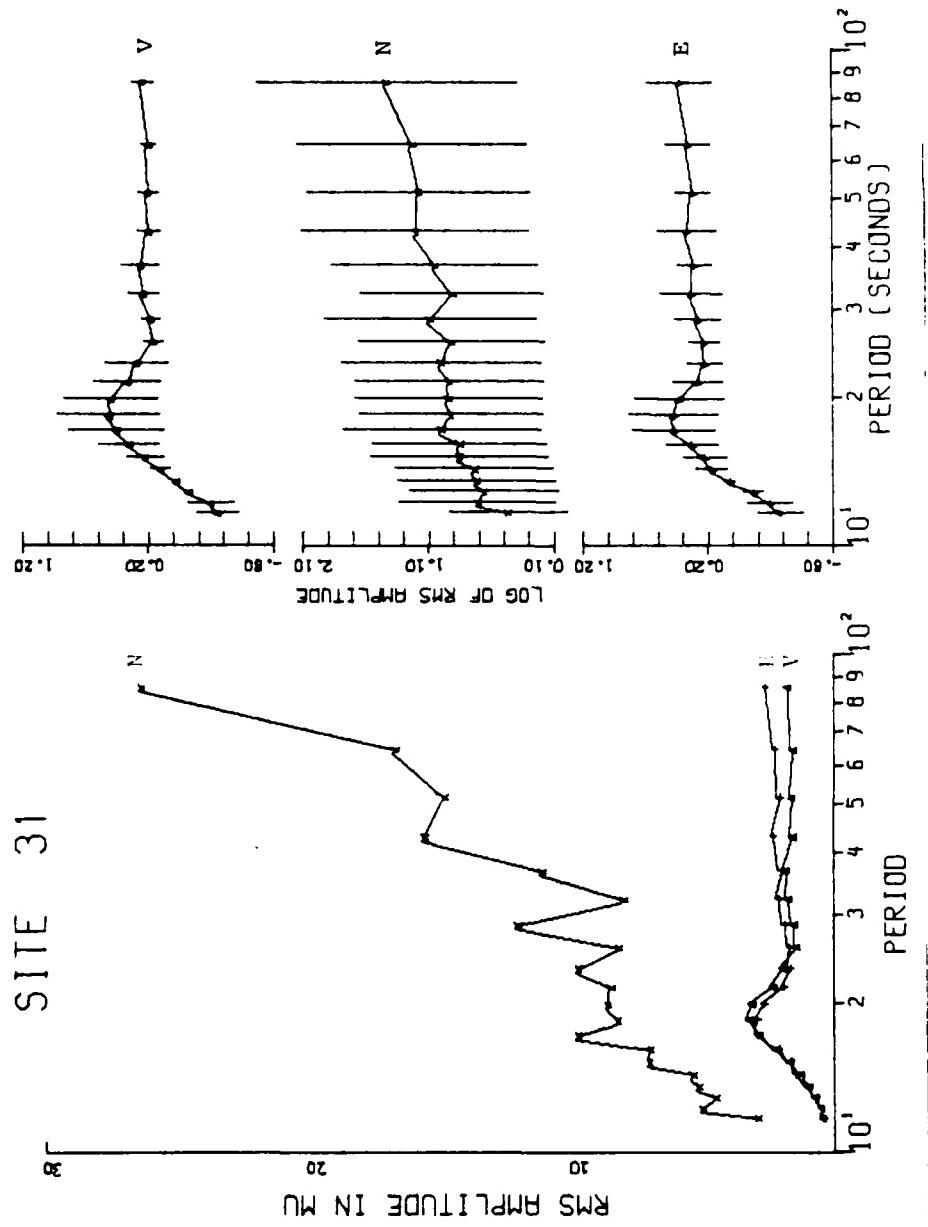
FIGURE III-30

AVERAGE RMS AMPLITUDE SPECTRA - ANTO LONG-PERIOD NOISE
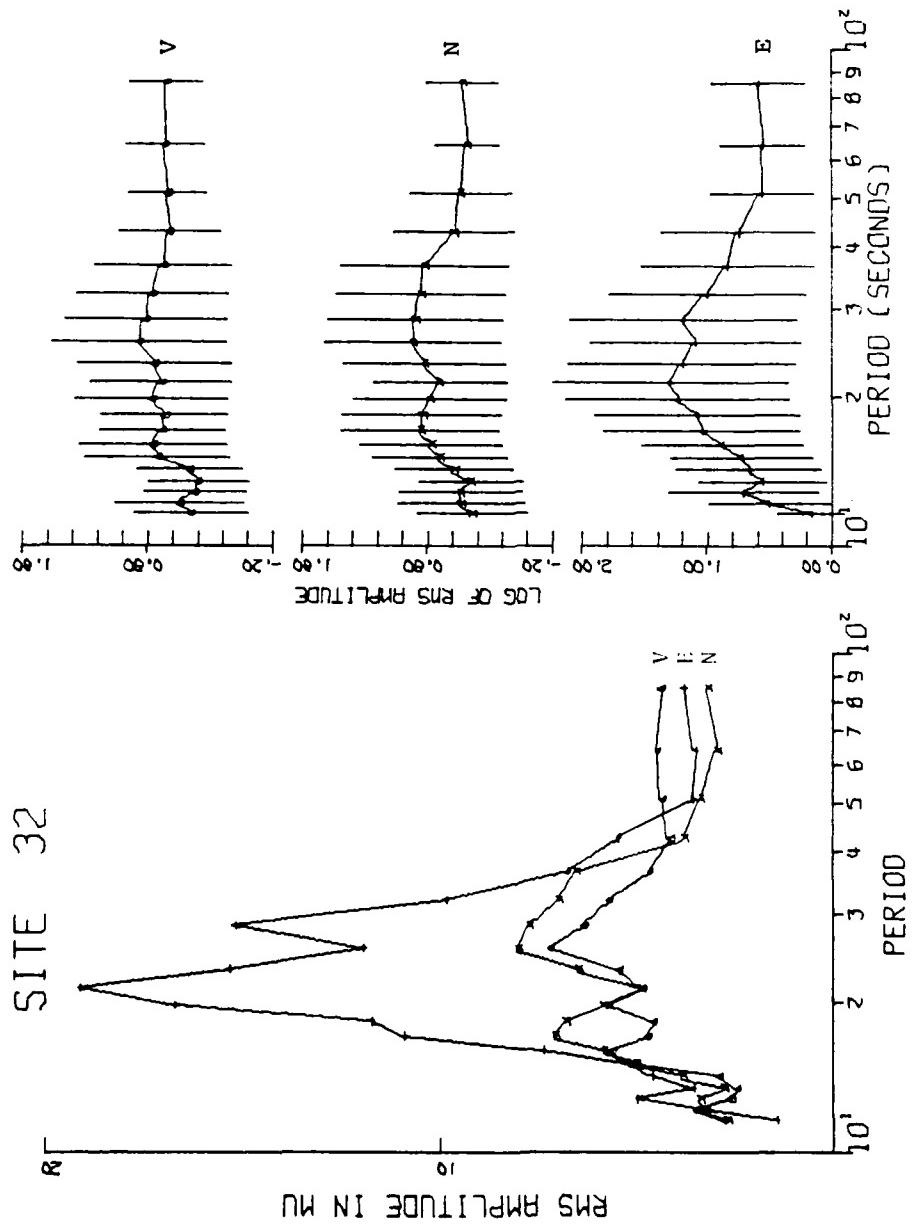
FIGURE III-31

AVERAGE RMS AMPLITUDE SPECTRA - BOCO LONG-PERIOD NOISE

SITE 33
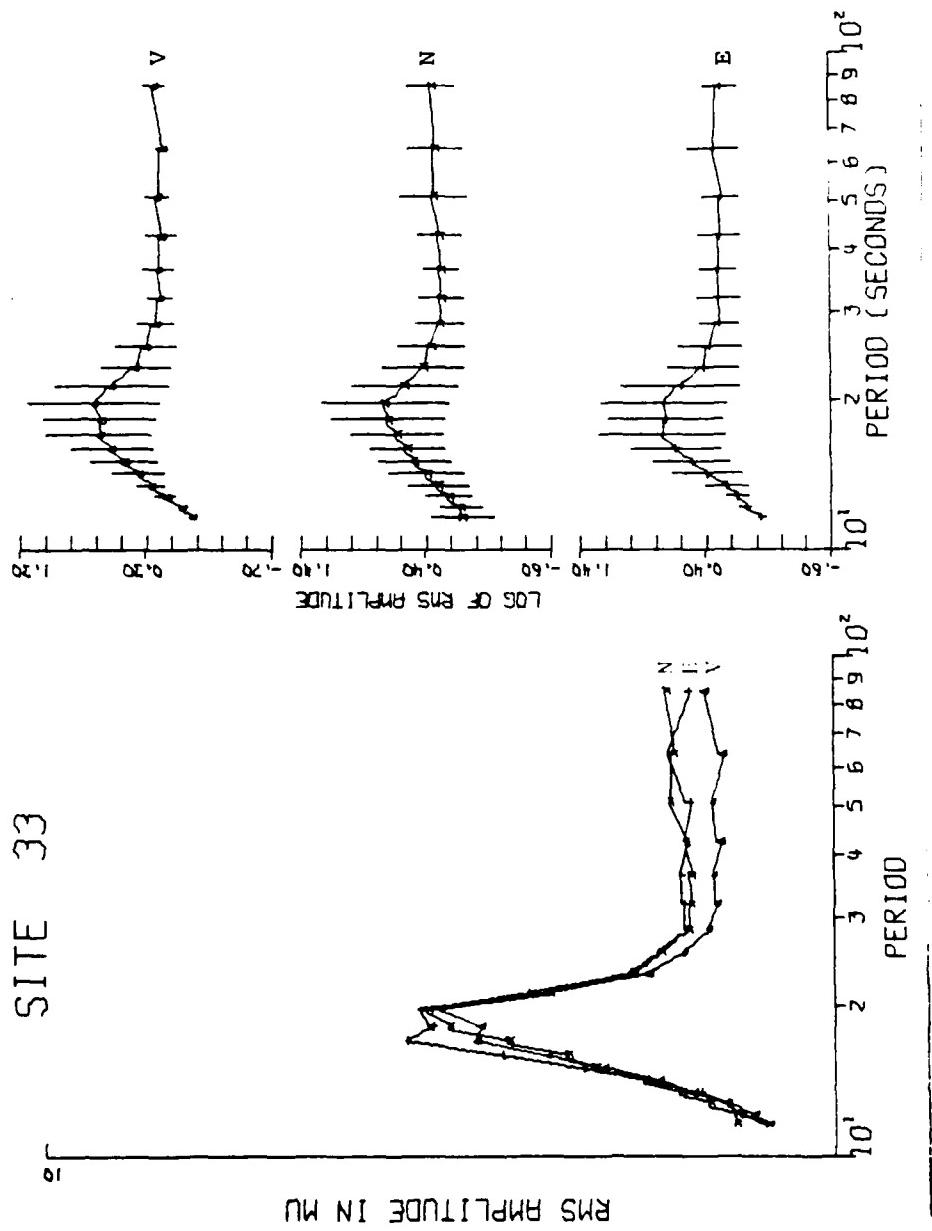
FIGURE III-32

AVERAGE RMS AMPLITUDE SPECTRA - CIITO LONC-PERIOD NOISE

SITE 39
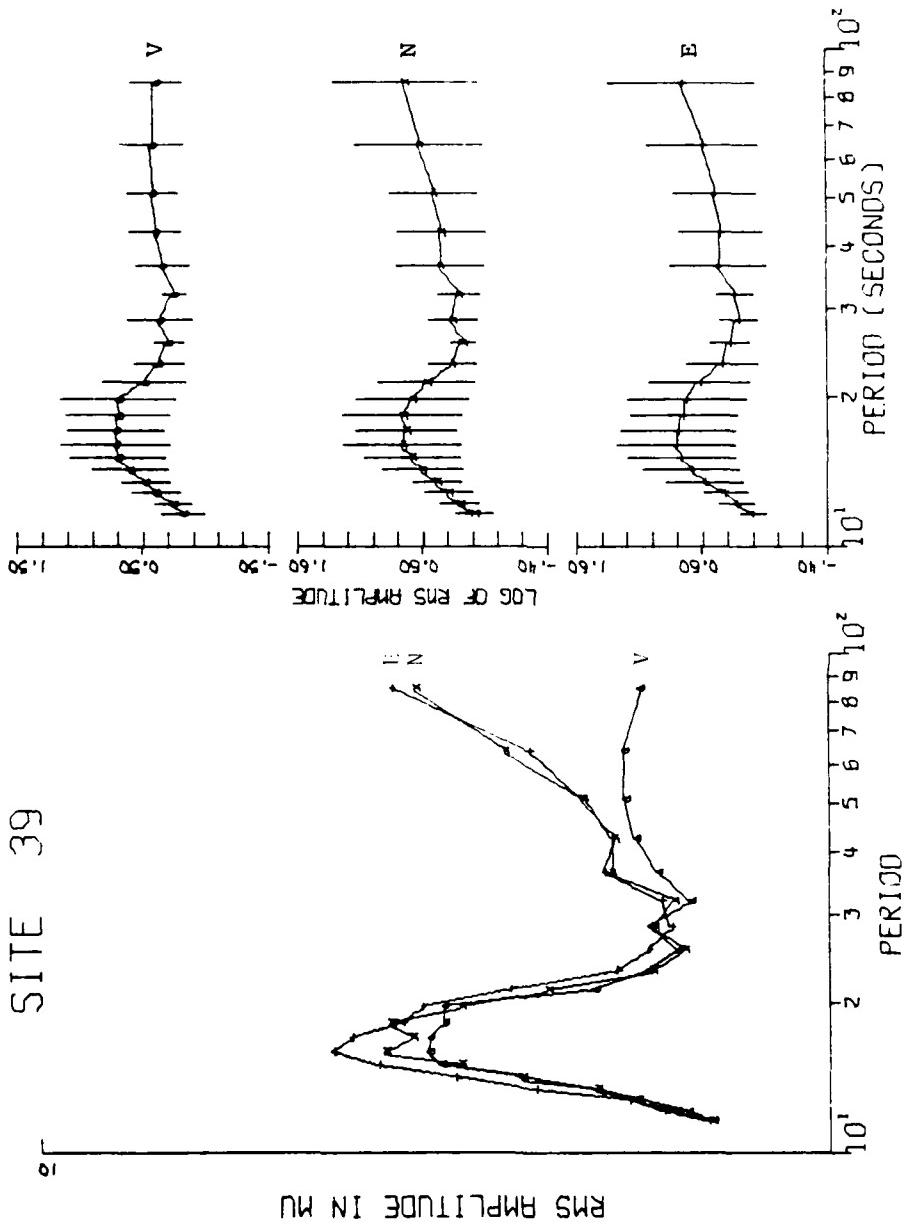
FIGURE III-33

AVERAGE RMS AMPLITUDE SPECTRA - GRFO LONG-PERIOD NOISE
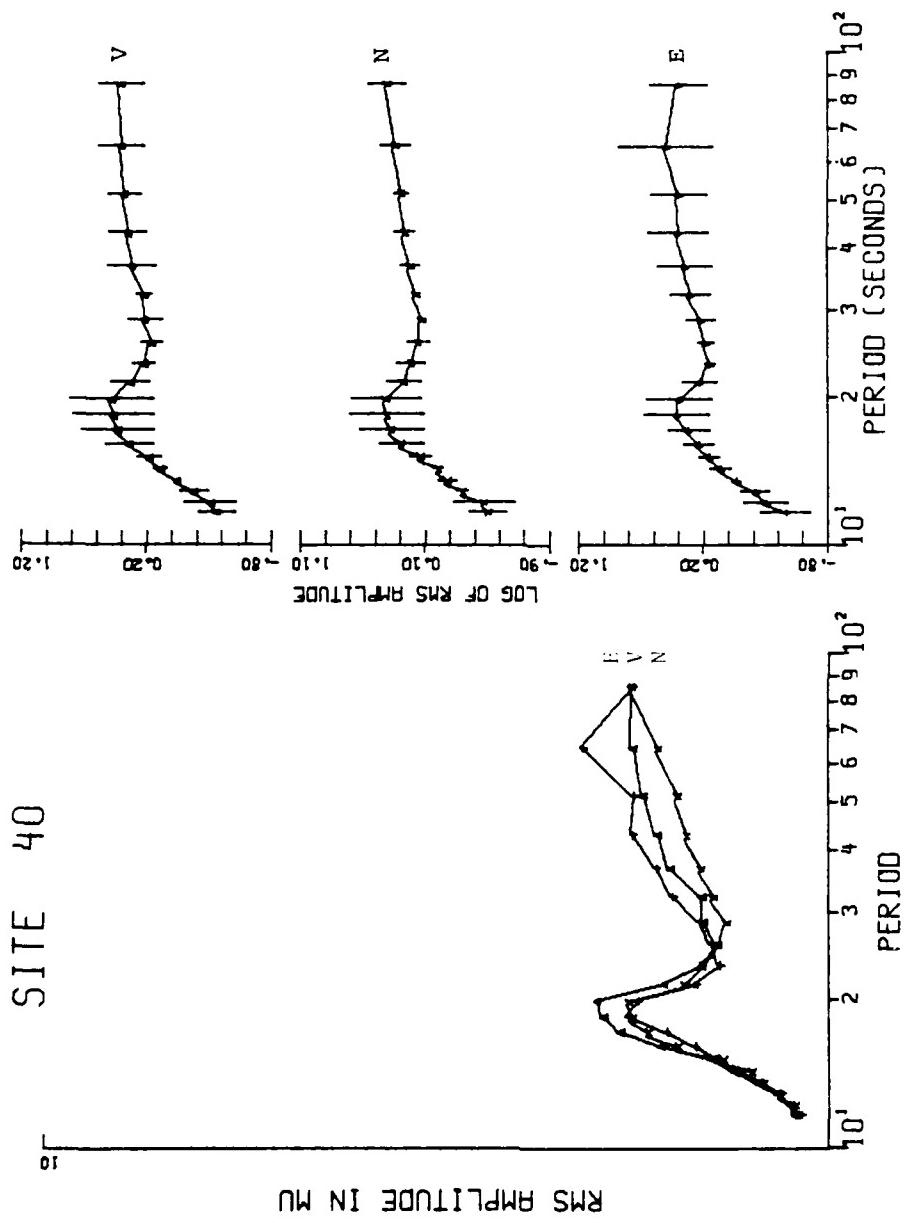
FIGURE III-34

AVERAGE RMS AMPLITUDE SPECTRA - SII1O LONG-PERIOD NOISE

SITE 51
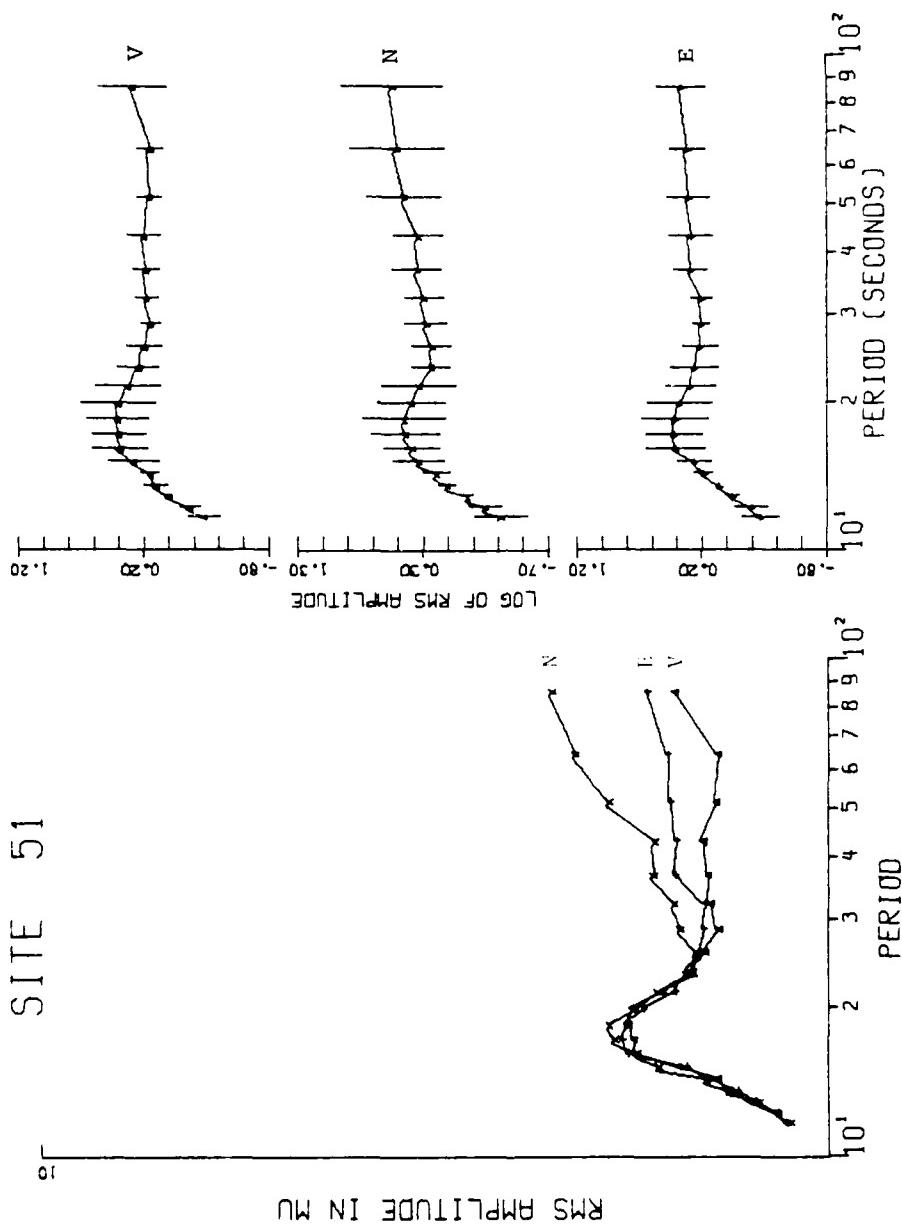
FIGURE III-35

AVERAGE RMS AMPLITUDE SPECTRA - ZOBO LONG-PERIOD NOISE
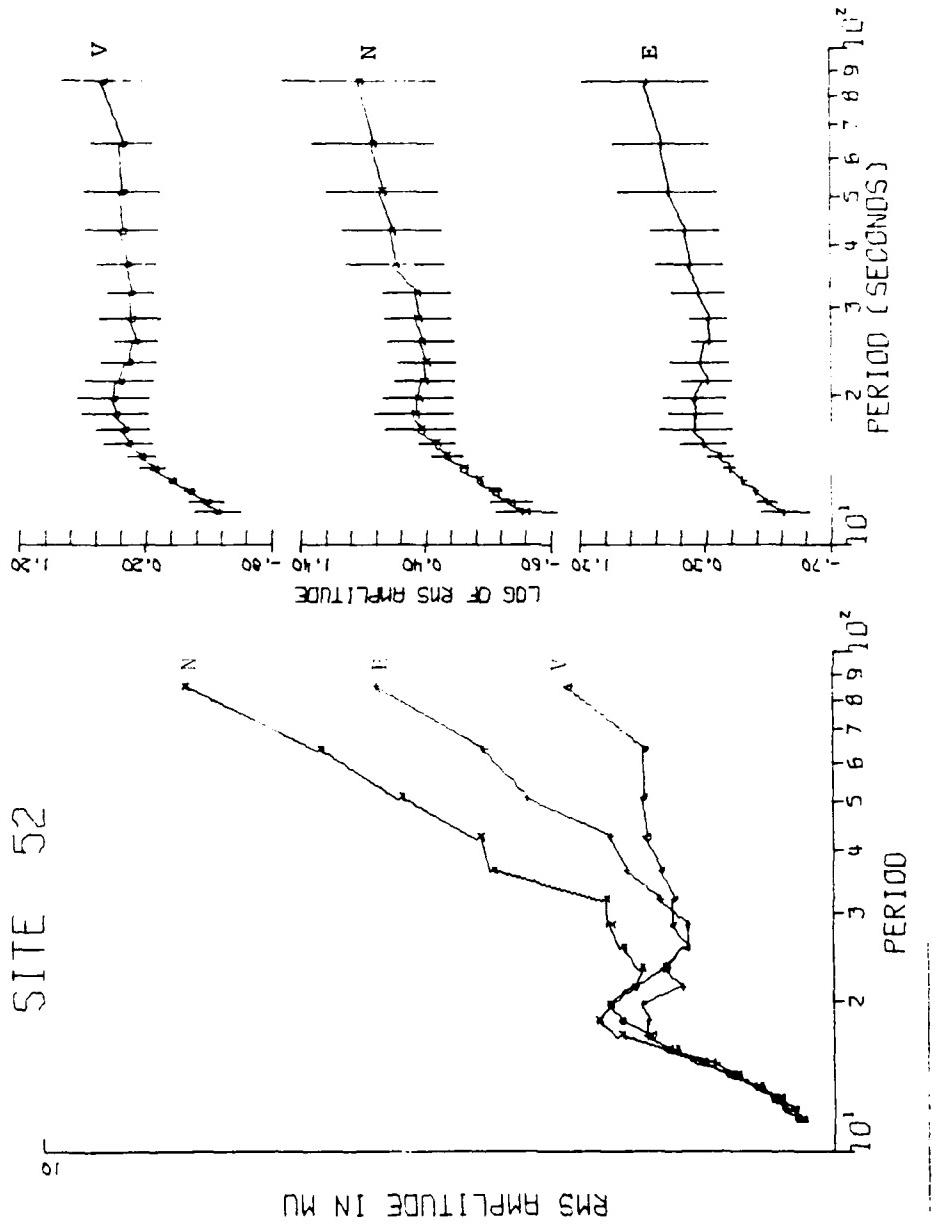
FIGURE III-36

AVERAGE RMS AMPLITUDE SPECTRA - KAAO LONG-PERIOD NOISE
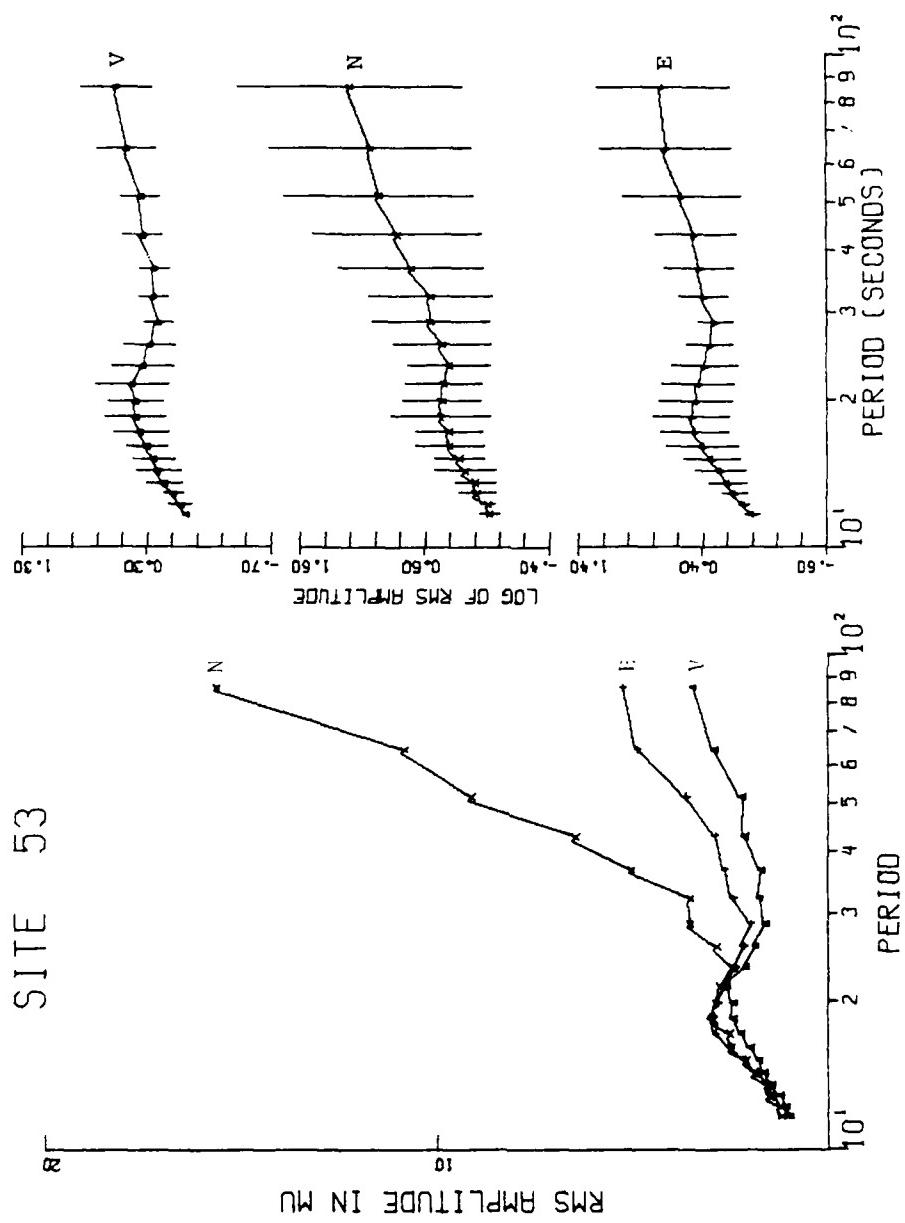
FIGURE III-37

AVERAGE RMS AMPLITUDE SPECTRA - MAJO LONG-PERIOD NOISE

SITE 54

RMS AMPLITUDE IN MU

PERIOD

LOG OF RMS AMPLITUDE
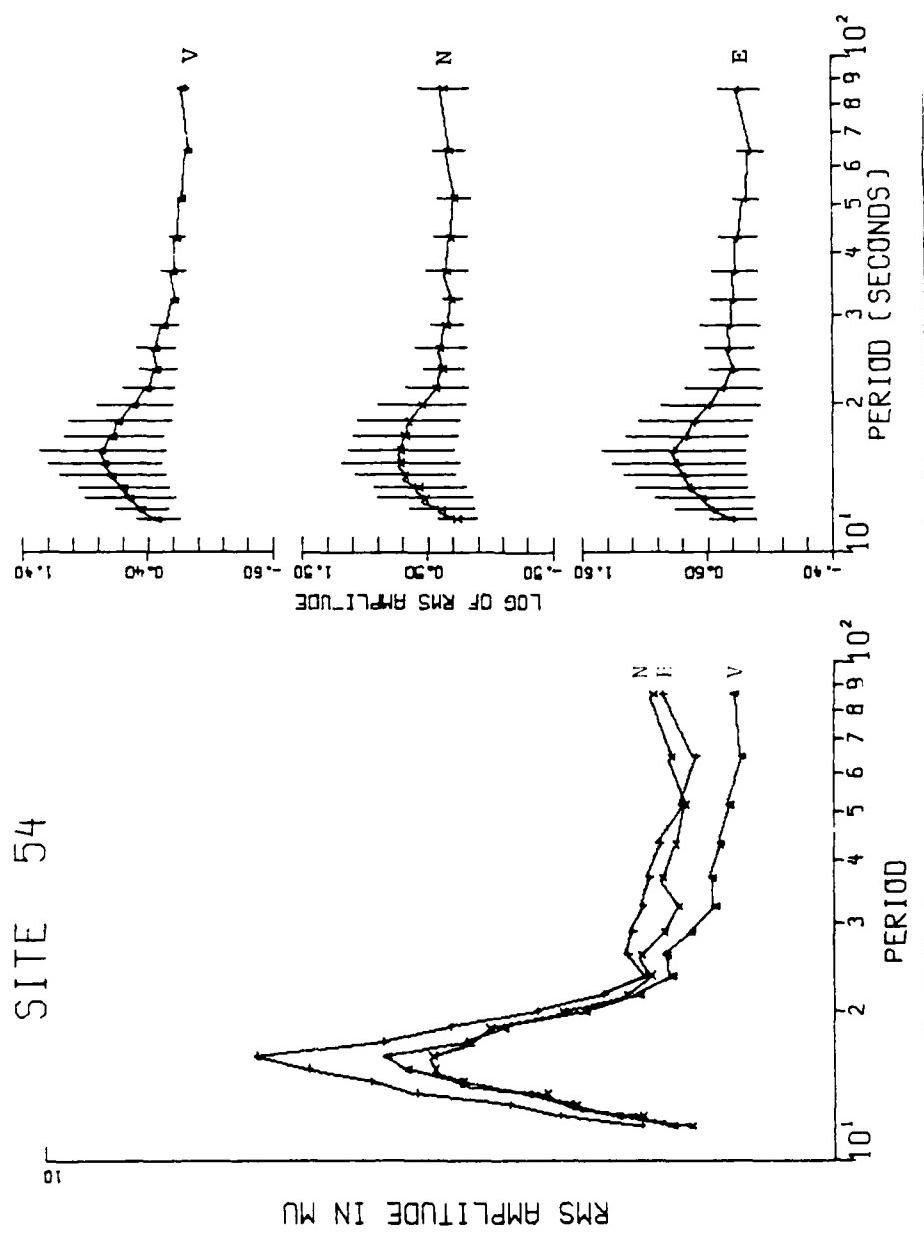
PERIOD (SECONDS)

FIGURE III-38

AVERAGE RMS AMPLITUDE SPECTRA - KONO LONG-PERIOD NOISE

TABLE III-6

MEAN PEAK 25 SECOND NOISE AMPLITUDES IN MILLIMICRONS (mµ)

Station	Vertical		North		East	
	Mean	S.D.*	Mean	S.D.*	Mean	S.D.*
ANTO	19.42	7.38	22.04	7.70	54.55	160.32
BOCO	48.25	126.66	116.25	611.00	55.32	201.32
CHTO	21.21	12.22	26.46	13.38	23.66	12.21
GRFO	28.25	10.68	30.21	13.48	30.01	12.94
SHIO	22.81	6.27	23.56	9.82	20.56	5.83
ZOBO	18.43	7.75	20.18	6.00	23.01	9.03
KAAO	22.73	9.22	23.90	8.51	29.84	11.84
MAJO	22.65	8.01	34.18	44.03	23.33	9.11
KONO	24.54	9.16	33.35	11.86	30.14	9.64

*S.D. = Standard Deviation

ENSCO, INC.   III-51

TABLE III-7

MEAN $\log_{10}$ PEAK 25 SECOND NOISE AMPLITUDES IN MILLIMICRONS (mμ)

Station	Vertical		North		East	
	Mean	S.D.*	Mean	S.D.*	Mean	S.D.*
ANTO	1.26	0.15	1.32	0.14	1.44	0.34
BOCO	1.50	0.24	1.52	0.33	1.45	0.28
CHTO	1.28	0.20	1.38	0.18	1.33	0.20
GRFO	1.42	0.16	1.45	0.17	1.44	0.18
SHIO	1.34	0.14	1.30	0.17	1.30	0.12
ZOBO	1.24	0.16	1.29	0.12	1.33	0.15
KAAO	1.32	0.17	1.35	0.15	1.44	0.18
MAJO	1.33	0.15	1.44	0.22	1.34	0.15
KONO	1.36	0.14	1.50	0.14	1.46	0.15

*S.D. = Standard Deviation

Section V in an estimate of theoretical network detection
capability.

SECTION IV
SRO/ASRO DETECTION CAPABILITY

A. DISCUSSION

The SRO/ASRO detection capability statistics for six new stations are presented in this section: ANTO, BOCO, GRFO, SHIO, ZOBO, and KONO. For any given event, only one to five conditions can exist:

- Event is detected.

- Event is not detected.

- Event is mixed.

- No data are recorded for the time period.

- Equipment is malfunctioning.

A mixed event is one that is partially or completely masked by another signal. This occurs when two events arrive at a station at essentially the same time, or when a larger signal arrives before the signal of interest, burying the event in the former's coda. The cause of no data being recorded is simply the 'shutting down' of the station. Malfunctions refer to the partial failure of the system (i.e., a malfunction anywhere in the chain from the sensor unit to the reception of data at the Seismic Data Analysis Center) which causes degradation of the data.

In its simplest form, a station's detection capability would be determined by whether the analyst either saw the

ENSCO, INC. IV-1

event of interest or seismic noise. However, a better estimate of detection capability is one which properly interprets mixed events, malfunctions, periods of no recorded data, etc. For this reason, the SRO/ASRO detection capability estimates are calculated in two ways:

1. The first is labeled the 'ideal detection capability.' When calculating this estimate, mixed events, events for which no data were recorded, and events containing malfunctions, were dropped from the data base. The value of this ideal estimate is that it shows the detection capability improvement possible if the reliability of the instrumentation could be improved and if methods of separating mixed events could be found.

2. The second estimate is labeled 'actual detection capability.' It considers mixed events, events for which no data were recorded, and events which were affected by malfunctions (designated as non-detections). This approach gives a 'real-world' detection capability estimate.

Detection capabilities are estimated by a maximum likelihood method which was developed by Ringdal (1974). This method fits a cumulative Gaussian probability function to the detection statistics.

As described in detail in Section II, detection capabilities were estimated with respect to a Eurasian area of interest for stations ANTO, GRFO, SHIO, and KONO, and with respect to a South American area of interest for stations BOCO and ZOBO. Each station's event data base was unique as were the mean event epicentral distances of each data base to its associated station (see Table II-2). Thus, the results

ENSCO, INC.   IV-2

presented are not intended to provide measures of a station's worth other than with respect to its associated area of interest.

B.   SHORT-PERIOD DETECTION CAPABILITY ESTIMATES

Short-period detection capability was estimated by a comparison between detections made by an automatic detector and those made by an analyst. The latter were based on microfiche analysis.

The criteria for determining whether an event was detected were as follows:

- The waveform is at least 3.5 dB above the surrounding noise waveform.

- The waveform begins within $\pm$ 20 seconds of the predicted arrival time.

The detection threshold seemed low at first, but it was pointed out that noise trends and characteristics are easily seen on a microfiche, which displays 24 hours of data at once. Signal identifications could therefore be made with confidence.

Emergent waveforms were also identified; however, this was done only when the observed start time satisfied the second requirement. It should be noted that although these emergent start times were chosen at the most obvious break from the noise level, they are not necessarily the actual P-wave arrival times,which could be several seconds earlier.

Use of the second detection criterion provided no assurance that the proper arrival was picked. It is possible

that errors in computation of origin time and location, and in choice of start time, may combine to place the first point of detection outside the $\pm$ 20 second gate. Also, the expected arrival times were calculated assuming a normal (33 km) depth of focus. In cases where a P wave was observed outside the gate, and where no other events could be found in available earthquake bulletins, a detection was declared. Such cases, however, were rare.

The short-period detection capability estimates are presented for both the ideal and actual cases in Figures IV-1 through IV-12. Ideal detection capability assumes that a station operate perfectly (i.e., without downtime, malfunction, or event mixing). All events for which station problems were encountered were deleted from the ideal detection capability estimates. These events are counted as nondetections in the estimates of actual detection capabilities.

The upper portions of Figures IV-1 through IV-12 are histograms giving the detection statistics as a function of bodywave magnitude. The lower portions show the percentage of events detected at each bodywave magnitude (represented by asterisks), the fitted maximum likelihood curve (represented by a solid line), and the 90 percent confidence limits for this curve (represented by dashed lines). The values for 'MB50' and 'MB90' shown on the figures are the 50 and 90 percent detection thresholds as picked from the maximum likelihood curve. The value shown for 'SIGMA' is the standard deviation of the Gaussian probability function obtained by the maximum likelihood method. Both the confidence limits and 'SIGMA' depend upon the number and m_b distribution of events (see Ringdal, 1974).

ENSCO, INC.   IV-4
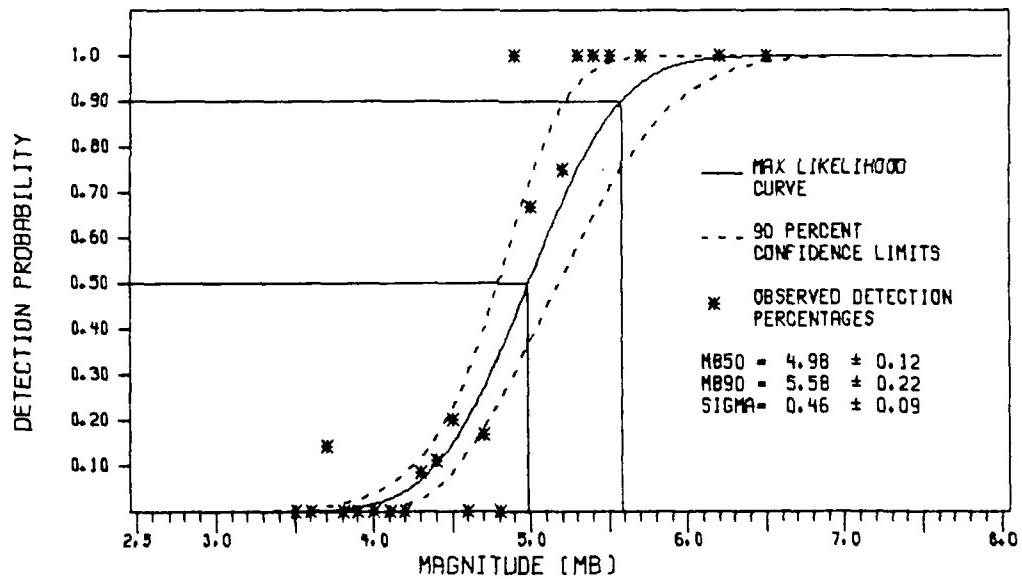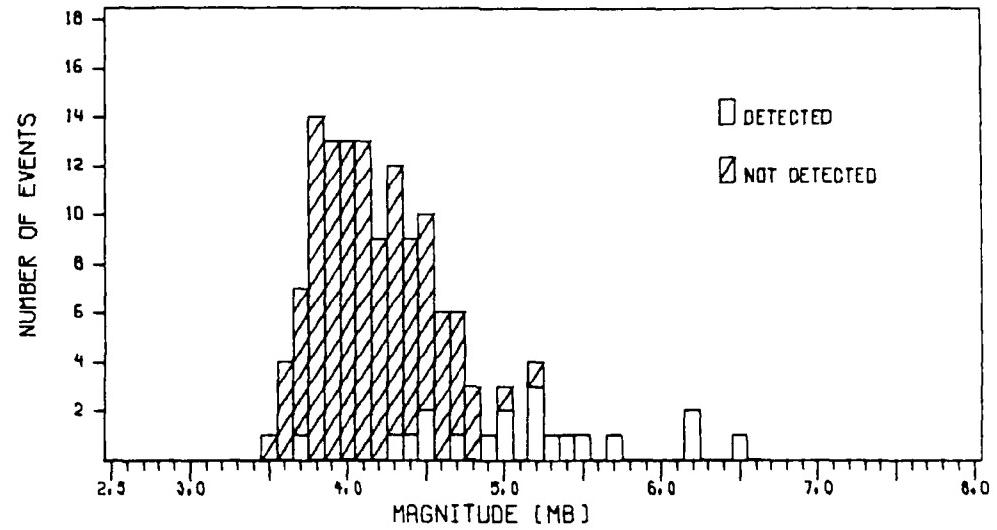
FIGURE IV-1

IDEAL ANTO SHORT-PERIOD DETECTION CAPABILITY
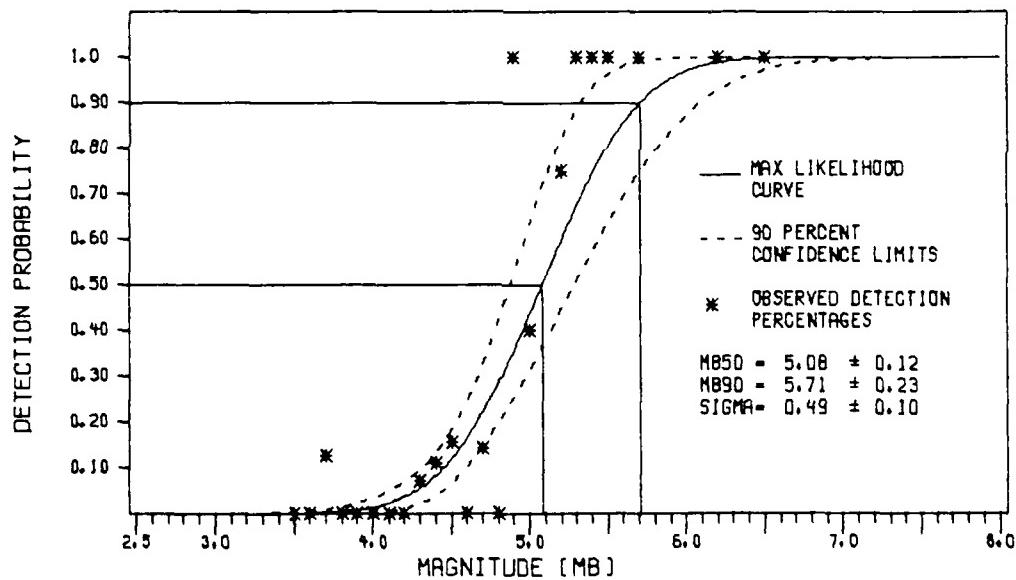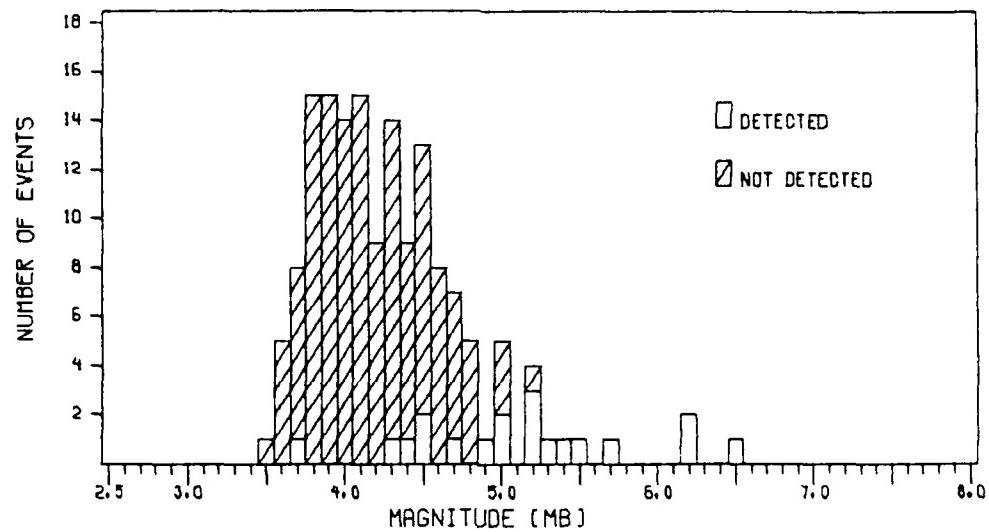
FIGURE IV-2

ACTUAL ANTO SHORT-PERIOD DETECTION CAPABILITY
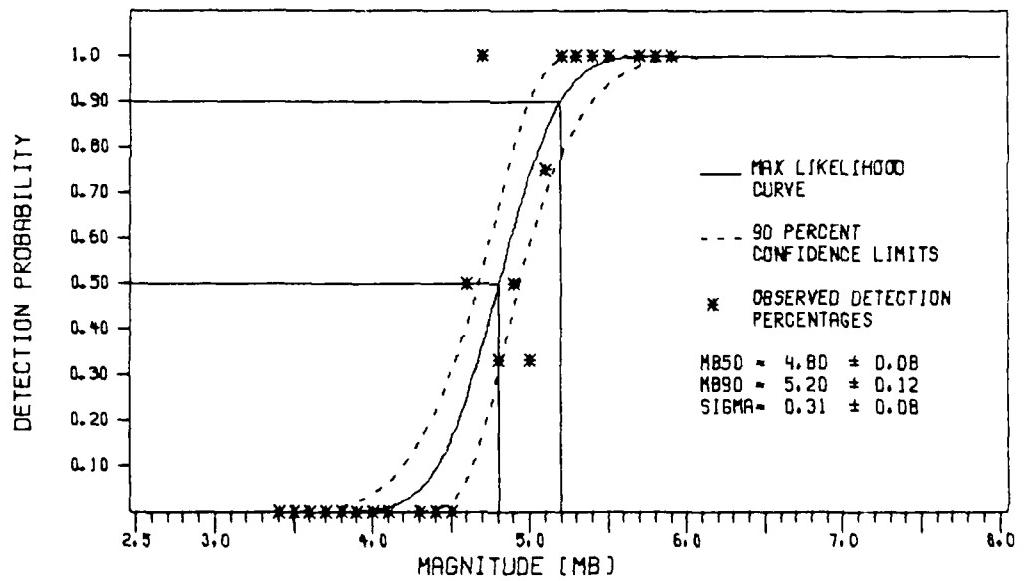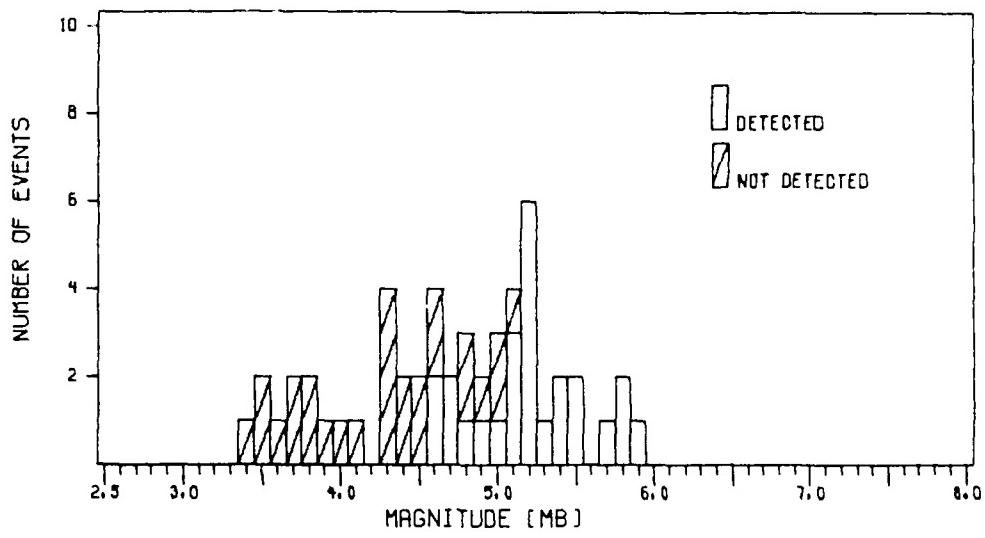
FIGURE IV-3

IDEAL BOCO SHORT-PERIOD DETECTION CAPABILITY

ENSCO, INC.   IV-7
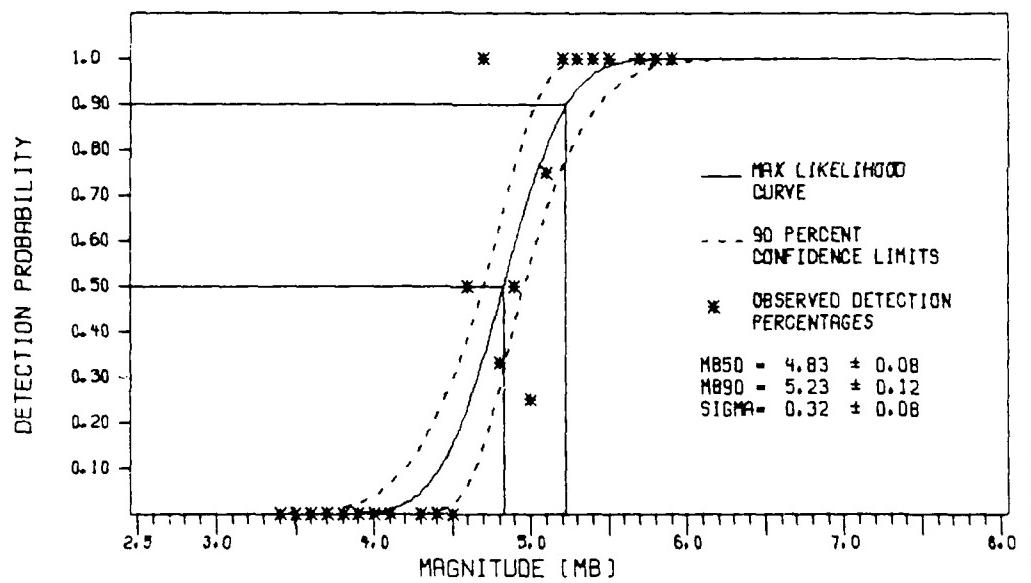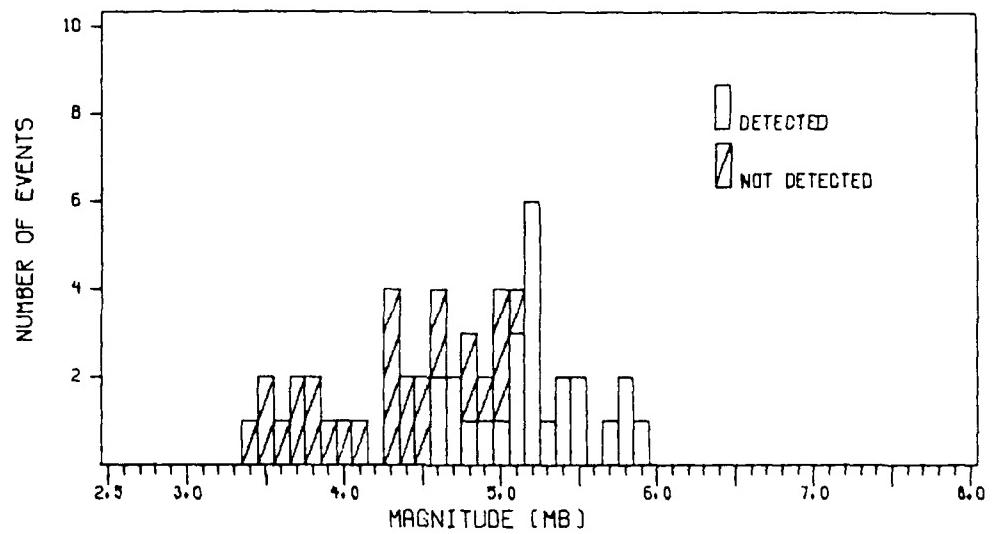
FIGURE IV-4

ACTUAL BOCO SHORT-PERIOD DETECTION CAPABILITY
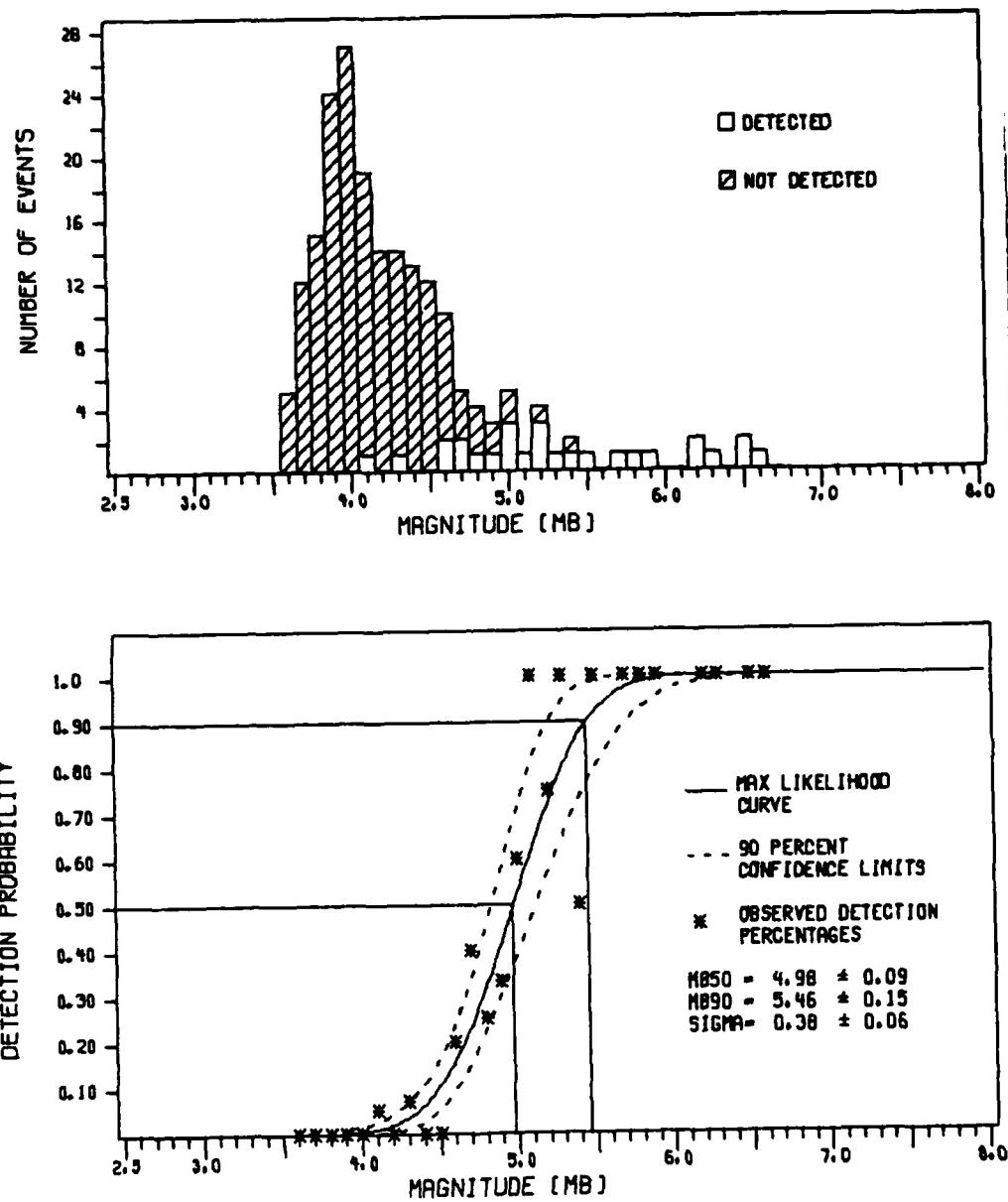
FIGURE IV-5

IDEAL GRFO SHORT-PERIOD DETECTION CAPABILITY
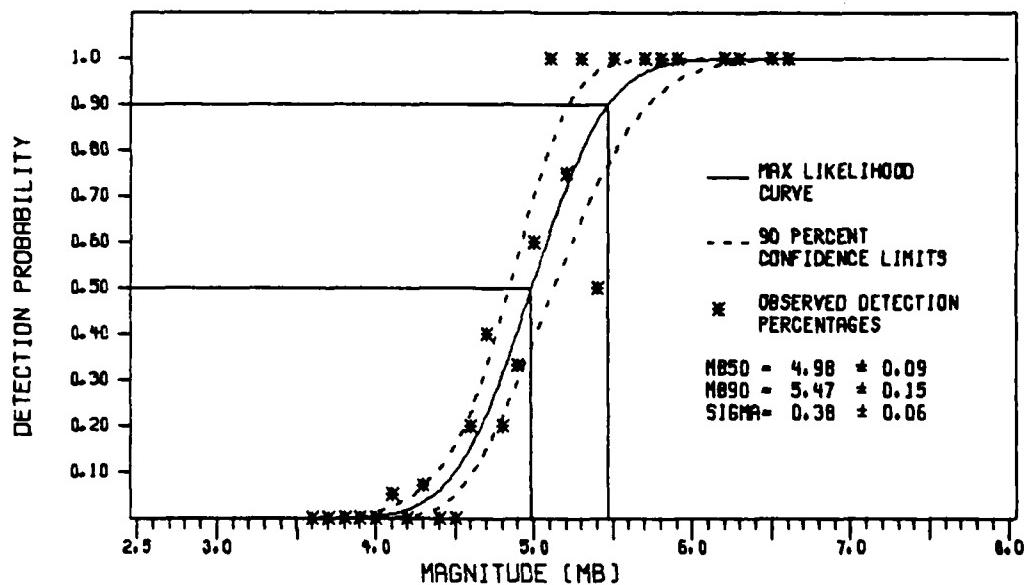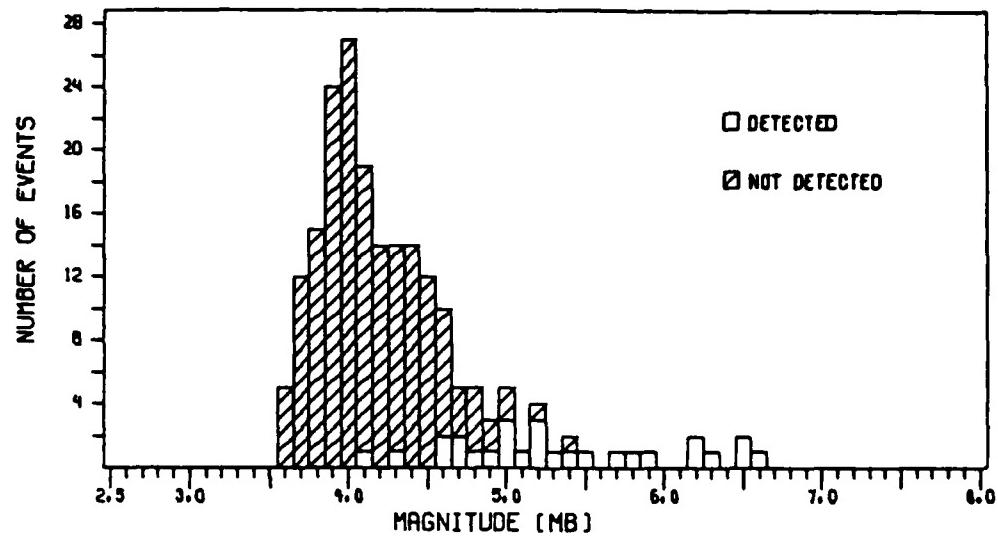
FIGURE IV-6

ACTUAL GRFO SHORT-PERIOD DETECTION CAPABILITY

ENSCO, INC.   IV-10

Number of events histogram:

NUMBER OF EVENTS (y-axis: 10, 8, 6, 4, 2)

DETECTED
NOT DETECTED

MAGNITUDE (MB) (x-axis: 2.5, 3.0, 4.0, 5.0, 6.0, 7.0, 8.0)

DETECTION PROBABILITY (y-axis: 1.0, 0.90, 0.80, 0.70, 0.60, 0.50, 0.40, 0.30, 0.20, 0.10)

MAX LIKELIHOOD CURVE

90 PERCENT CONFIDENCE LIMITS

*   OBSERVED DETECTION PERCENTAGES

MB50 = 4.45 ± 0.13
MB90 = 5.22 ± 0.32
SIGMA= 0.60 ± 0.19

MAGNITUDE (MB) (x-axis: 2.5, 3.0, 4.0, 5.0, 6.0, 7.0, 8.0)
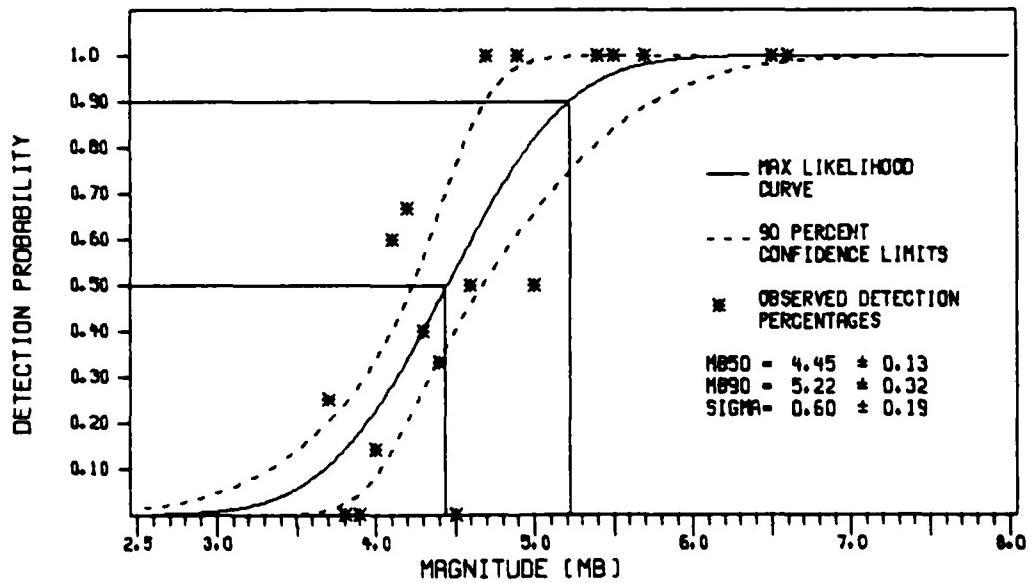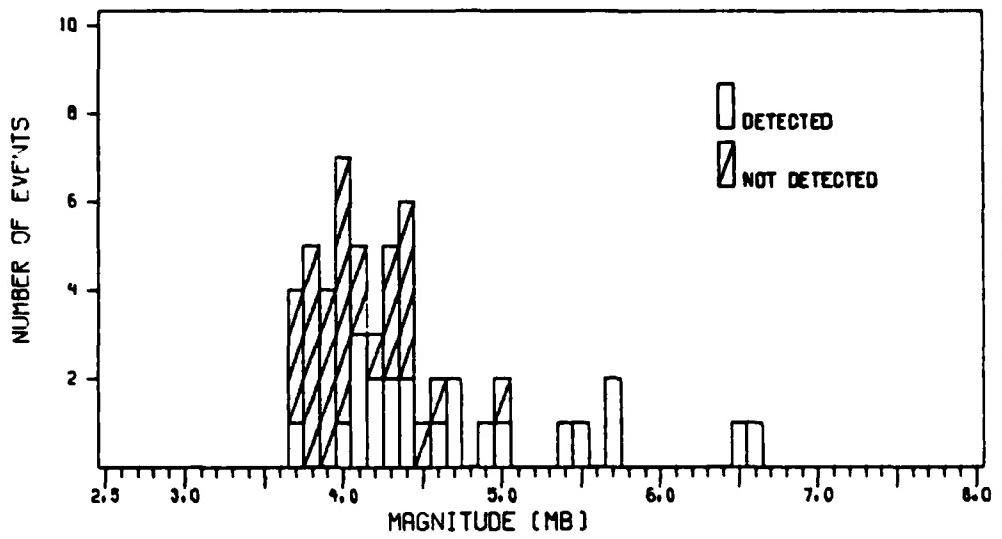
FIGURE IV-7

IDEAL SHIO SHORT-PERIOD DETECTION CAPABILITY
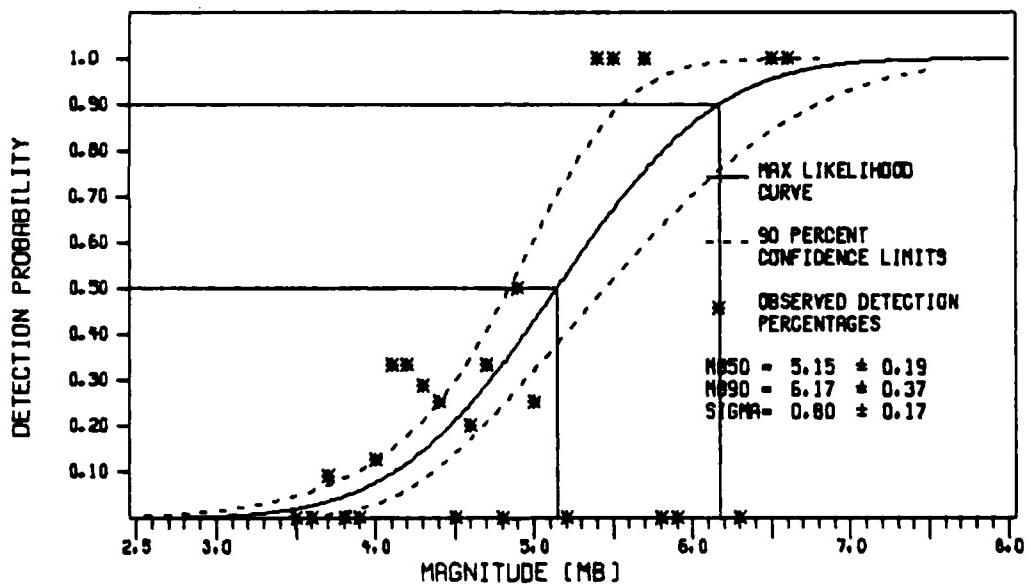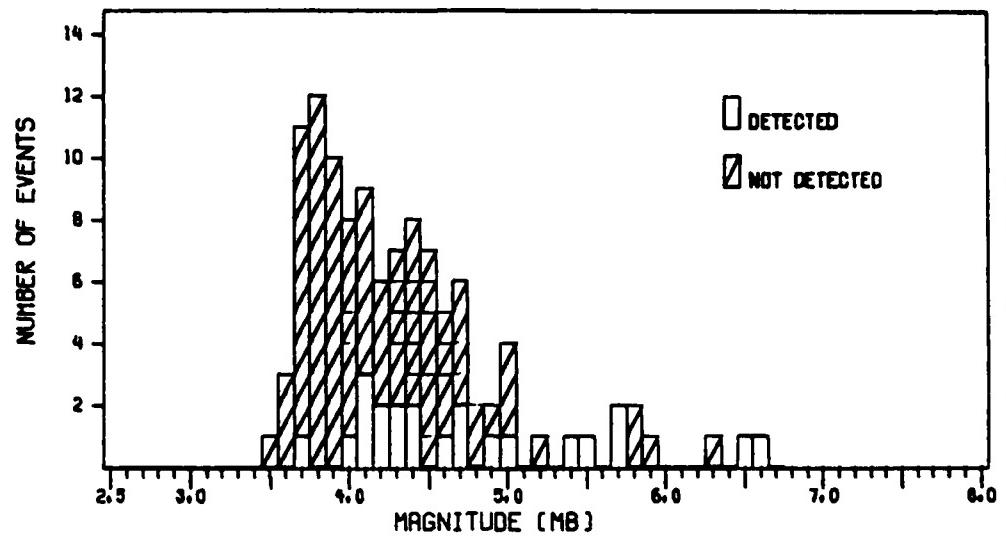
FIGURE IV-8

ACTUAL SHIO SHORT-PERIOD DETECTION CAPABILITY
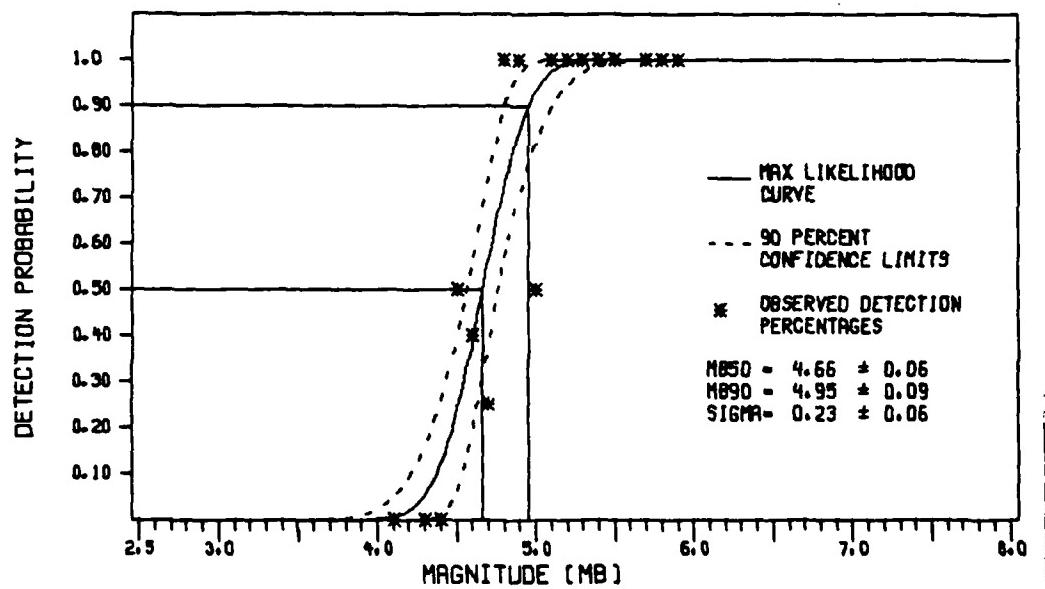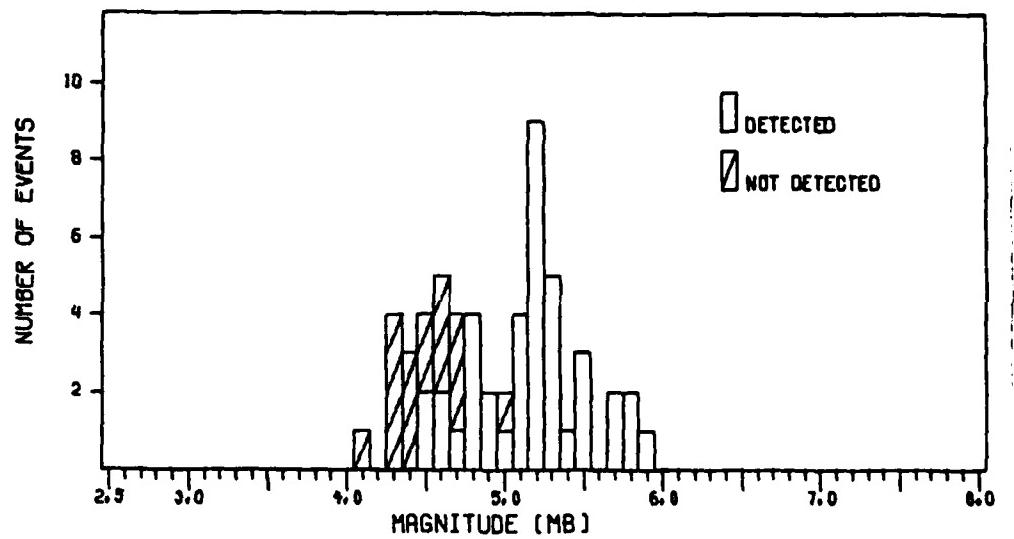
FIGURE IV-9

IDEAL ZOBO SHORT-PERIOD DETECTION CAPABILITY
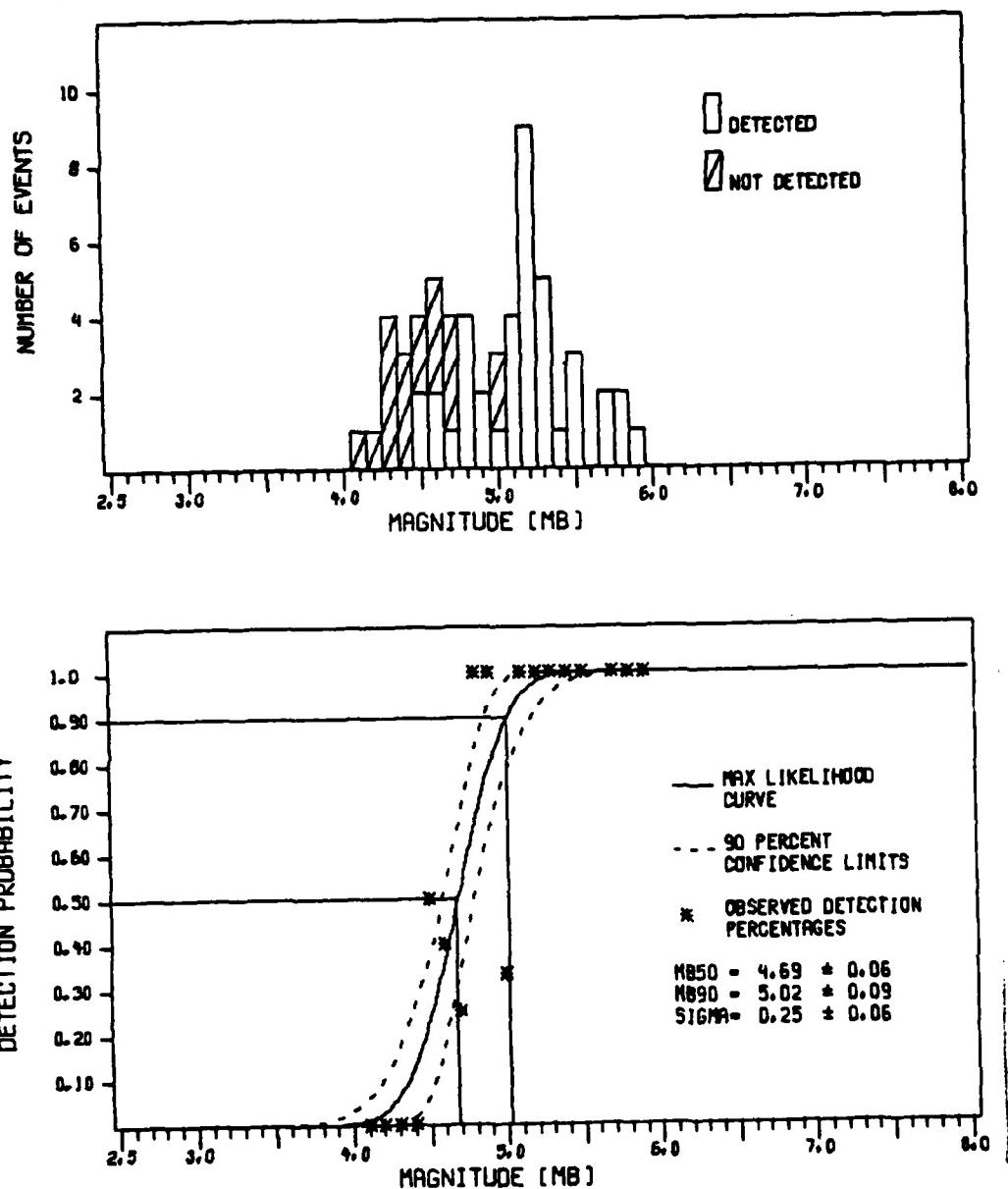
FIGURE IV-10

ACTUAL ZOBO SHORT-PERIOD DETECTION CAPABILITY
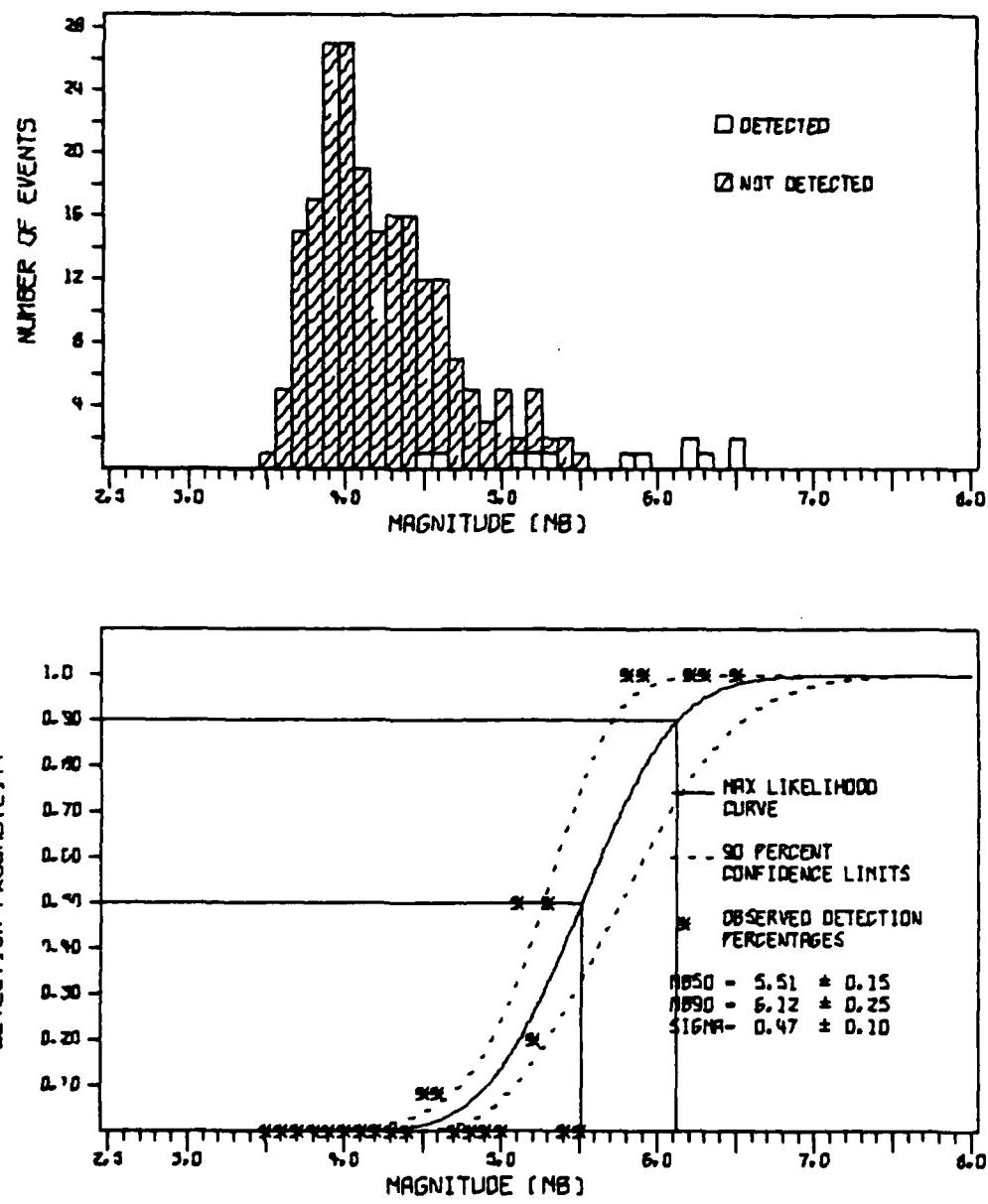
FIGURE IV-11

IDEAL KONO SHORT-PERIOD DETECTION CAPABILITY
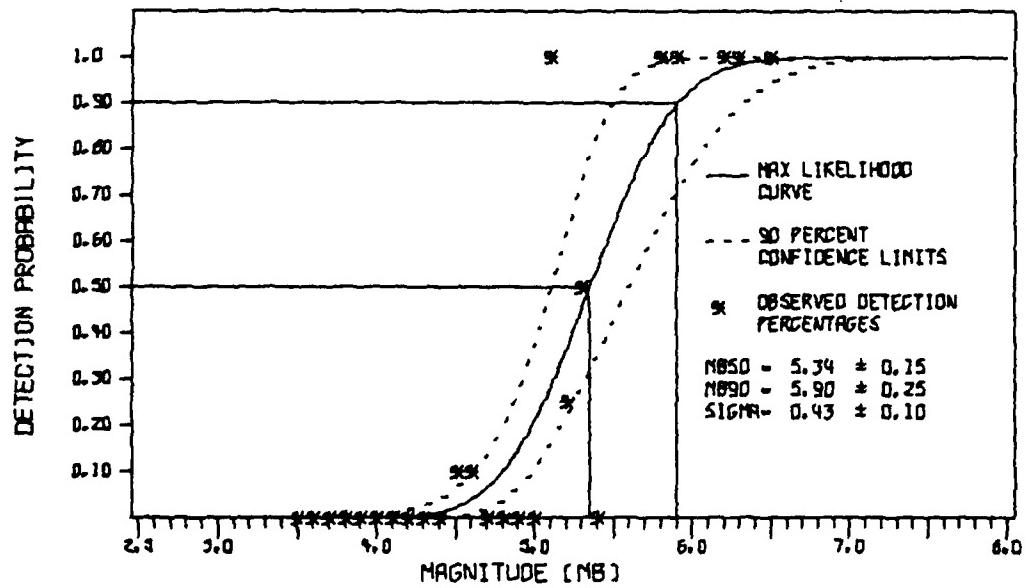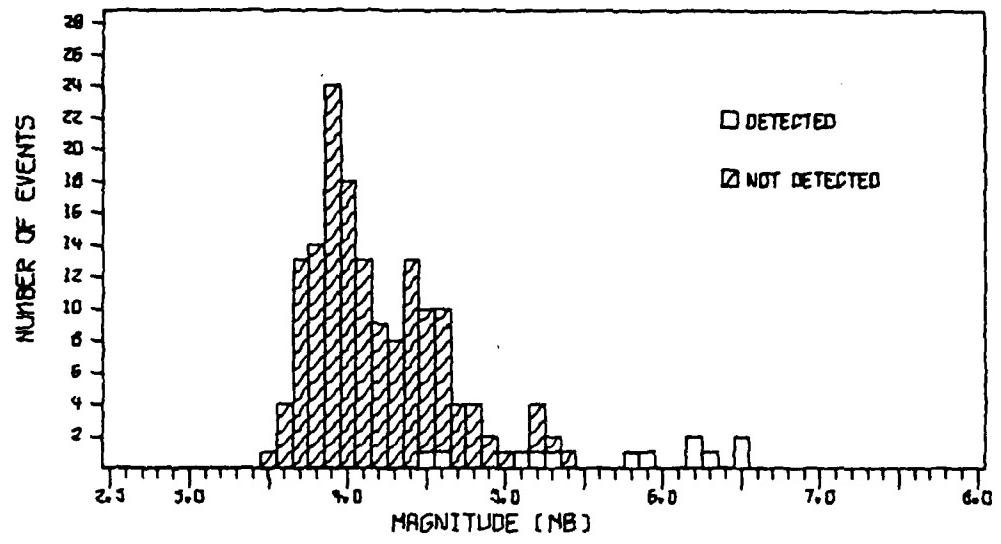
FIGURE IV-12

ACTUAL KONO SHORT-PERIOD DETECTION CAPABILITY

The titles for each figure define the station under evaluation and the type of estimation, which can be ideal or actual as defined previously. In all cases, the difference between ideal and actual detection capability reflect periods of station down time.

The short-period ideal detection capabilities are most easily discussed in terms of the event magnitude which a station can detect with a probability of 50%. The best Eurasian value, 4.45, was estimated for station SHIO. That station recorded the lowest noise levels and was nearest to the area of interest. Stations GRFO and ..ONO were further from Eurasia, recorded higher noise levels, and consequently demonstrated poorer 50% levels of m_b 4.98 and m_b 5.34, respectively. ANTO's estimate of m_b 4.98 was poorer than expected. However, that station's event data base represented a small geographic region as compared to those of the other stations. The detection capability may have been affected by a greater than average attenuation along a particular travel path.

The BOCO short-period South American ideal 50% detection capability was calculated at m_b 4.80, a reasonable value considering the station's noise level and the epicentral distances represented in that station's event base. ZOBO's 50% detection capability, estimated at m_b 4.66, was expected to be lower because of the low noise levels recorded at that station. Travel path effects may again be responsible. However, the geographic region represented here is wider than that of station ANTO.

C.   LONG-PERIOD DETECTION CAPABILITY ESTIMATES

Estimates of long-period Seismic Research Observatory detection capability are presented for the six stations: ANTO, BOCO, GRFO, SHIO, ZOBO, and KONO. The criteria for determining whether a detection has been achieved for a given event are:

- The presence of dispersion in the signal gate.

- The presence of a peak in the dispersed wave train which is 3 dB or more above any peak outside the dispersed wave train, and inside a time gate starting 600 seconds before the predicted Love wave arrival time and ending 600 seconds after the estimated Rayleigh wave end time.

- The occurrence of the signal onset within $\pm$ 180 seconds of the predicted signal onset time.

- Detection of the event on at least two components.

Occasionally, an event was considered to be detected when not all criteria were satisfied. For example, signal peaks were sometimes less than 3 dB above the noise peaks, but the signal was still recognized from its dispersion characteristics. Then, too, at a given station, it was sometimes possible to find specific features of a seismic waveform from a given region; this enabled the analyst to detect the event even though not all of the detection criteria have been satisfied. An example of this is discussed in an earlier SRO report (Strauss, 1976).

The problem of mixed events is often difficult to resolve, and may be a source of error (i.e., a detection may

be declared when, in fact, the observed signal is from an event other than that under analysis). In this study, when a signal was observed in the time gate of the event under analysis, the analyst first checked the waveforms on the three components of motion to see that their phase interrelationships were correct. If doubts existed, the analyst checked available event lists to determine whether any other reported event could have arrived in the signal gate. In general, the analyst declared a detection if a dispersed signal was observed having the correct interrelationships between the Love and Rayleigh waves, and if no other event had been reported which could be mistaken for the event under analysis.

The long-period detection statistics and derived maximum likelihood curves are presented in Figures IV-13 to IV-24. The detection capability estimates were calculated and are presented in the manner described in the first portion of this section (i.e., an 'ideal detection capability' and an 'actual detection capability'). However, because of the advantages in using filtered data, microfiche were not used for the long-period detection statistics. Each of the figures represents one long-period detection capability estimate, where the upper portions show a histogram of the detection statistics and the lower portions show the maximum likelihood curve fitted to these statistics.

Differences in ideal and actual detection capabilities for each station reflect the effects of malfunction, downtime, and signal mixing (as is discussed in Section II).

As in the short-period case, ideal long-period detection capabilities are discussed in terms of the event magnitude
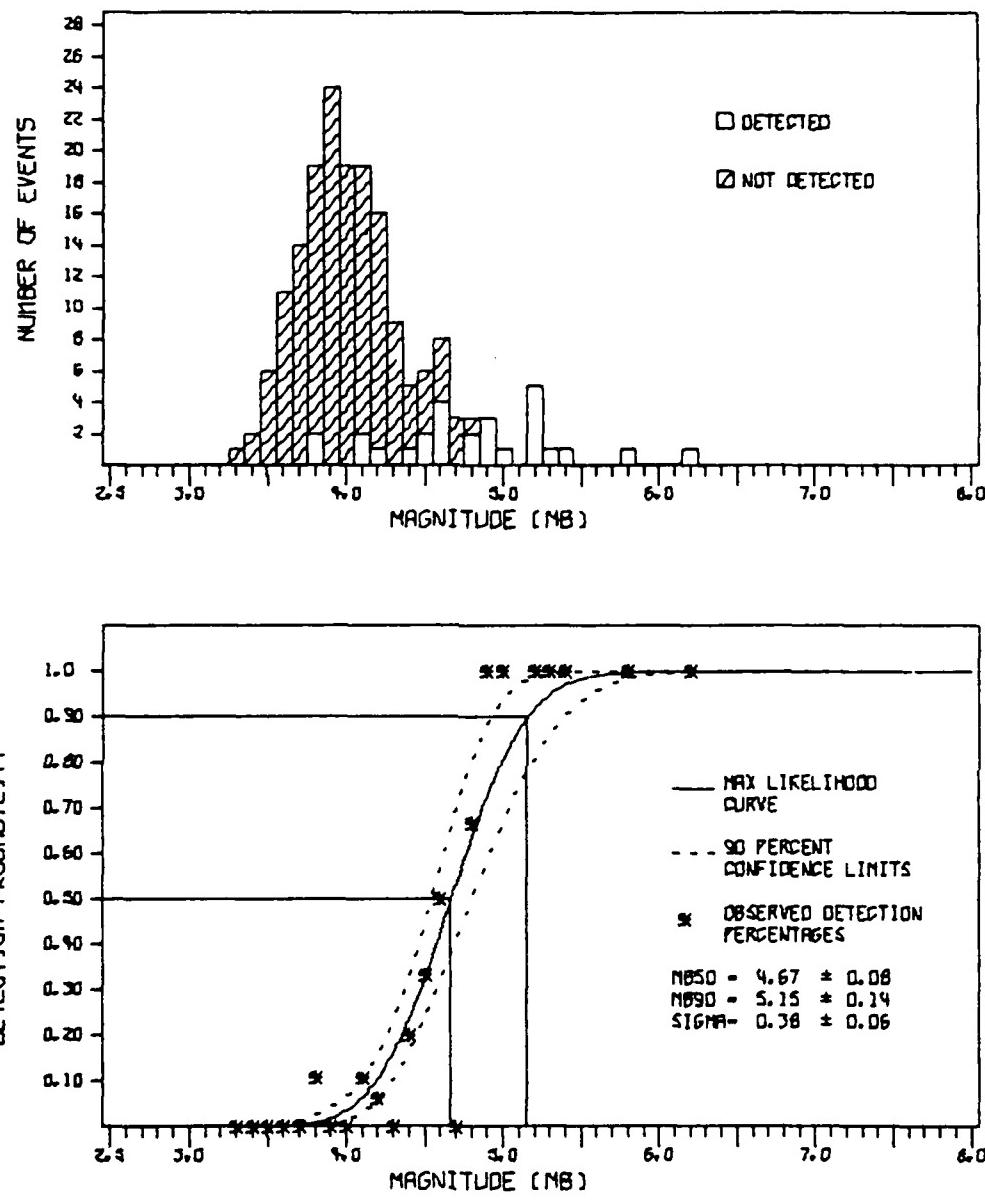
FIGURE IV-13

IDEAL ANTO LONG-PERIOD DETECTION CAPABILITY
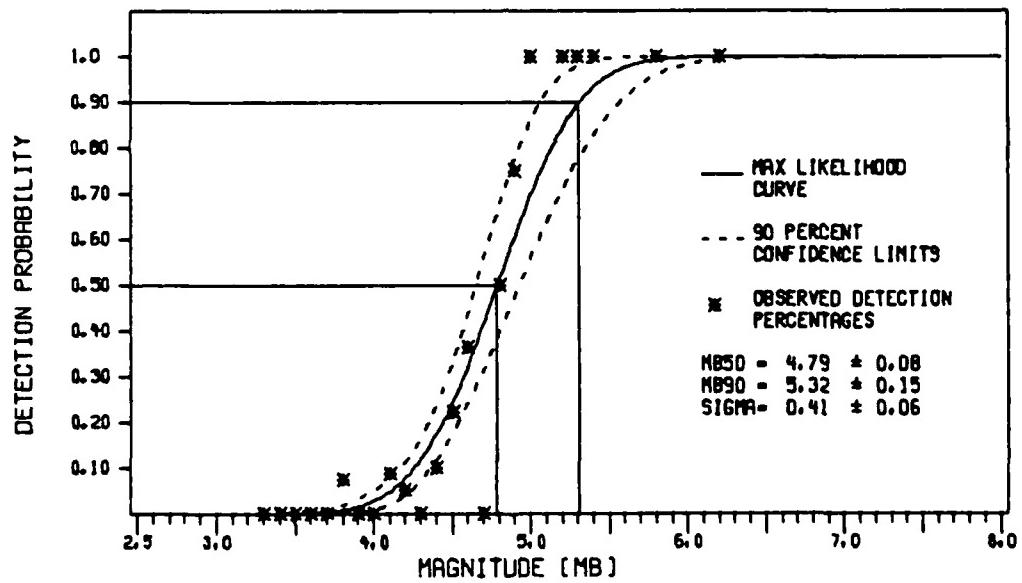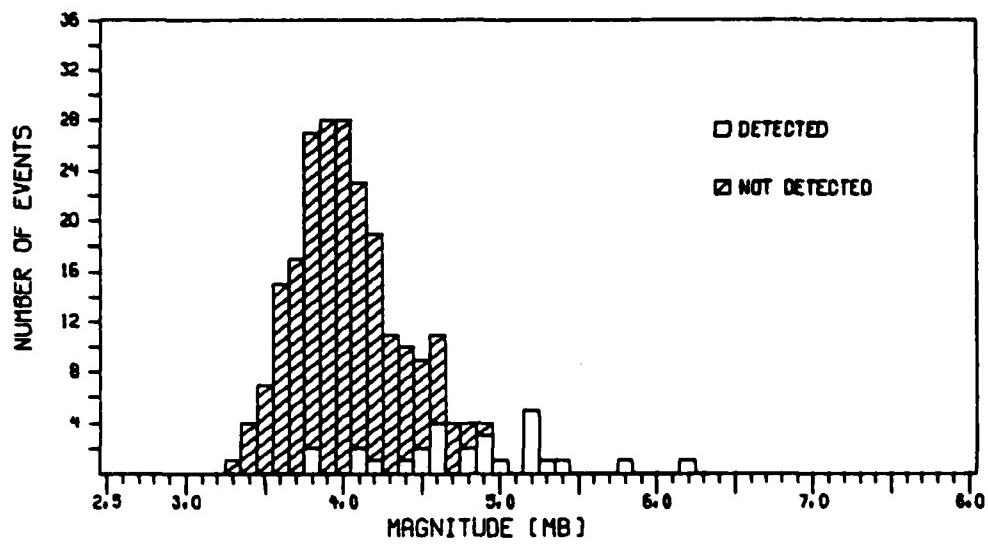
FIGURE IV-14

ACTUAL ANTO LONG-PERIOD DETECTION CAPABILITY
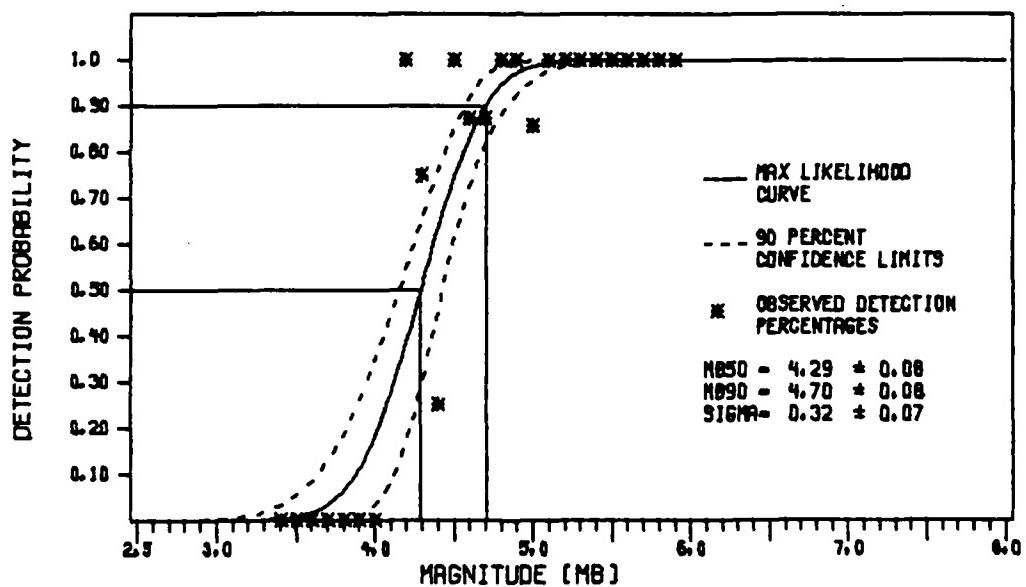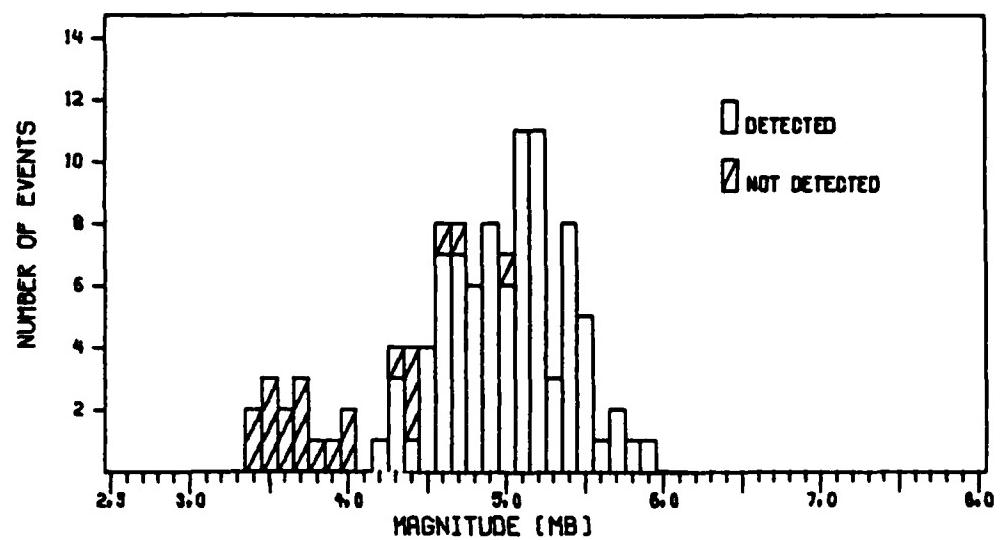
FIGURE IV-15

IDEAL BOCO LONG-PERIOD DETECTION CAPABILITY
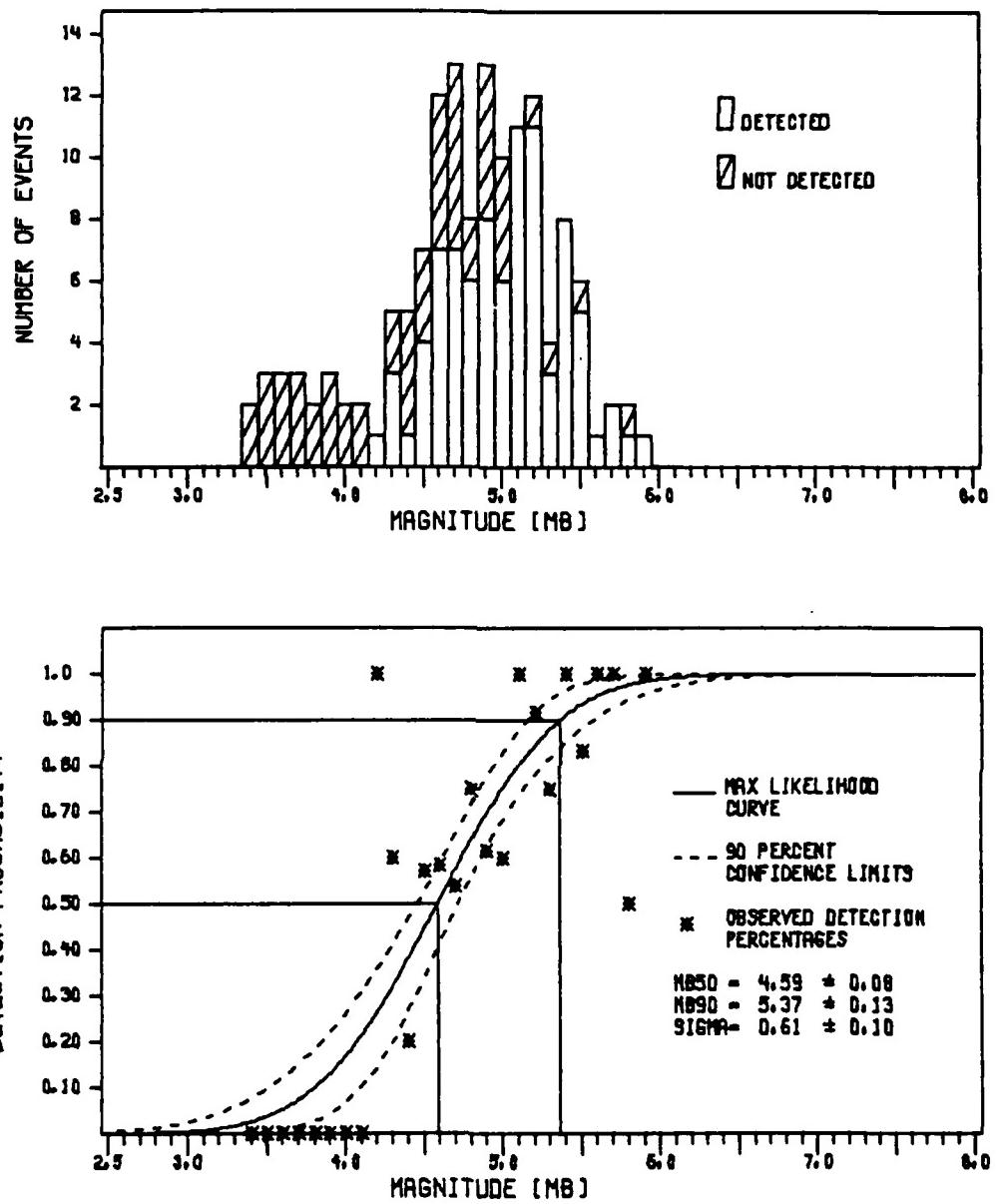
FIGURE IV-16

ACTUAL BOCO LONG-PERIOD DETECTION CAPABILITY
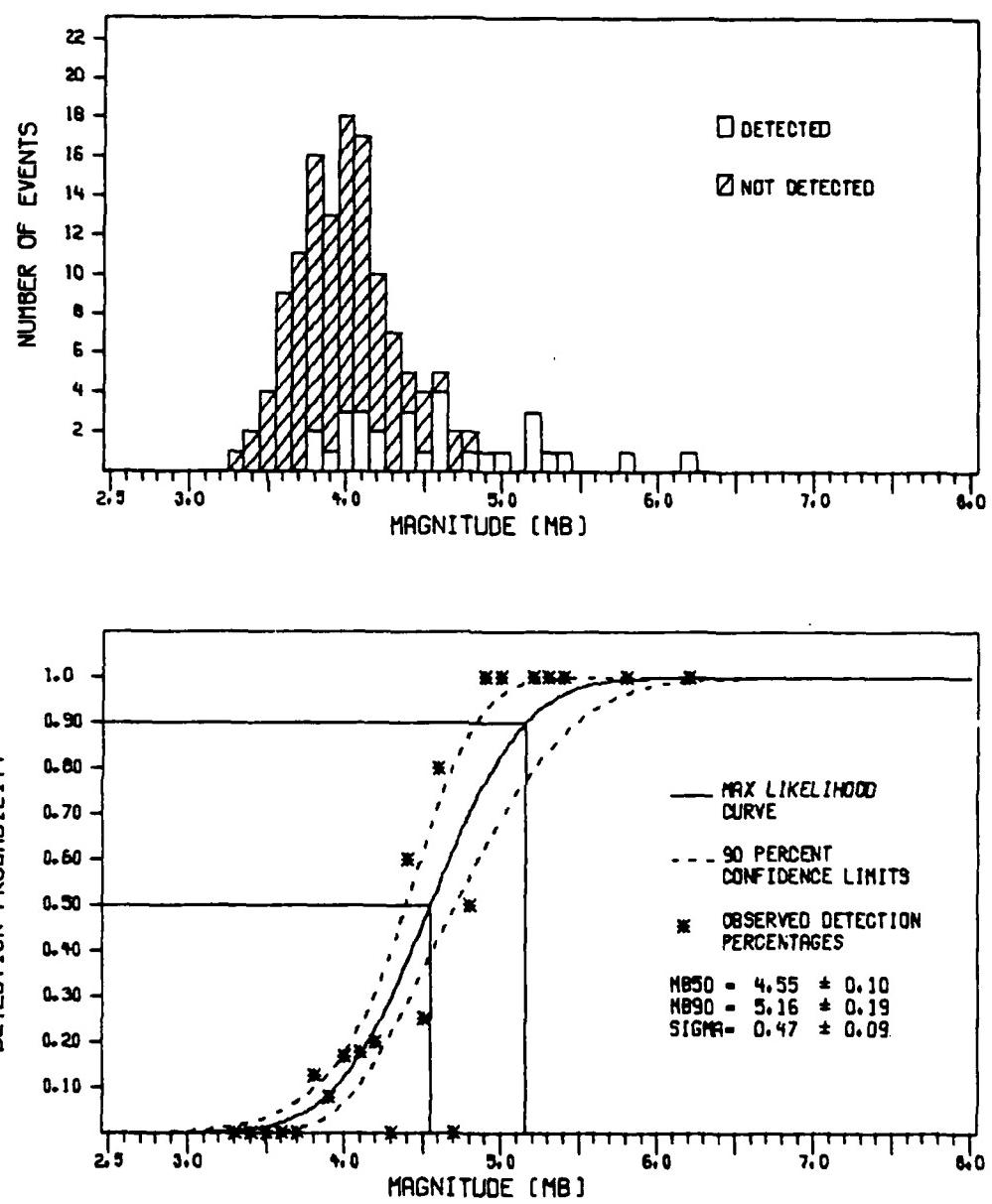
FIGURE IV-17

IDEAL GRFO LONG-PERIOD DETECTION CAPABILITY
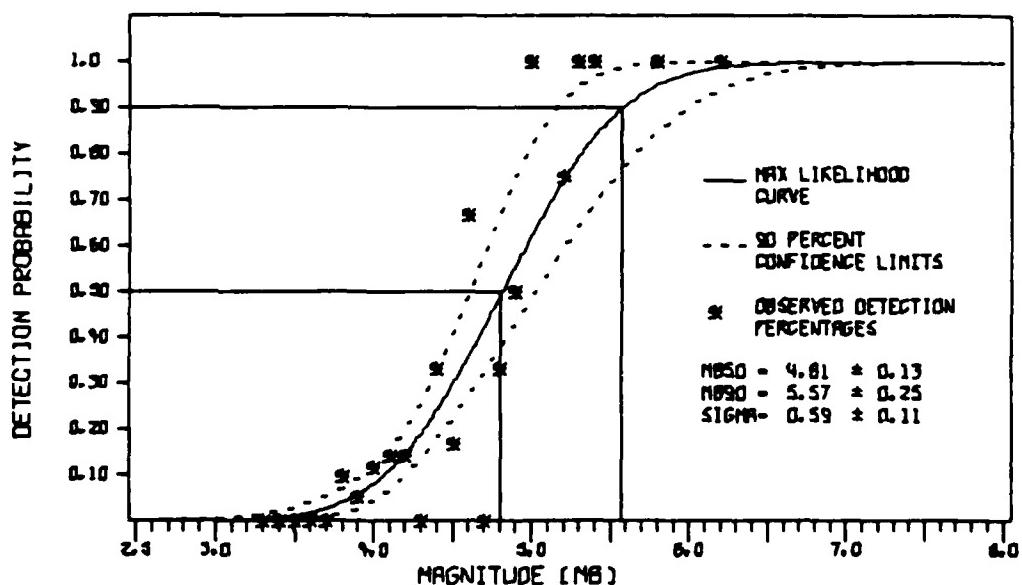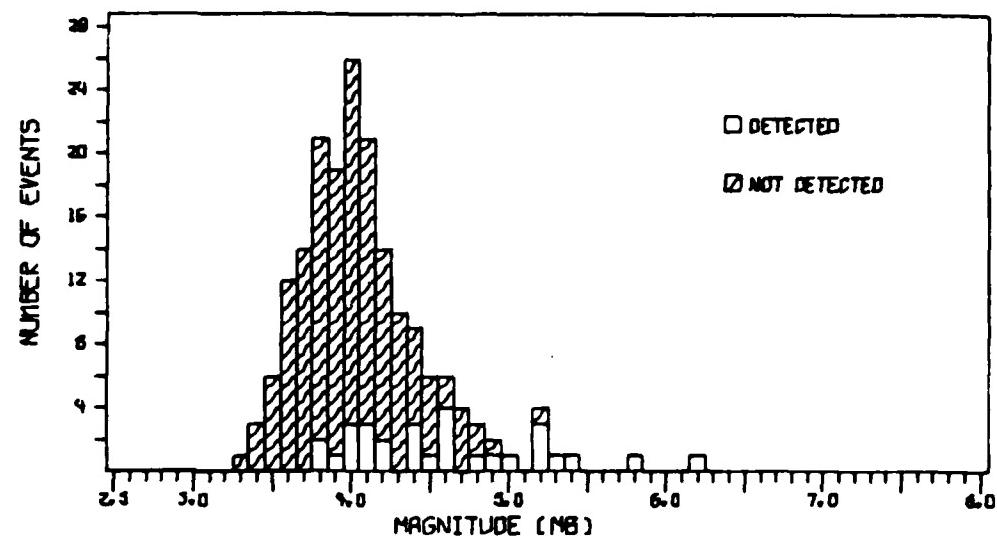
FIGURE IV-18

ACTUAL GRFO LONG-PERIOD DETECTION CAPABILITY
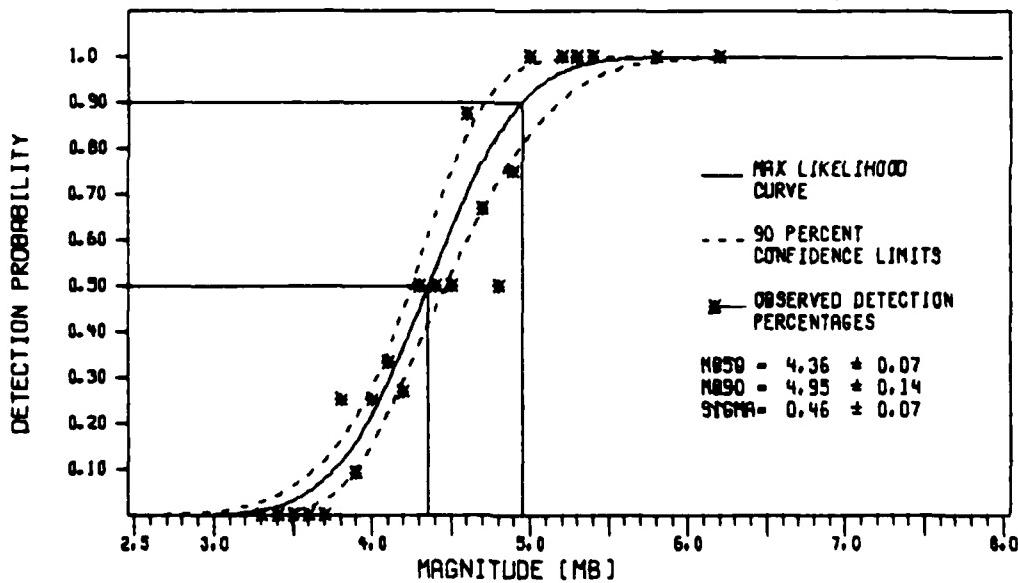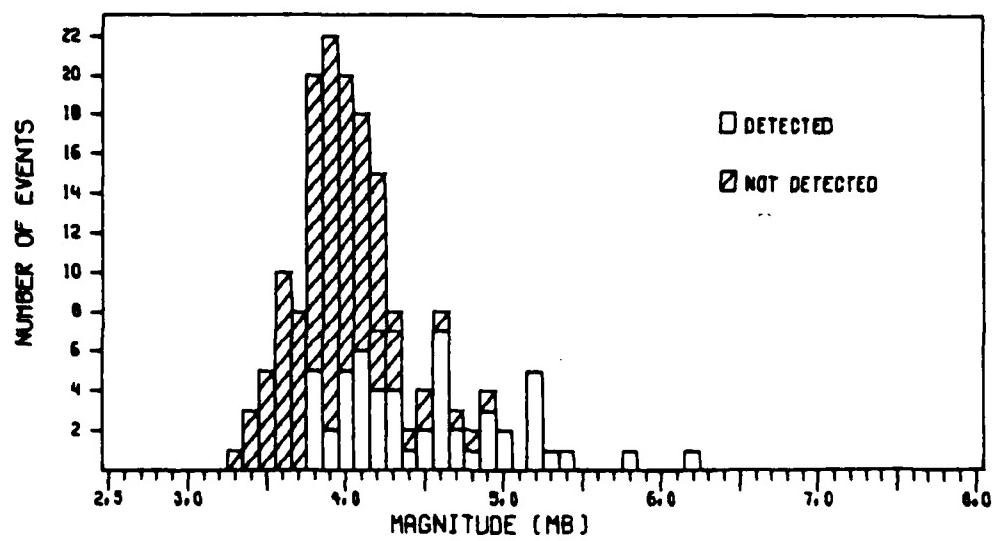
FIGURE IV-19

IDEAL SHIO LONG-PERIOD DETECTION CAPABILITY
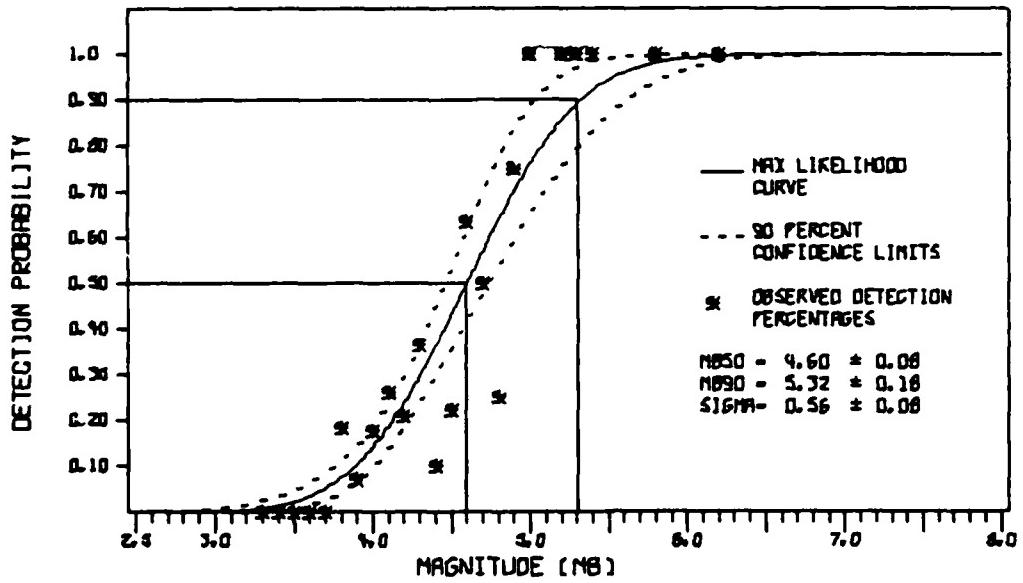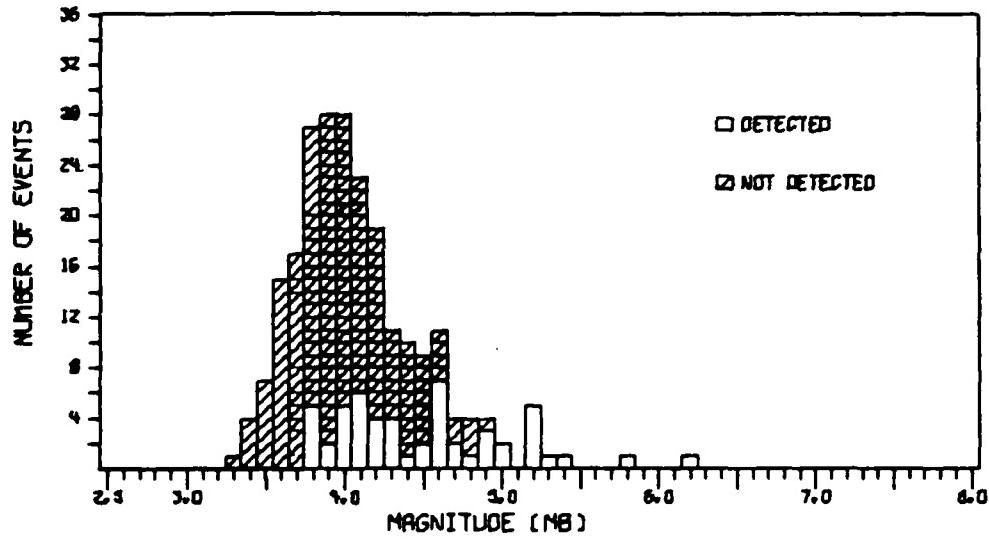
FIGURE IV-20

ACTUAL SHIO LONG-PERIOD DETECTION CAPABILITY
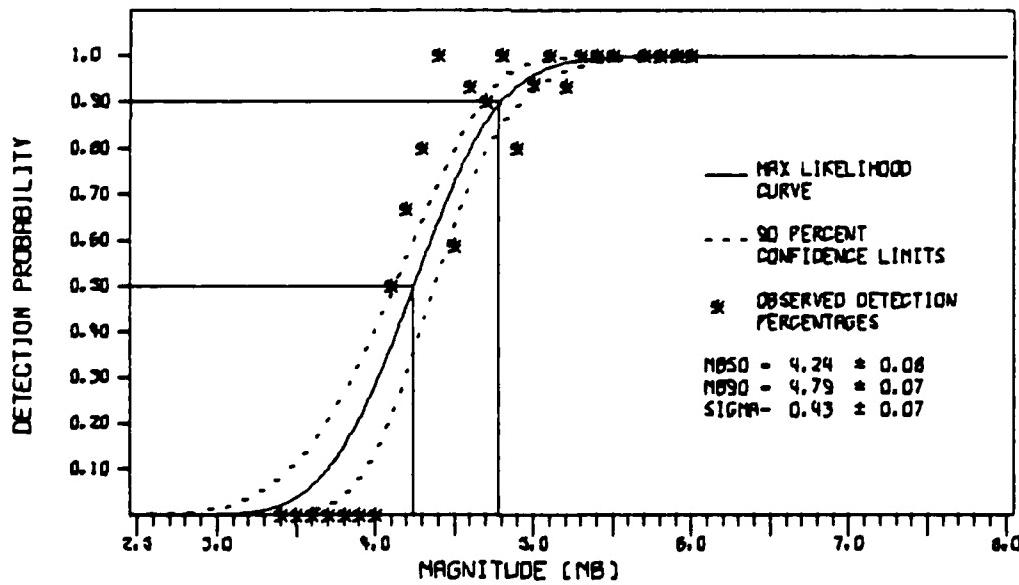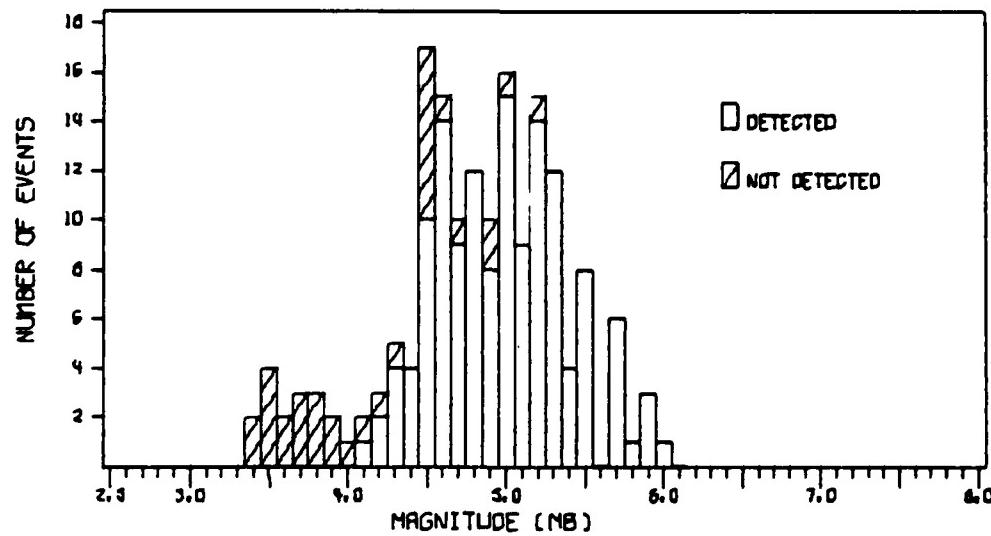
FIGURE IV-21

IDEAL ZOBO LONG-PERIOD DETECTION CAPABILITY
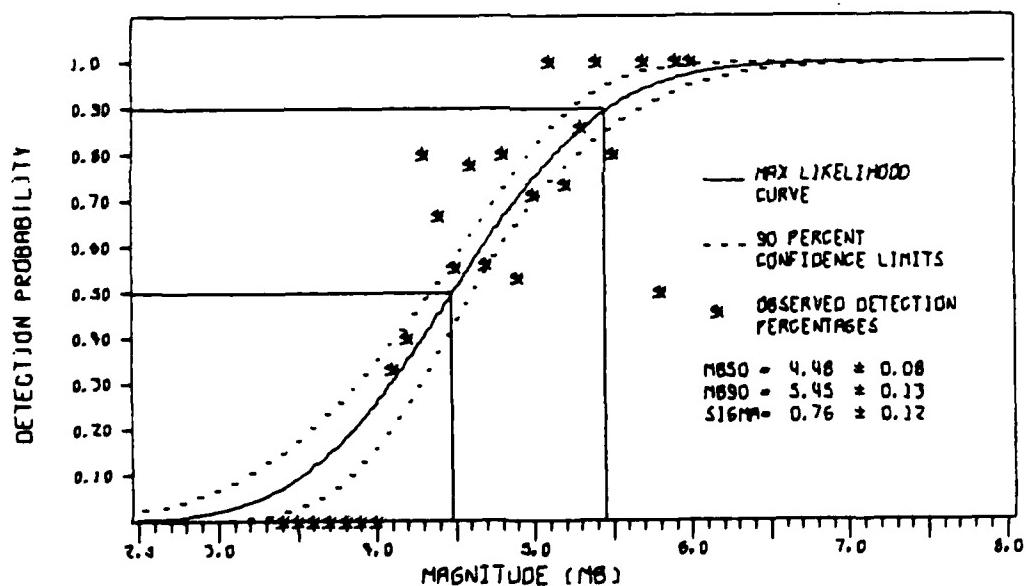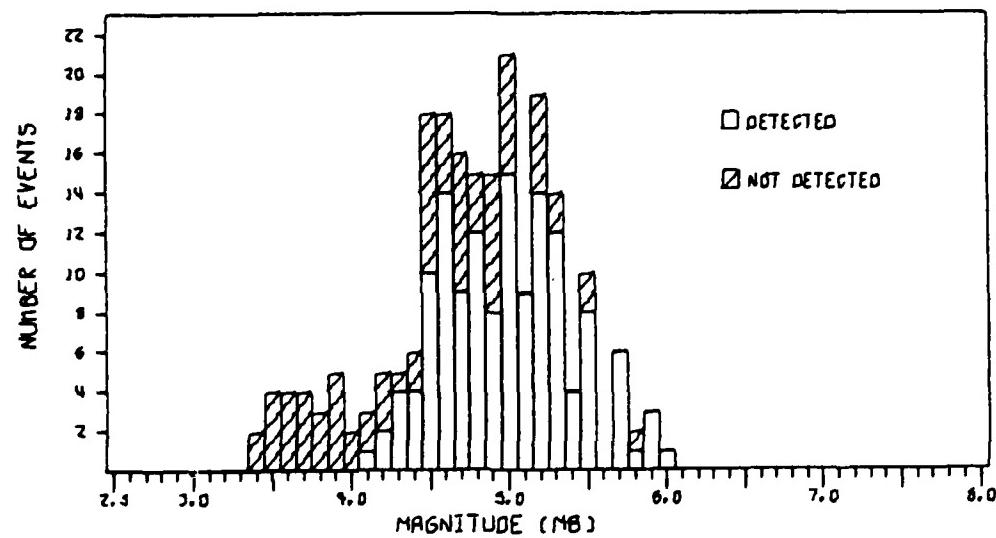
FIGURE IV-22

ACTUAL ZOBO LONG-PERIOD DETECTION CAPABILITY
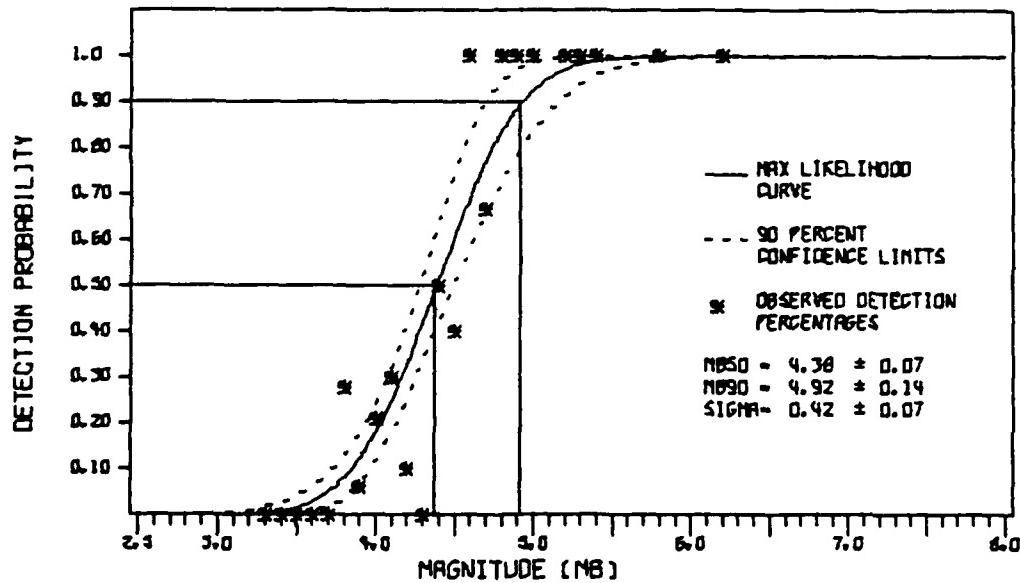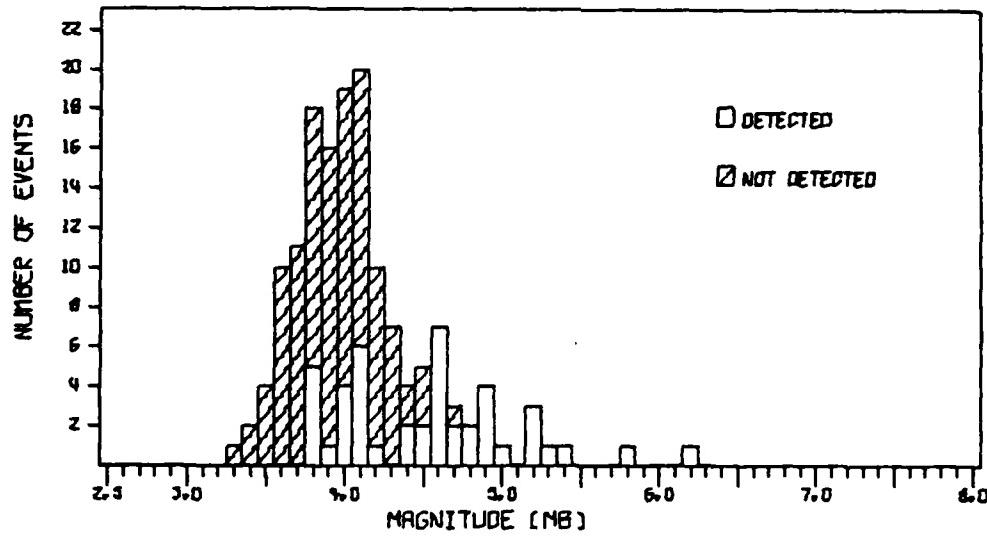
FIGURE IV-23

IDEAL KONO LONG-PERIOD DETECTION CAPABILITY
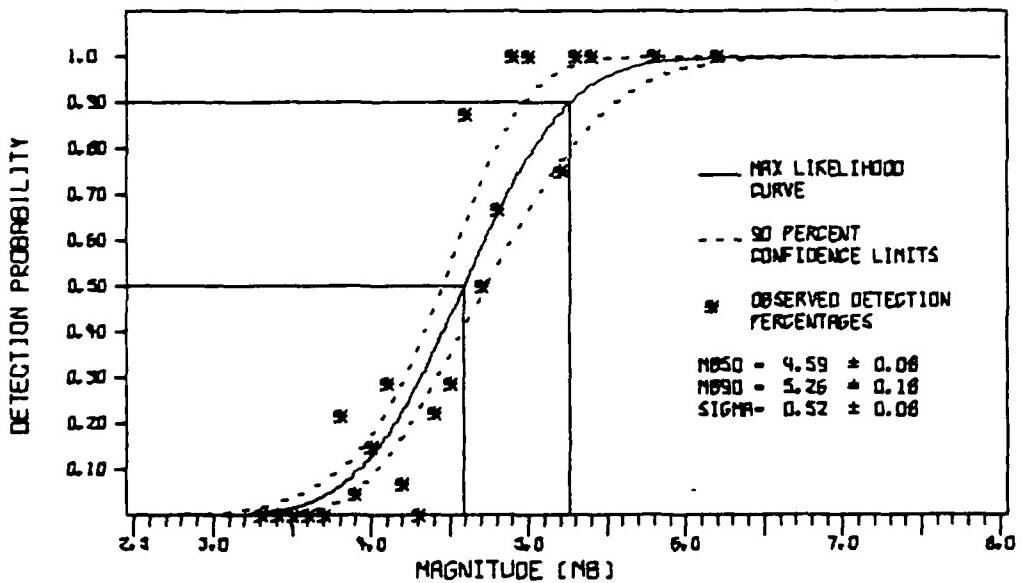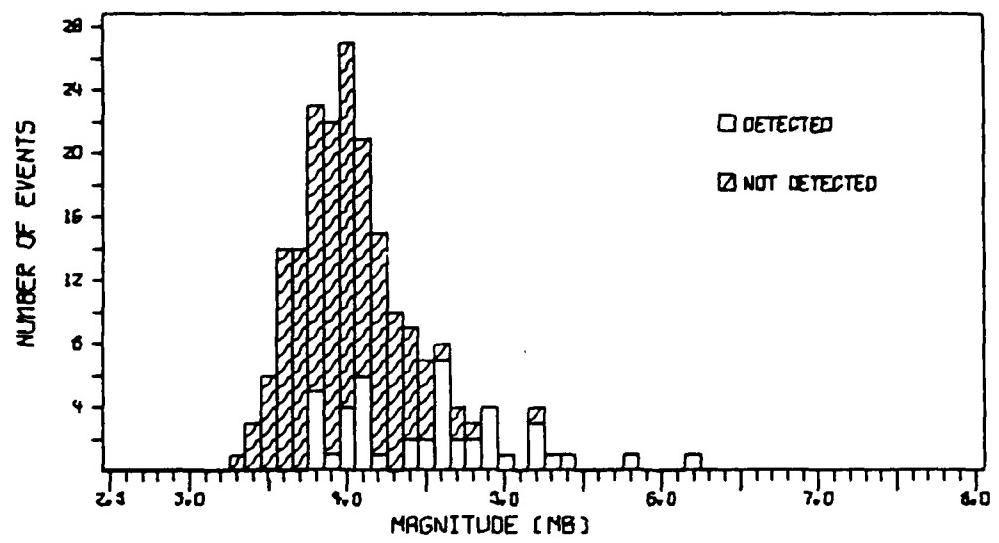
FIGURE IV-24

ACTUAL KONO LONG-PERIOD DETECTION CAPABILITY

which a station can detect with a probability of 50%. The Eurasian 50% values for stations ANTO, GRFO, SHIO, and KONO are 4.67, 4.55, 4.36, and 4.38 m_b units, respectively. These estimates are reasonable (except for station ANTO) considering recorded noise levels and event epicentral distance ranges. Station ANTO's long-period detection capability estimates were likely biased by the aforementioned intermittemt high noise level recorded on the north-south component.

The South American 50% ideal detection capabilities for stations BOCO and ZOBO were estimated at 4.29 and 4.24 m_b units, respectively. These stations, on the bases of noise level and event epicentral distances alone, were expected to exhibit poorer detection capabilities. Their unexpectedly good capabilities illustrate the regional dependence of detection capability estimates.

SECTION V

SUMMARY

A.   INTRODUCTION

This section combines the results of this year's study
with those of previous years (Weltman and Oliver, 1978;
Strauss and Weltman, 1977; Strauss, 1976). Efforts were made
in all of the evaluations to maintain a consistent methodology;
this was done to insure that all comparisons would be meaning-
ful*.

B.   STATION RELIABILITY

Reliability factors for each station are summarized in
Table V-1. Reliabilities were calculated from the results
of an analysis of each station's detection capability event
data base, where the reliability factor is defined as:

$$R = 1 - \frac{N_d + N_m}{T}$$

---

*NB, Data from stations BOCO and TATO, the N-S component at
ANTO, and from all long-period components at SNZO were, at
times, degraded by hardware malfunctions during the evalua-
tions of those stations. Analysis results for these data,
therefore, may not be representative of true station perfor-
mance.

ENSCO, INC.   V-1

TABLE V-1

STATION RELIABILITY

Station	Short-Period	Long-Period
ANMO	0.91	0.87
ANTO	0.88	0.94
BOCO	0.98	0.91
CHTO	0.85	0.84
GUMO	0.76	0.70
MAIO	0.89	0.92
NWAO	1.00	0.91
GRFO	1.00	0.94
SHIO	0.53	0.83
TATO	0.94	0.90
SNZO	0.94	0.80
CTAO	0.99	0.99
ZOBO	0.98	0.99
KAAO	0.93	0.89
MAJO	0.71	0.66
KONO	0.74	0.96
Average	0.88	0.88

where

    R = Reliability factor

    N_d = Number of events for which no data were recorded

    N_m = Number of events for which the data indicated an instrument malfunction

    T = Total number of events.

The average station reliability is approximately 0.9. Reliability would be expected to improve slightly as stations are brought to optimal operating efficiency.

C.   STATION NOISE CHARACTERISTICS

Short- and long-period noise samples were collected from each station every fourth station day over time periods of from six months to one year. Analysis yielded mean RMS noise amplitudes, noise magnitudes, and long-period mean RMS noise amplitude spectra. All values presented here are without correction for instrument response. Mean short- and long-period RMS noise values are presented in Table V-2.

The stations, based on their RMS noise levels, may be divided into a high noise group represented by the coastal stations GUMO, TATO, SNZO, and KONO; a low noise group represented by the inland stations ANMO, CHTO, MAIO, SHIO, ZOBO, and KAAO; and a medium noise group composed of the remaining inland and coastal stations. Without exception, the stations in the high noise group are located in areas which subject them to severe ocean storm activity.

TABLE V-2
MEAN RMS NOISE AMPLITUDES IN MILLIMICRONS (mµ)

Station	Short-Period 0.5-4.0 Hz		Long-Period 0.023-0.059 Hz					
	Vertical		Vertical		North		East	
	Mean	S.D.*	Mean	S.D.*	Mean	S.D.*	Mean	S.D.*
SRO								
ANMO	0.38	0.09	9.73	3.61	8.80	3.67	10.01	3.32
ANTO	3.46	0.96	8.37	4.88	8.62	4.31	16.42	40.50
BOCO	3.88	0.81	13.50	16.00	20.02	48.89	14.60	19.13
CHTO	1.67	0.67	11.13	6.30	12.93	7.35	11.87	6.49
GUMO	40.25	16.83	11.25	3.45	17.20	5.34	18.23	5.34
MAIO	0.57	0.17	7.70	2.96	7.80	2.73	8.07	2.91
NWAO	7.69	2.80	13.44	4.85	17.29	5.67	11.61	4.79
GRFO	5.01	2.57	12.48	6.38	14.36	7.34	13.05	7.41
SHIO	1.62	0.42	8.42	3.01	8.08	2.94	7.50	3.18
TATO	20.61	8.66	14.22	6.04	15.65	7.14	18.12	9.56
SNZO	28.92	11.05	45.92	17.28	27.26	14.22	30.17	14.41
ASRO								
CTAO	5.55	2.27	9.41	3.29	9.90	3.02	8.78	3.18
ZOBO	1.02	0.36	7.57	3.07	8.06	2.97	8.75	3.53
KAAO	1.94	0.69	9.06	3.51	9.05	3.02	11.86	4.56
MAJO	3.53	1.31	8.40	3.22	10.20	4.08	10.85	9.75
KONO	12.64	4.27	10.34	4.23	12.94	6.17	11.59	4.84

*S.D. = Standard Deviation

Table V-3 lists the means and standard deviations of measured $\log_{10}$ peak noise amplitudes. Short-period and long-period measurements were made at periods of 1.0 ± 0.2 and 25 ± 2 seconds, respectively. A comparison between SRO and ASRO peak noise amplitudes reveals, as was expected, that short-period standard deviations appear reduced for the buried SRO instruments. This evidence, together with comparisons of the typical SRO and ASRO long-period noise spectra (shown in Figure V-1) demonstrates how instrument burial reduces and stablizes the ambient noise field.

Figures V-2 and V-3 present the theoretical short- and long-period capabilities of at least one station in the SRO/ASRO network to detect an m_b 4.5 event. The program used was developed by M. H. Wirth (1970) and assumed that both signal and noise are lognormally distributed. Snell (1976) modified that program to consider station reliability. The numbers on the figure contours were calculated as follows:

$$\log_{10} \frac{P_D}{1-P_D}$$

where P_D is the probability of detection. The contour values are translated into detection probabilities in Table V-4. The probability of detection must never reach one or the logarithm would be infinite and so the last detection probability listed in Table V-4 may actually be calculated as 0.99997. Figures V-2 and V-3 show that the SRO/ASRO network can detect medium magnitude events with certainty.

Short- and long-period detection capabilities for each station are presented in Table V-5. These capabilties were

TABLE V-3

MEAN LOG PEAK NOISE AMPLITUDES IN MILLIMICRONS (mμ)

Station	1 Second Period		25 Seconds Period					
	Vertical		Vertical		North		East	
	Mean	S.D.*	Mean	S.D.*	Mean	S.D.*	Mean	S.D.*
SRO								
ANMO	-0.06	0.16	1.33	0.16	1.28	0.17	1.35	0.16
ANTO	0.82	0.17	1.26	0.15	1.32	0.14	1.44	0.34
BOCO	0.87	0.13	1.50	0.24	1.52	0.33	1.45	0.28
CHTO	0.37	0.18	1.28	0.20	1.38	0.18	1.33	0.20
GUMO	1.85	0.14	1.62	0.16	1.73	0.15	1.73	0.17
MAIO	0.06	0.15	1.28	0.15	1.28	0.16	1.29	0.16
NWAO	0.95	0.20	1.54	0.15	1.59	0.15	1.43	0.17
GRFO	0.72	0.18	1.42	0.16	1.45	0.17	1.44	0.18
SHIO	0.43	0.19	1.34	0.14	1.30	0.17	1.30	0.12
TATO	1.49	0.17	1.59	0.15	1.63	0.18	1.68	0.19
SNZO	1.79	0.17	2.10	0.16	1.84	0.17	1.88	0.16
ASRO								
CTAO	0.61	0.26	1.26	0.22	1.32	0.13	1.30	0.20
ZOBO	0.10	0.20	1.24	0.16	1.29	0.12	1.33	0.15
KAAO	0.46	0.21	1.32	0.17	1.35	0.15	1.44	0.18
MAJO	0.56	0.21	1.33	0.15	1.44	0.22	1.34	0.15
KONO	0.83	0.23	1.36	0.14	1.50	0.14	1.46	0.15

*S.D. = Standard Deviation
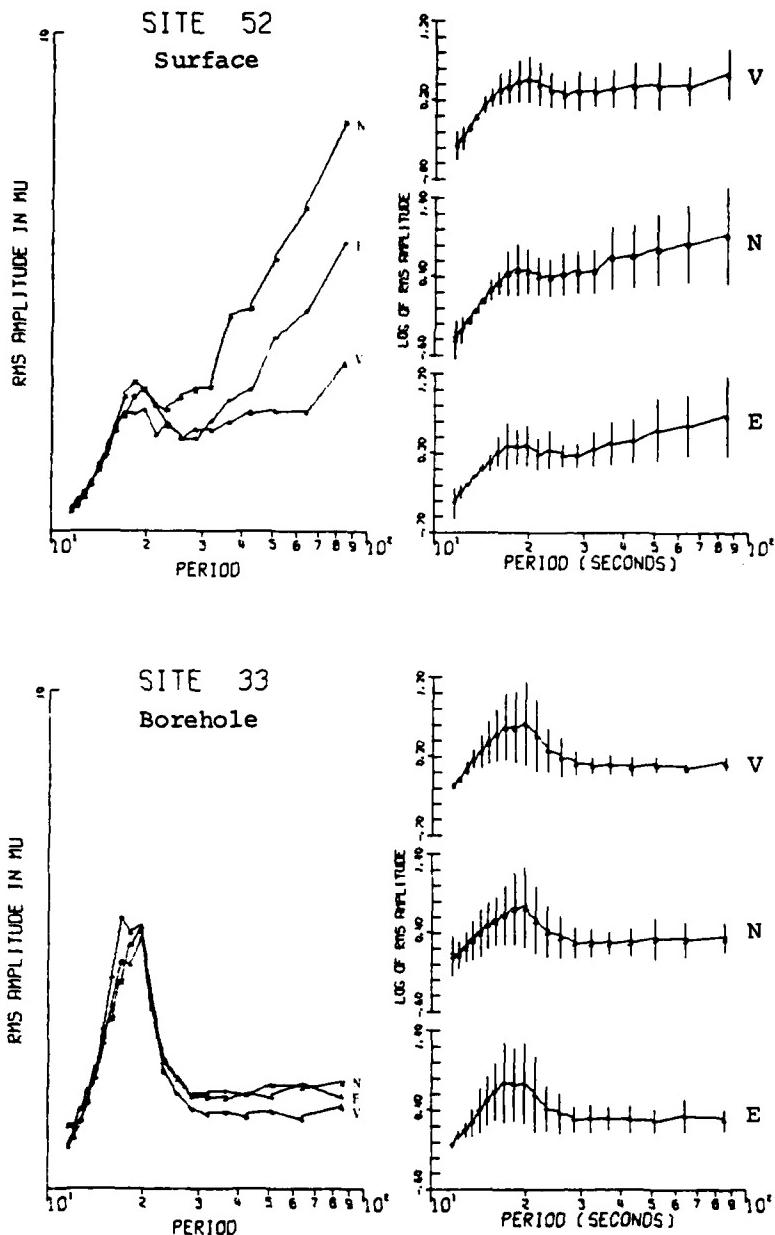
FIGURE V-1

LONG-PERIOD NOISE SPECTRA FROM
SURFACE AND BOREHOLE INSTRUMENTS
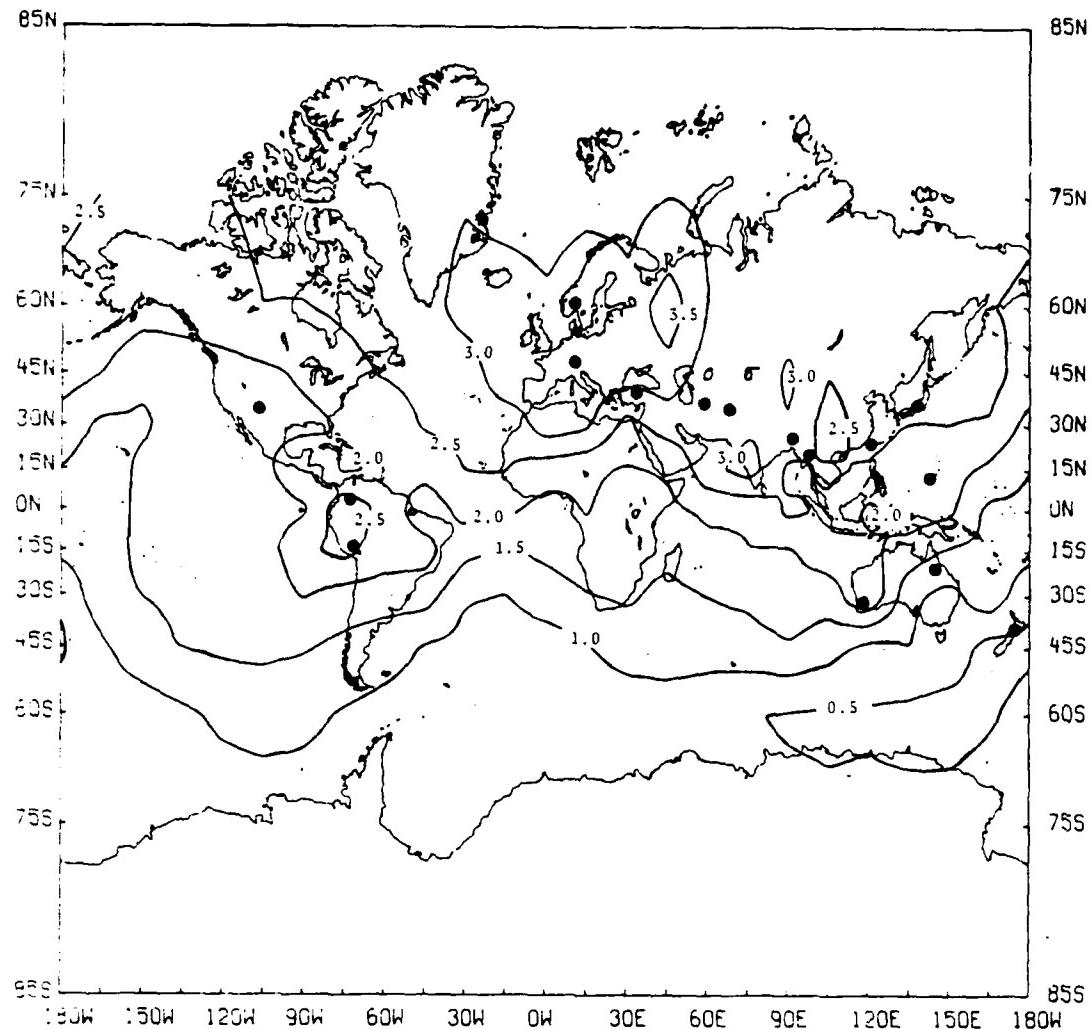
FIGURE V-2

THEORETICAL NETWORK SHORT-PERIOD DETECTION CAPABILITY
WITH REGARD TO AN m_b 4.5 EVENT

ENSCO, INC.   V-8
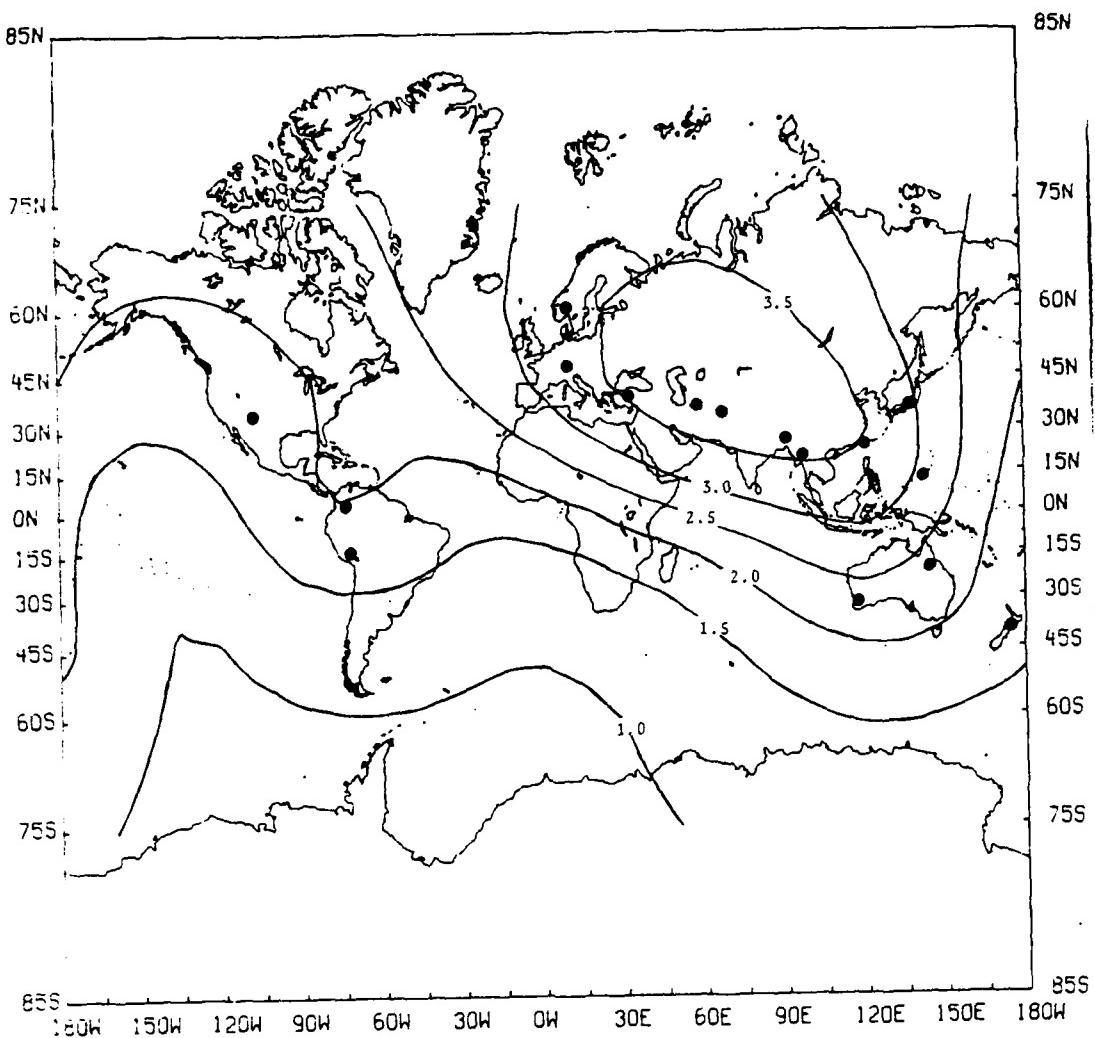
FIGURE V-3

THEORETICAL NETWORK LONG-PERIOD DETECTION CAPABILITY
WITH REGARD TO AN m_b 4.5 EVENT

ENSCO, INC.   V-9

TABLE V-4

CORRESPONDENCE OF DETECTION CAPABILITY CONTOURS
WITH DETECTION PROBABILITY

Contour	Probability Of Detection
0.5	0.7597
1.0	0.9091
1.5	0.9693
2.0	0.9901
2.5	0.9968
3.0	0.9990
3.5	0.9997

TABLE V-5

m_{b50} SRO/ASRO DETECTION CAPABILITY

	Short-Period		Long-Period		$\bar{\Delta}*$
	Ideal	Actual	Ideal	Actual	(degrees)
SRO					
ANMO	4.8	5.1	4.6	5.0	92 + 16
ANTO	5.0	5.1	4.7	4.8	32 + 2
BOCO	5.2	5.2	4.3	4.6	42 + 16
CHTO	4.6	5.0	4.6	4.9	46 + 20
GUMO	>6.0	>6.0	4.5	5.1	63 + 30
MAIO	4.7	4.8	4.1	4.6	38 + 22
NWAO	6.1	6.1	4.9	5.2	87 + 17
GRFO	5.0	5.0	4.6	4.8	46 + 4
SHIO	4.4	5.2	4.4	4.6	21 + 6
TATO	5.5	5.7	4.1	4.5	44 + 24
SNZO	>6.0	>6.0	5.0	5.3	120 + 28
ASRO					
CTAO	5.4	5.4	5.0	5.2	86 + 26
ZOBO	4.7	4.7	4.2	4.5	49 + 17
KAAO	4.3	4.4	4.1	4.5	39 + 24
MAJO	4.9	5.3	4.4	5.0	42 + 29
KONO	5.3	5.5	4.6	4.6	45 + 5

* Mean and standard deviation of station-to-epicenter distances

ENSCO, INC.   V-11

estimated by the analysis of event data bases which were constructed from available event lists. The region of interest for all except two of the stations was Eurasia. Stations BOCO and ZOBO, which are distant from Eurasia, were evaluated with regard to their South American detection capabilities.

The ideal and actual detection capabilities differ in their treatment of signals for events which were undetected due to their masking by other signals, equipment malfunction, or equipment failure. These events were ignored in the ideal estimates and were counted as nondetections in the actual estimates.

The ideal detection capabilities, with few exceptions, reflect station noise levels and the mean epicentral distances of the events in the station's evaluation data bases. Based on these two factors alone, the two South American *stations detect better than their Eurasian counterparts,* illustrating the regional dependence of detection capability.

In general, the SRO/ASRO instruments are considered reliable and are thought to produce high quality seismic data. The studies confirm that instrument burial results in a significant reduction of, and increased stability in, the recorded noise field. Consequently, these stations are valuable assets for use in event detection, location, and discrimination.

SECTION VI
REFERENCES AND RELATED MATERIAL

Chiburis, E. F., 1967; Long-Period L-Array Noise Coherence, Report No. 199, AFTAC Contract Number F33657-67-C-1313, Teledyne Incorporated, Garland, TX.

Douze, E. J., 1967; Short-Period Seismic Noise, Bulletin of the Seismological Society of America, 57, 55-81.

Eterno, J. S., D. S. Burns, L. J. Freier, and S. W. Buck, 1974; Special Event Detection for an Unattended Seismic Observatory, Report No. R-765, ARPA Contract Number F44620-73-C-0057, The Charles Stark Draper Laboratory, Incorporated, Cambridge, MA.

Fix, J. E., 1972; Ambient Earth Motion in the Period Range from 0.1 to 2560 Seconds, Bulletin of the Seismological Society of America, 62, 1753-1760.

Hudson, J. A., and A. Douglas, 1975; On the Amplitudes of Seismic Waves, Geophys. J. R. Astron. Society, 42, 1039-1044.

Operation and Maintenance Manual, Seismic Research Observatory Data Recording System, Unitech, Incorporated, Austin, TX (date unknown).

Peterson, J., H. M. Butler, L. G. Holcomb, and C. R. Hutt, 1976; The Seismic Research Observatory, Bulletin of the Seismological Society of America, 66, 2049-2068.

Prahl, S. R., 1974; Earth Noise at Very Long Period Experiment Stations, Technical Report No. 3, Texas Instruments Report No. ALEX(01)-TR-74-03, AFTAC Contract Number F08606-74-C-0033, Texas Instruments Incorporated, Dallas, TX.

Ringdal, F., 1974; VLPE Network Evaluation and Automatic Processing Research, Technical Report No. 2, Texas Instruments Report No. ALEX(01)-TR-74-02, AFTAC Contract Number F08606-74-C-0033, Texas Instruments Incorporated, Dallas, TX.

Schmidt, A. W., and K. S. Wilson, 1978; Seismic Data Preparation Procedures, Technical Report No. 22, Texas Instruments Report No. ALEX(01)-TR-78-10, AFTAC Contract Number F08606-77-C-0004, Texas Instruments Incorporated, Dallas, TX.

Snell, N. S., 1976; Network Capability Estimation, Technical Report No. 4, Texas Instruments Report No. ALEX(01)-TR-76-04, AFTAC Contract Number F08606-76-C-0011, Texas Instruments Incorporated, Dallas, TX.

Sorrels, G. G., 1971; A Preliminary Investigation into the Relationship between Long-Period Seismic Noise and Local Fluctuations in the Atmospheric Pressure Field, Geophysical Journal of the Royal Astronomical Society, 26, 71-82.

Sorrels, G. G., J. A. McDonald, Z. A. Der, and E. Herrin, 1971; Earth Motion Caused by Local Atmospheric Pressure Changes, Geophysical Journal of the Royal Astronomical Society, 26, 83-98.

Strauss, A. C., 1976; Preliminary Evaluation of the Seismic Research Observatories, Technical Report No. 2, Texas

ENSCO, INC. VI-2

Instruments Report No. ALEX(01)-TR-76-02, AFTAC Contract
Number F08606-76-C-0011, Texas Instruments Incorporated,
Dallas, TX.

Strauss, A. C., and L. C. Weltman, 1977; Continuation of the
Seismic Research Observatories Evaluation, Technical
Report No. 2, Texas Instruments Report No. ALEX(01)-TR-
77-02, AFTAC Contract Number F08606-77-C-0004, Texas In-
struments Incorporated, Dallas, TX.

Von Seggern, D. H., 1970; A Long-Period Noise Study at Murphy
Dome Alaska Seismic Data Laboratory, Report No. 247,
AFTAC Contract Number F33657-69-C-0913-PZ01, Teledyne
Industries Incorporated, Garland, TX.

Weltman, L. C., and R. R. Oliver, 1978; Continuation of the
Seismic Research Observatories, Technical Report No. 13,
Texas Instruments Report No. ALEX(01)-TR-78-01, AFTAC
Contract Number F08606-77-C-0004, Texas Instruments
Incorporated, Dallas, TX.

Wirth, M. H., 1970; Estimation of Network Detection and Loca-
tion Capability, Research Memorandum, AFTAC Contract
Number F33657-70-C-0941, Teledyne Geotech, Alexandria,
VA.